Państwowy Instytut Geologiczny
Państwowy Instytut Badawczy
państwowa służba geologiczna
państwowa służba hydrogeologiczna

HYDROCARBON PROSPECTIVE OF POLAND

NFEP&WM agreement No. 307/2021/Wn-07/FG-sm-dn/D of 21-04-2021
PGI–NRI project No. 22.5004.2101.00.1

BLOCK 208

TENDER AREA

GEOLOGICAL PACKAGE ENGLISH ABSTRACT

VI LICENSING ROUND
FOR CONCESSIONS FOR PROSPECTION AND EXPLORATION
OF HYDROCARBON FIELDS AND PRODUCTION OF HYDROCARBONS FROM FIELDS
IN POLAND

Team leader:
Adam WÓJCICKI

Project manager:
Krystian WÓJCIK

NATIONAL FUND
FOR ENVIRONMENTAL PROTECTION
AND WATER MANAGEMENT

Dariusz BRZEZIŃSKI, Martyna CZAPIGO-CZAPLA, Joanna FABIAŃCZYK,
Anna FELDMAN-OLSZEWSKA, Anna GABRYŚ-GODLEWSKA,
Marek JASIONOWSKI, Anna KALINOWSKA, Hubert KIERSNOWSKI,
Sylwia KIJEWSKA, Paulina KOSTRZ-SIKORA, Przemysław KOWALSKI,
Aleksandra KOZŁOWSKA, Olimpia KOZŁOWSKA, Marta KUBERSKA,
Krzysztof LESZCZYŃSKI, Marcin ŁOJEK, Elżbieta PRZYTUŁA,
Olga ROSOWIECKA, Leszek SKOWROŃSKI, Marcin TYMIŃSKI,
Krzysztof WAŚKIEWICZ,Piotr WESOŁOWSKI, Dorota WĘGLARZ,
Michał WOROSZKIEWICZ, Krystian WÓJCIK, Jarosław ZACHARSKI

Warsaw, 2023

1. GENERAL INFORMATION
1.1. LOCATION

The Block 208 tender area of 946.1 km^2 is located onshore in central Poland (concession block 208; Fig. 1.1). The precise location is defined by geographic coordinates listed below.

Border points	1992 coordinate system	
	X	Y
1	487578.09	431753.89
2	488166.79	397632.46
3	515963.52	398208.96
4	515376.16	432138.19

Tab. 1.1. Border points' coordinates of the Block 208 tender area (Fig. 1.2).

The Block 208 tender area was previously subjected to hydrocarbon prospection and exploration concession No. 5/03/p Blok 208 (Energia Zachód Sp. z o.o.). Currently, in the neighborhood of the tender area the following concessions are active:

- Block 207 No. 4/03/p (Energia Zachód Sp. z o.o.),
- Kórnik-Środa No. 32/96/p (ORLEN S.A.),
- Pyzdry No. 18/99/p (ORLEN S.A.),
- Malanów No. 5/2017/Ł (ORLEN S.A.).

Within the Kórnik-Środa and Pyzdry concessions, which are located SW from the Block 208, 8 gas fields in the Rotliegend sandstone are documented. These are: Kromolice S, Kromolice, Środa Wielkopolska, Winna Góra, Miłosław, Miłosław E, Lisewo, Komorze (CGDB, 2023; MIDAS, 2023).

Moreover, the Block 208 is adjacent to the east to the Konin tender area, which was subjected to the 3rd tender round for hydrocarbon concessions (Figs 1.1–1.2).

The Block 208 is prospective for exploration of conventional and unconventional oil and gas fields in the Permian Upper Rotliegend (tight gas) and Main Dolomite (conventional oil and gas) horizons. Unconventional accumulations of gas in the Carboniferous, as well as conventional gas occurrences in the Zechstein Limestone are also possible.

→**Fig. 1.1.** Location of the Block 208 tender area on the map of concessions for hydrocarbon exploration and production, and non-reservoir storage of substances in the subsurface, and storage of wastes in the subsurface, as of 30-06-2023.

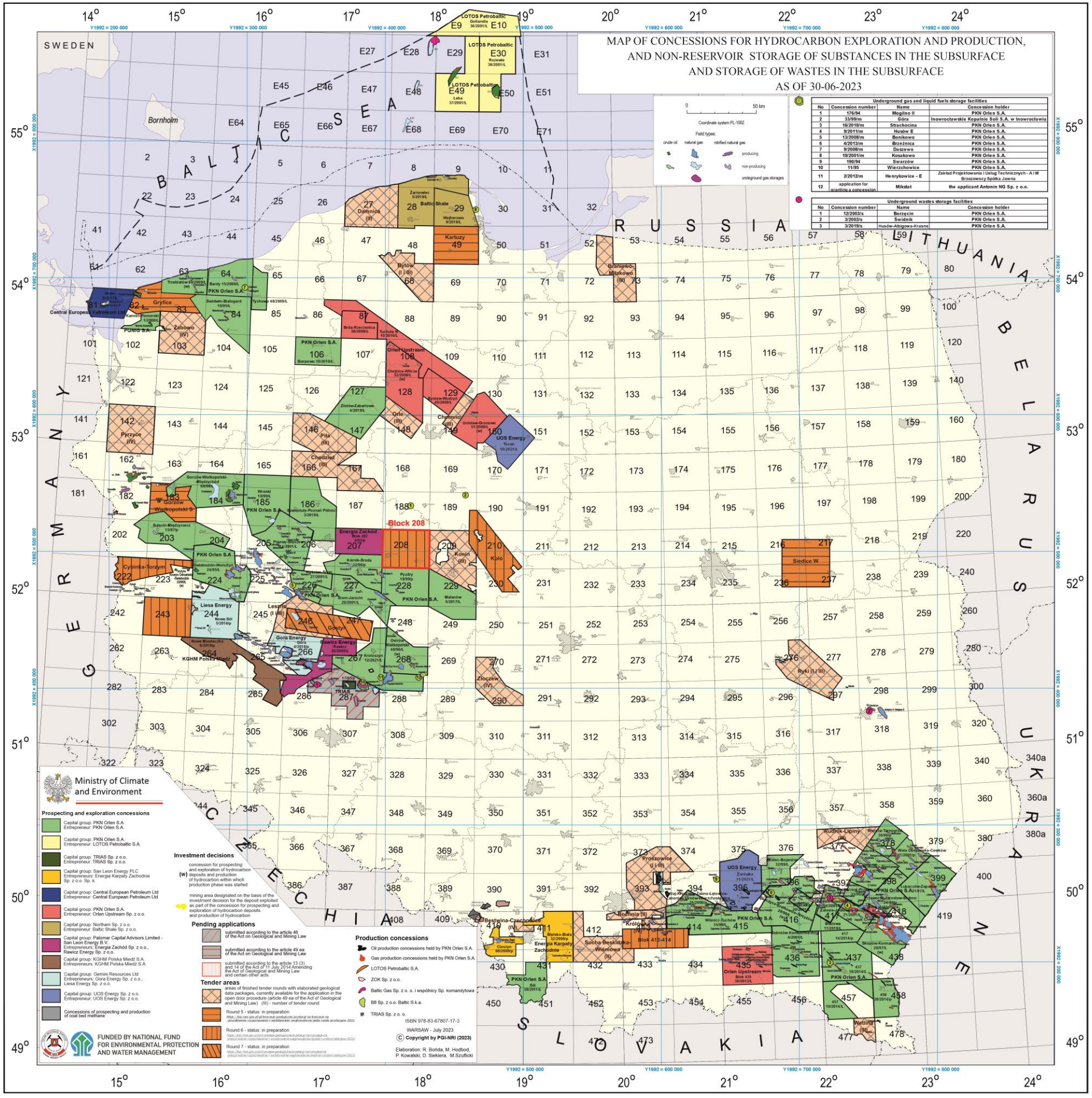
MAP OF CONCESSIONS FOR HYDROCARBON EXPLORATION AND PRODUCTION,
AND NON-RESERVOIR STORAGE OF SUBSTANCES IN THE SUBSURFACE
AND STORAGE OF WASTES IN THE SUBSURFACE
AS OF 30-06-2023
Underground gas and liquid fuels storage facilities
No | Concession number | Name | Concession holder
1 | 176/94 | Mogilno II | PKN Orlen S.A.
2 | 33/99/m | Góra | Inowrocławskie Kopalnie Soli S.A. w Inowrocławiu
3 | 16/2010/m | Strachocina | PKN Orlen S.A.
4 | 9/2011/m | Husów E | PKN Orlen S.A.
5 | 13/2008/m | Bonikowo | PKN Orlen S.A.
6 | 4/2013/m | Brzeźnica | PKN Orlen S.A.
7 | 9/2008/m | Daszewo | PKN Orlen S.A.
8 | 19/2001/m | Kosakowo | PKN Orlen S.A.
9 | 190/94 | Swarzów | PKN Orlen S.A.
10 | 11/95 | Wierzchowice | PKN Orlen S.A.
11 | 2/2012/m | Henrykowice - E | Zakład Projektowania i Usług Technicznych - A i M Brzozowscy Spółka Jawna
12 | application for granting a concession | Mikstat | the applicant Antonin NG Sp. z o.o.
Underground wastes storage facilities
No | Concession number | Name | Concession holder
1 | 12/2003/s | Borzęcin | PKN Orlen S.A.
2 | 3/2003/s | Świdnik | PKN Orlen S.A.
3 | 3/2019/s | Husów-Abigowa-Krasne | PKN Orlen S.A.
Block 208
Ministry of Climate and Environment
Prospecting and exploration concessions
Investment decisions
Pending applications
Tender areas
Production concessions
FUNDED BY NATIONAL FUND FOR ENVIRONMENTAL PROTECTION AND WATER MANAGEMENT
ISBN 978-83-67807-17-3
WARSAW - July 2023
Copyright by PGI-NRI (2023)
Elaboration: R. Bońda, M. Hodbod, P. Kowalski, D. Siekiera, M.Szuflicki

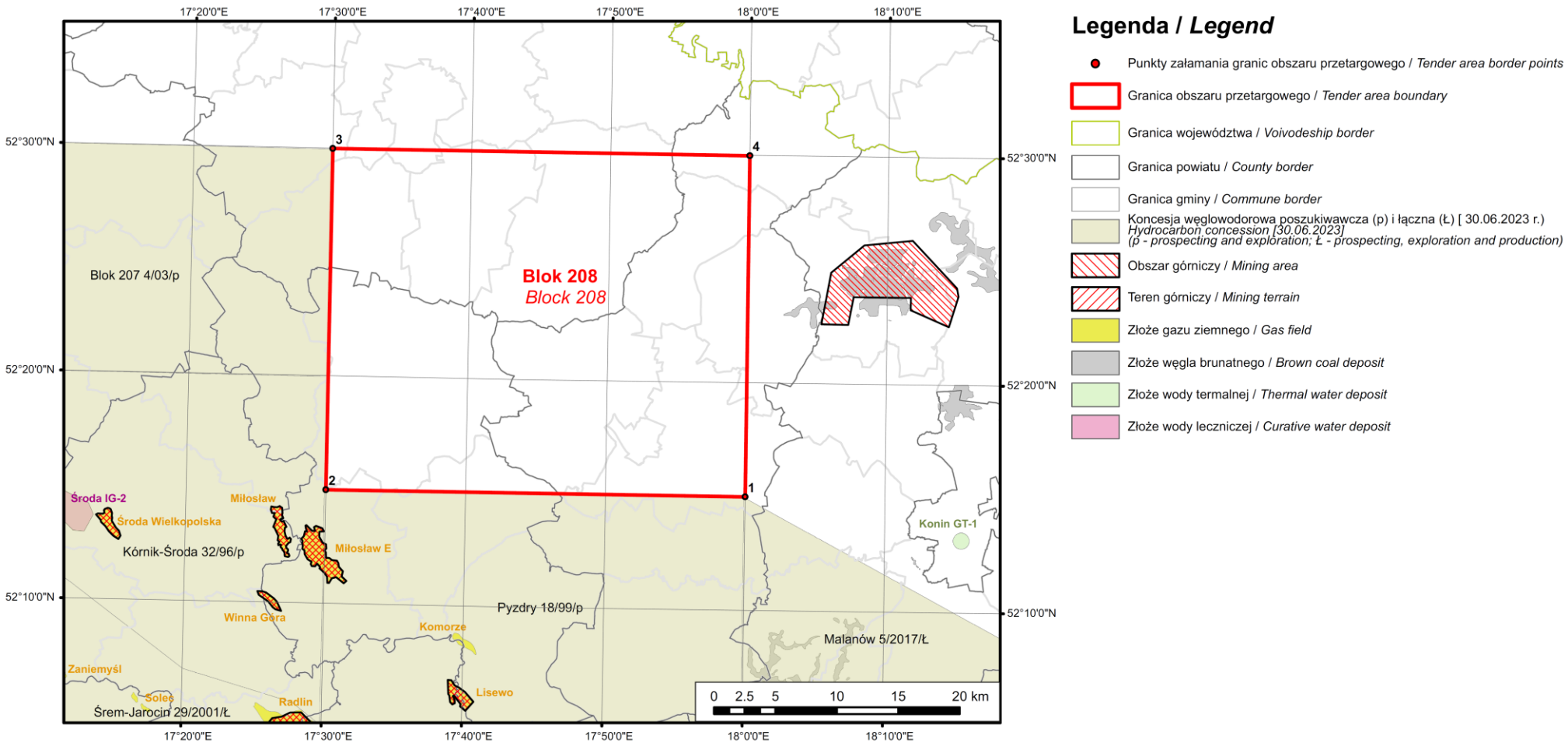

Fig. 1.2. Border points of the Block 208 tender area and location of the hydrocarbon concessions in the neighborhood, as of 30-06-2023 (CGDB, 2023).

1.2. ENVIRONMENTAL CONDITIONS

THE ENVIRONMENTAL CONDITIONS DATASHEET FOR THE BLOCK 208 TENDER AREA				
1.	LOCATION OF THE TENDER AREA ON THE MAP	Name and number of the map sheet at a scale 1: 50 000	Psary Polskie 474, Witkowo 475, Września 510, Słupca 511	
2.	ADMINISTRATIVE LOCATION	Voivodeship	Wielkopolskie	
		County	Gniezno	
		The commune and % of the area within the tendering area	Witkowo (16.92%), Gniezno (0.33%), Gniezno City (0.62%), Niechanowo (10.67%), Czerniejewo (6.44%), Łubowo (0.10%)	
		County	Słupca	
		Commune	Strzałkowo (15.02%), Orchowo (1.28%), Powidz (7.65%), Ostrowite (4.16%), Słupca (10.91%), Słupca City (1.09%)	
		County	Września	
		Commune	Września (21.51%), Kołaczkowo (2.85%), Nekla (0.03%), Miłosław (0.42%)	
3.	PHYSIOGRAPHIC REGIONALIZATION (after KONDRACKI, 2013 and SOLON et al., 2018)	Macroregion	Pojezierze Wielkopolskie (315.5)	
		Mesoregion	Pojezierze Gnieźnieńskie (315.54), Równina Wrzesińska (315.56), Pojezierze Żnińsko-Mogileńskie (315.58)	
4.	COORDINATES OF THE TENDER AREA BORDER POINTS	PL-1992 coordinate system	487578.09	431753.89
			488166.79	397632.46
			515963.52	398208.96
			515376.16	432138.19
5.	SURFACE OF THE TENDER AREA	[km^2]	946.10	
6.	CONCESSION TYPE		prospecting, exploration and production of hydrocarbons	
7.	AGE OF HYDROCARBON FORMATION		Carboniferous, Permian – Rotliegend, Zechstein Limestone, Main Dolomite	
8.	PROTECTED NATURAL AREAS:	[yes/ no] if "yes": the name of the tender area and its % within the total area		
	National Parks		no	
	Natural Reserves		no	
	Landscape Parks		Powidzki Park Krajobrazowy (13,65%)	
	Protected landscape areas		Powidzko-Bieniszewski OChK (24,83%)	
	Natura 2000, (Special Area of Conservation, SAC)		PLH300049 Grądy w Czerniejowie (<1%), PLH300026 Pojezierze Gnieźnieńskie (7%)	
	Natura 2000, (Special Bird Protection, SPA)		no	
	Natura 2000, (SAC+SPA)		no	
	Nature and landscape complexes		no	
	Ecological area	[yes (quantity) / no]	1	
	Nature monuments		39	
	Documentation positions		no	
9.	PROTECTED SOIL	[yes / no]	yes	
10.	FOREST COMPLEXES	[yes / no]	yes	
11.	PROTECTIVE FORESTS	[yes (% of the total area / no]	94.9 km^2 (10,0%)	
12.	CULTURAL HERITAGE FACILITIES Archaeological monuments	[yes (quantity) / no]		
		Hillfort	5	
		Hamlet	1	
		Cemetery	1	
		others	no	
13.	MAJOR GROUNDWATER RES-	[yes (number, name and	(143, Inowrocław-Gniezno, Ng; 144, Dolina	

THE ENVIRONMENTAL CONDITIONS DATASHEET FOR THE BLOCK 208 TENDER AREA			
	ERVOIRS	age of the aquifer) / no]	Kopalna Wielkopolska, Q)
14.	PROTECTIVE ZONES OF WATER INTAKE	[yes / no]	yes
15.	SPA PROTECTION ZONES	[yes / no]	no
16.	FLOOD HAZARD AREA	[yes / no]	no
17.	POROVEN MINERAL DEPOSITS	[yes (type of mineral deposit) / no]	yes (natural aggregates, clays)
18.	PROGNOSTIC AND PERSPEC-TIVE AREAS OF OCCURRENCE OF MINERAL RESOURCES (excluding hydrocarbons)	[yes (type of mineral deposit)/ no]	yes (sand, sand and gravel, peat, brown coal)
19.	NATURAL GAS PIPELINES	[yes / no]	no
20.	UNDERGROUND GAS STORAGE	[yes / no]	no
21.	DATE OF THE DATASHEET COMPLETION	26.02.2021	
22.	DATA COLLECTION AND ELABORATION	Joanna Szyborska-Kaszycka, Dominika Kafara	

Tab. 1.2. The environmental conditions datasheet for the Block 208 tender area.

→**Fig. 1.3.** Environmental Map of the Block 208 area.

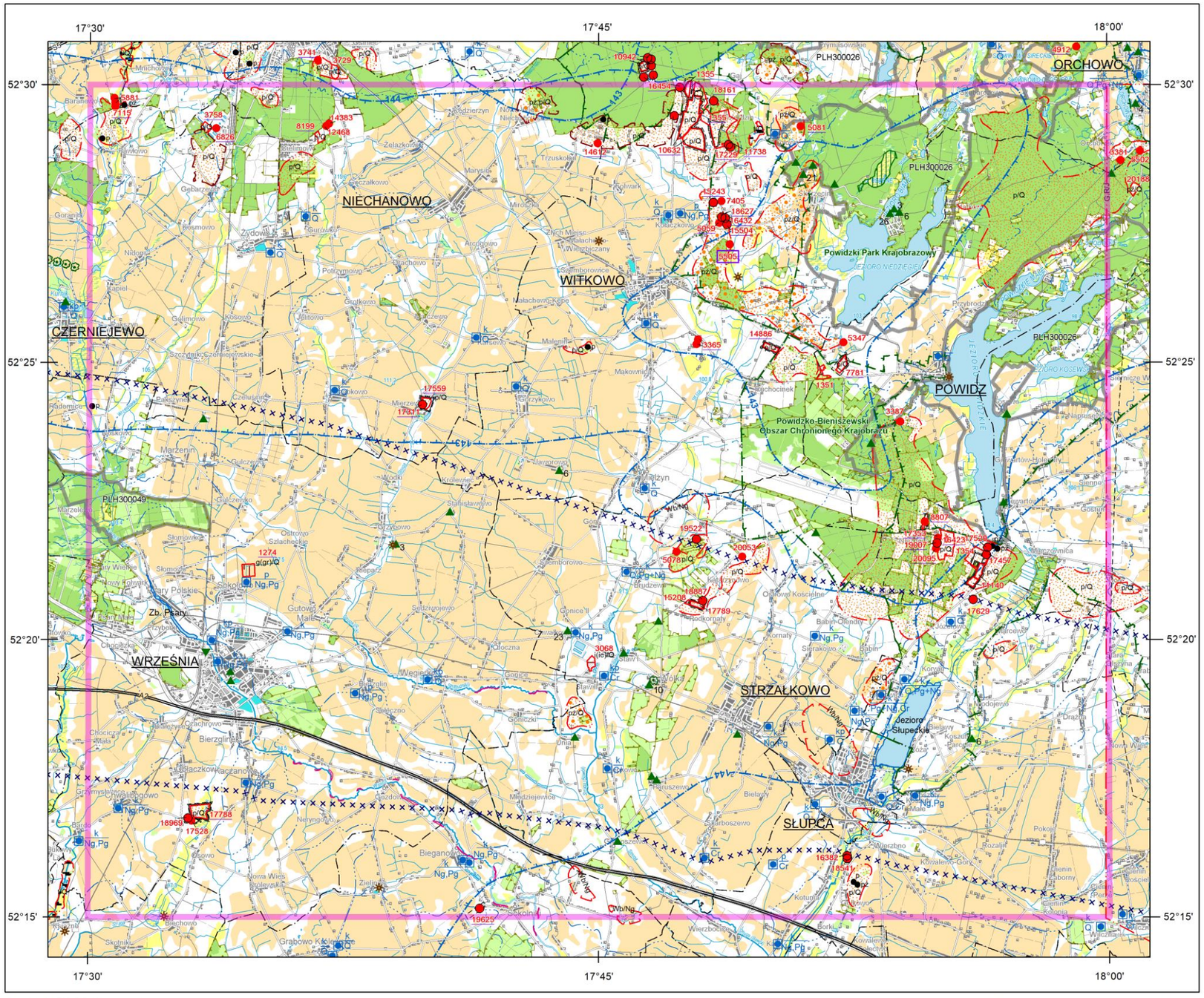

Współrzędne prostokątne w układzie PL-1992, podkład topograficzny na podstawie VMap L2

PAŃSTWOWY INSTYTUT GEOLOGICZNY
PAŃSTWOWY INSTYTUT BADAWCZY

Narodowy Fundusz Ochrony Środowiska i Gospodarki Wodnej

Ministerstwo Klimatu i Środowiska

Mapa środowiskowa obszaru Blok 208

Environmental Map of the Blok 208 area

1000 m 0 1 2 3 4 5 6 7 8 9 km

Położenie obszaru przetargowego na tle podziału administracyjnego
Location of tender area on administrative division map

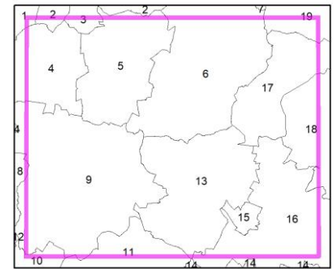

woj. WIELKOPOLSKIE
powiat gnieźnieński
1 - gm. Łubowo
2 - gm. Gniezno
3 - m.Gniezno
4 - gm. Czerniejewo
5 - gm. Niechanowo
6 - gm. Witkowo
7 - gm. Trzemeszno
powiat wrzesiński
8 - gm. Nekla
9 - gm. Września
10 - gm. Miłosław
11 - gm. Kołaczkowo
powiat średzki
12 - gm. Dominowo
powiat słupecki
13 - gm. Strzałkowo
14 - gm. Lądek
15 - m. Słupca
16 - gm. Słupca
17 - gm. Powidz
18 - gm.Ostrowite
19 - gm. Orchowo

Położenie obszaru przetargowego na arkuszach 1:50 000
Location of tender area on maps with a scale of 1:50 000

435 Kłecko	*436 Gniezno*	*437 Mogilno*	*438 Strzelno*
473 Pobiedziska	*474 Psary Polskie*	*475 Witkowo*	*476 Kleczew*
509 Środa Wielkopolska	*510 Września*	*511 Słupca*	*512 Golina*

Zestawienie danychoraz redakcja komputerowa mapy: *Anna Gabryś-Godlewska*
Data compilation and map edition:

Weryfikacja: *Olimpia Kozłowska*
Verification:

Objaśnienia do Mapy środowiskowej obszaru Blok 208

Legend of the Environmental Map of the Blok 208 area

(opracowano na podstawie bazy MGśP z zasobów PIG-PIB)*

(based on MGśP database)*

ZŁOŻA KOPALIN ORAZ PERSPEKTYWY I PROGNOZY ICH WYSTĘPOWANIA

MINERAL DEPOSIT AND PERSPECTIVE AREA'S, PROGNOSTIC AREA'S FOR DOCUMENTING DEPOSITS

- piaski i żwiry — sands and gravels
- iły i łupki ilaste — raw materials
- piaski — sands
- torfy — peat
- gliny — tills
- 12468 — identyfikator z bazy MIDAS złoża małokonfliktowego; ID from the MIDAS database of the small environmental conflict
- 8199 — identyfikator z bazy MIDAS złoża konfliktowego; ID from the MIDAS database of the environmental conflict
- 5505 — identyfikator z bazy MIDAS złoża bardzo konfliktowego; ID from the MIDAS database of the major environmental conflict
- granica złoża — deposit boundary
- granica obszaru prognostycznego — prognostic area boundary
- granica zweryfikowanego obszaru prognostycznego — verified prognostic area boundary
- granica obszaru perspektywicznego — perspective area boundary
- złoże o powierzchni ⩽ 5 ha — deposit with area ⩽ 5 ha

GÓRNICTWO I PRZETWÓRSTWO KOPALIN

MINING AND MINERAL PROCESSING

- granica obszaru górniczego — boundary of the mining area
- granica terenu górniczego — boundary of the mining terrain
- obszar i teren górniczy złoża o powierzchni ⩽ 5 ha — area and terrain of the deposit with area ⩽ 5 ha
- p — punkt niekoncesjonowanej eksploatacji kopaliny (p - rodzaj kopaliny); point of unlicensed exploitation of a mineral (p - type of mineral)

Symbol kopaliny: Mineral symbol:

- G - gaz ziemny — natural gas
- R - ropa naftowa — crude oil
- i(ic) - iły i łupki ilaste ceramiki budowlanej — building ceramics raw materials
- g(gc) - gliny ceramiki budowlanej — tills of ceramic
- pż - piaski i żwiry — sands and gravels
- p - piaski — sands
- t - torfy — peat
- Wb - węgiel brunatny — brown coal

Symbol jednostki stratygraficznej: Symbol of the stratigraphic unit:

- Q - Czwartorzęd — Quaternary
- Ng - Neogen — Neogene
- Pg - Paleogen — Paleogene
- Cr - Kreda — Cretaceous
- J - Jura — Jurassic

WODY POWIERZCHNIOWE I PODZIEMNE

SURFACE AND UNDERGROUNG WATERS

- granica działu wodnego trzeciego rzędu — water divide of third rank
- granica działu wodnego czwartego rzędu — water divide of fourth rank
- 143 — granica głównego zbiornika wód podziemnych wraz z jego numerem; principle boundary aquifer with ID number
- granica strefy ochrony ujęcia wód — water intake protected area boundary
- Zb. Psary — zbiornik retencyjny wraz z jego nazwą; water reservoir with its name
- k / Q — ujęcie wód podziemnych o wydajności ⩾ 50 m³/h (k - komunalne, p - przemysłowe, Q - wiek ujmowanych utworów); underground water intake with capacity ⩾ 50 m³/h (k - municipal, p - industrial, Q - age of exploited rocks)

WARUNKI PODŁOŻA BUDOWLANEGO

BUILDING SUBSTRATE CONDITIONS

- tereny osuwiskowe i zagrożone ruchami masowymi — landslides and mass movements hazard area

OCHRONA PRZYRODY, KRAJOBRAZU I DZIEDZICTWA KULTUROWEGO

PROTECTION OF NATURE, LANDSCAPE AND CULTURAL HERITAGE

- grunty orne (klasy I-IVa użytków rolnych) — arable land (class I-IVa)
- łąki na glebach pochodzenia organicznego — meadows on organic soils
- lasy — forests
- lasy ochronne — protected forests
- zieleń urządzona — urban greenery
- granice terenów zarządzanych przez Dyrekcję Generalną Lasów Państwowych — boundary of areas managed by General Directorate of the State Forests
- granica parku krajobrazowego; nazwa parku — boundary of landscape park; park name
- granica obszaru chronionego krajobrazu; nazwa obszaru — boundary of protected landscape area; area name
- Obszary Europejskiej Sieci Ekologicznej Natura 2000; kod obszaru — Natura 2000 ecological network; area code
- aleja drzew pomnikowych — avenue of monumental trees
- n — pomnik przyrody żywej (n - liczba obiektów); animate nature monument (n - numer of objects)
- pomnik przyrody nieożywionej — inanimate nature monument
- użytek ekologiczny — ecological area
- stanowisko archeologiczne — archeological site

INFORMACJE DODATKOWE

ADDITIONAL INFORMATIONS

- granica powiatu — distirct boundary
- granica gminy, miasta — commune or town boundary
- S3 — oś autostrady lub drogi szybkiego ruchu; highway or express route
- POWIDZ — siedziba urzędu gminy, miasta; commune or town office headquarter
- sieć elektroenergetyczna najwyższych napięć — high-voltage power network
- granica obszaru przetargowego — boundary of tender area

** Wykorzystano informacje udostępniane przez: RZGW, GDOŚ, GDLP, IMGW-PIB, NID, PSE, GAZ-SYSTEM, urzędy morskie oraz z baz danych PSG i PSH w PIG-PIB*

** Data source: RZGW, GDOŚ, GDLP, IMGW-PIB, NID, PSE, GAZ-SYSTEM, maritime offices and from database of PSG and PSH*

2. GEOLOGY
2.1. GENERAL GEOLOGY AND TECTONICS

The Block 208 tender area is located within the West European platform (Żelaźniewicz et al., 2011; Figs 2.1–2.2). Three structural units can be distinguished in its area: the Variscan basement and the Permian-Mesozoic and Cenozoic sedimentary covers.

In the Variscan structural plan, the tender area represents a part of the Variscan Orogen between the Wielkopolska Fold Belt and the Outer Variscan Externides (compare Figs 2.1 and 2.2). In the Permian-Mesozoic structural plane, the Block 208 is located in the central part of the Szczecin-Miechów Synclinorium, adjacent to the Fore-Sudetic Monocline (Fig. 2.1).

The Quaternary sediments with a thickness of several tens of meters cover older Cenozoic rocks (Neogene, in particular Miocene and Paleogene). The Mesozoic succession, comprising Cretaceous, Jurassic, and Triassic rocks, reaches a total thickness of 3–4 km. The deeper part is formed by the Zechstein and Rotliegend (still within the Permian-Mesozoic structural unit) and Carboniferous strata (Variscan structural unit). The formations older than Carboniferous have not been recognized within the tender area and its vicinity. Presumably, the Devonian, older Paleozoic, and crystalline basement of the West European Platform are present in here (Żelaźniewicz et al., 2011; Fig. 2.3), but their depths and structural setting are not precisely known.

The next sections provides a brief characterization of tectonics and individual stratigraphic units. To describe the stratigraphy and lithology in the Block 208 tender area, we used data from wells located within and in vicinity of th etender area. These are: Marzenin IG-1, Otoczna 1, Września IG-1, Grundy-2, Kłecko-1, Pławce 1, Pławce-2, Pławce-3/H, Siekierki 4, Siekierki Wielkie 1, Siekierki Wielkie 2, Trzek 1, Trzek 2, Trzek 3, Trzemżal 1, Trzemżal 2 and Wilczna 1. Their location can be found in Fig. 2.4.

Tectonic

According to information from the Września IG-1 and Otoczna 1 wells, the Quaternary, Neogene, and Palaeogene, Upper Cretaceous, Lower Cretaceous, Upper Jurassic, Middle Jurassic, Lower Jurassic, Upper Triassic, Middle Triassic, Lower Triassic, Zechstein, Rotliegend and Carboniferous strata form the stratigraphic succession within the Block 208 tender area.

In the south-western part of the area, the Upper Jurassic sediments belonging to the Fore-Sudetic Monocline occur under the Cenozoic. Then, further to the north-east, sub-Neogene outcrops of the Cretaceous appear (Fig. 2.5). A strong dip of the Permian-Mesozoic formations towards NE/ENE is observed. To the west, north-west and north-east of the tender area, several dislocation zones were identified within the Cretaceous deposits, as well (Fig. 2.5). Deeper part of the succession is formed by older Cretaceous and/or Jurassic and Triassic strata, respectively. The Zechstein was drilled only in the Września IG-1 well, having about 900 m thickness. Zechstein basement (Fig. 2.6) dips in NE/ENE direction and occurs at depths of 3700 to over 5500 m b.s.l. Numerous dislocations are present in the western, south-western and north-eastern vicinity of the tender area, while no such zones were found within (which can be related to the regional and not detailed character of the map). The report from the concession No. 5/03/p (Szpetnar-Skierniewska et al., 2015), which was operated by Energia Zachód Sp. z o.o. between 2003 and 2014, included a detailed map of the Rotliegend top surface, based on archival and current 2D seismic surveys, which, however, did not cover the northeastern part of the tender area. The map shows several small structures uplifted at the top of the Rotliegend, regional NE-dipping of this horizon and numerous dislocations, most often NW-SE. The map of Permian basement top surface (Fig. 2.7) presents generally similar (regional) structural setting as in the Zechstein case. The Permian basement dips strongly in NE direction and occurs at depths from ~4400 to over 6400 m b.s.l.

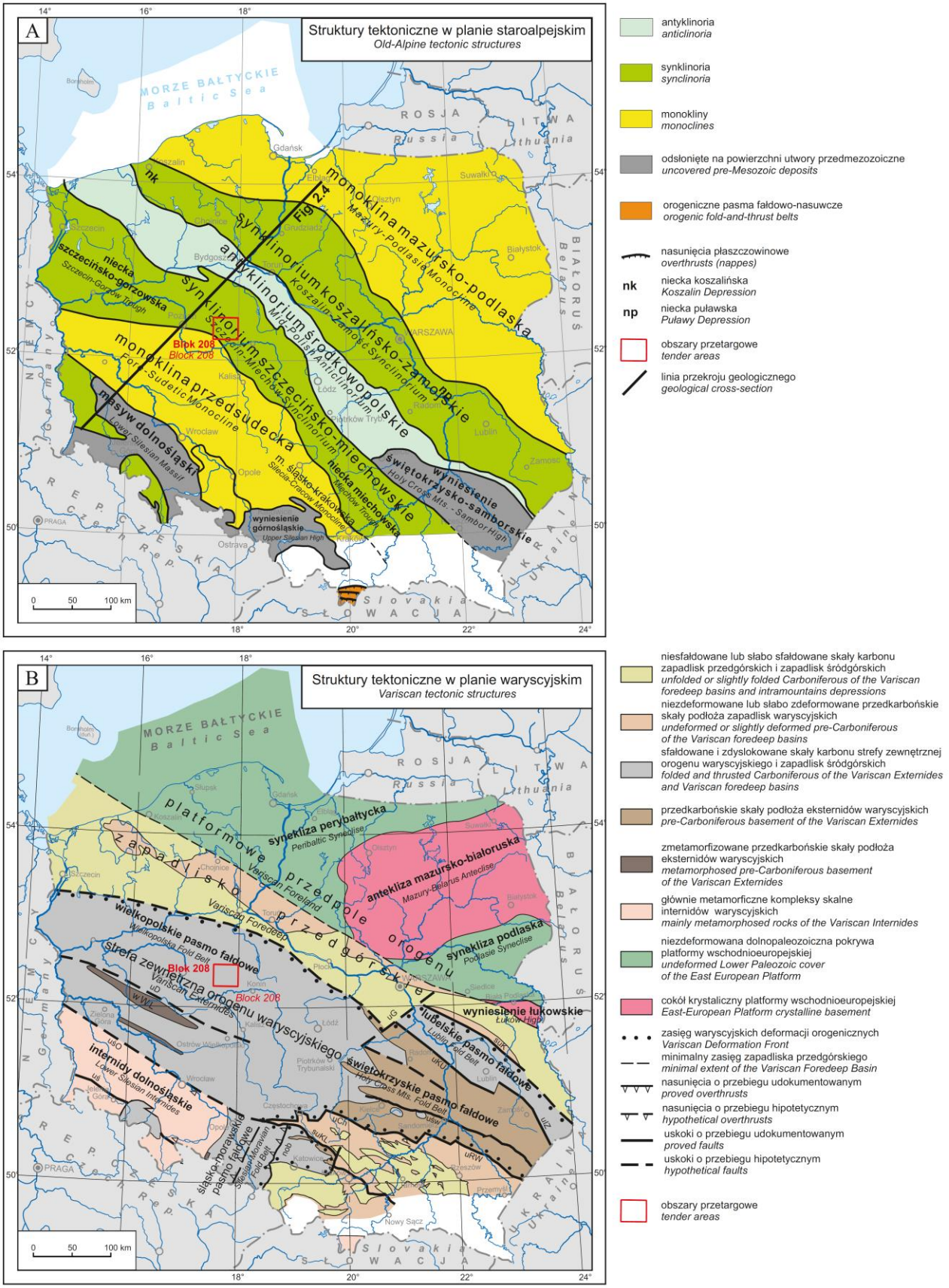

Fig. 2.1. A. Location of the Block 208 tender area in relation to the Old-Apline tectonic structures (Nawrocki and Becker, 2017; modified). **B**. Location of the Block 208 tender area in relation to the Variscan tectonic structures (Nawrocki and Becker, 2017; modified).

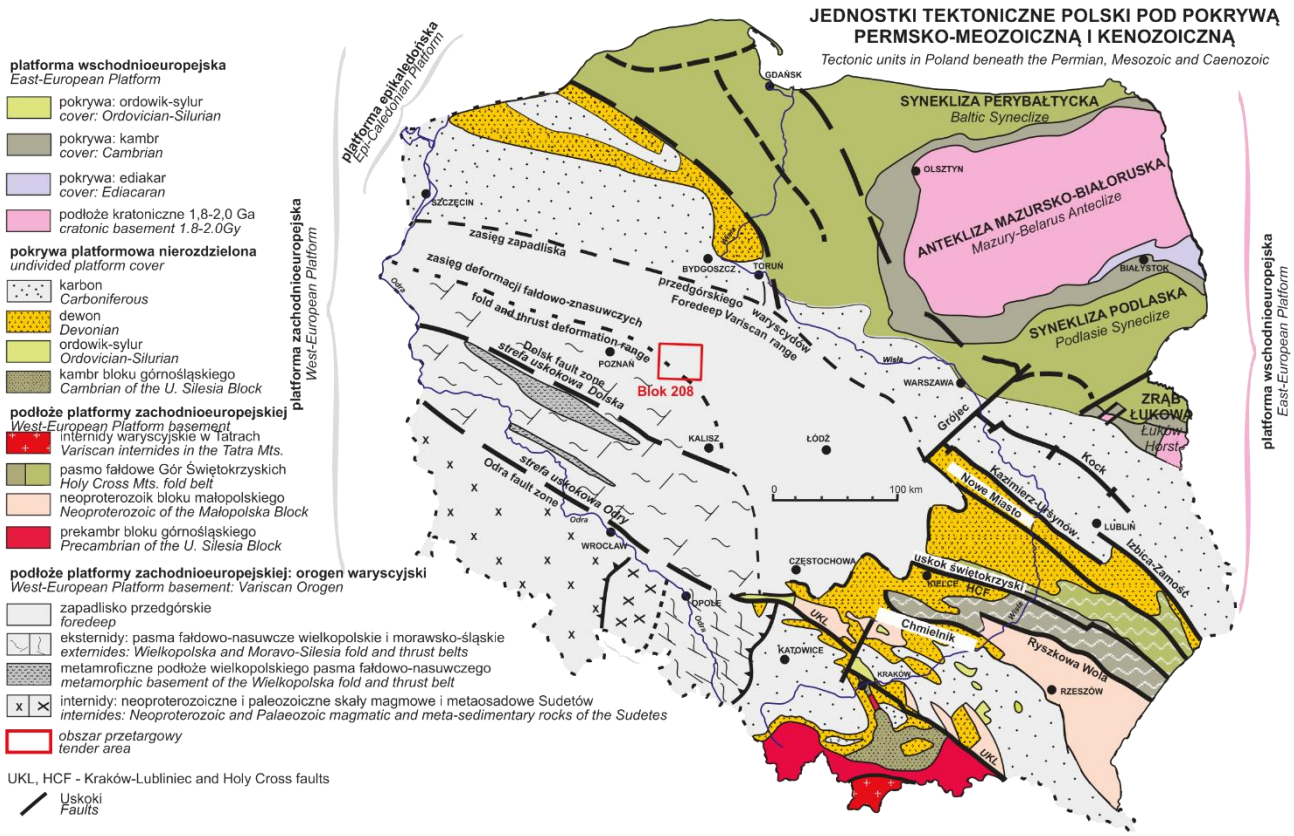

Fig. 2.2. Location of the Block 208 tender area in relation to the main tectonic units in Poland beneath the Permian, Mesozoic and Cenozoic (Żelaźniewicz et al., 2011; modified).

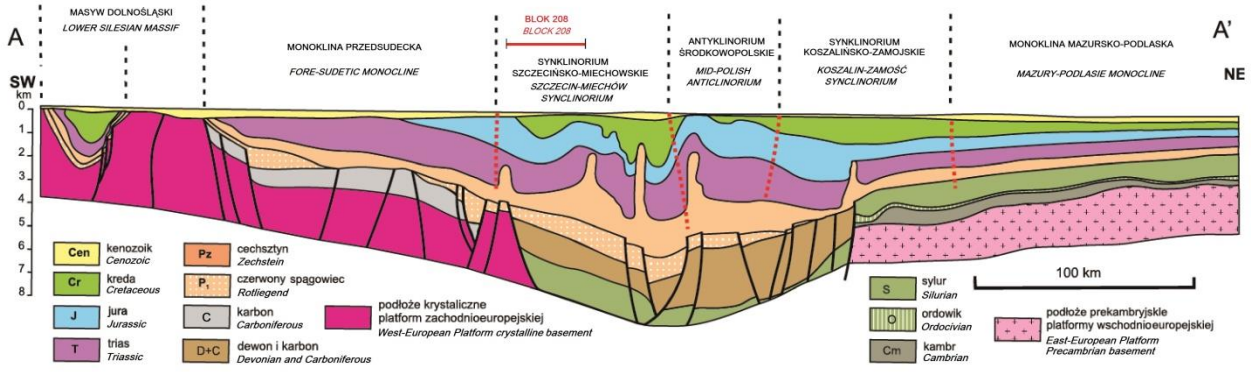

Fig. 2.3. Location of the Block 208 tender area on the geological cross-section illustrating general stratigraphy and tectonics of the Mid-Polish Anticlinorium (Żelaźniewicz et al., 2011). Cross-section location – see Fig. 2.1.

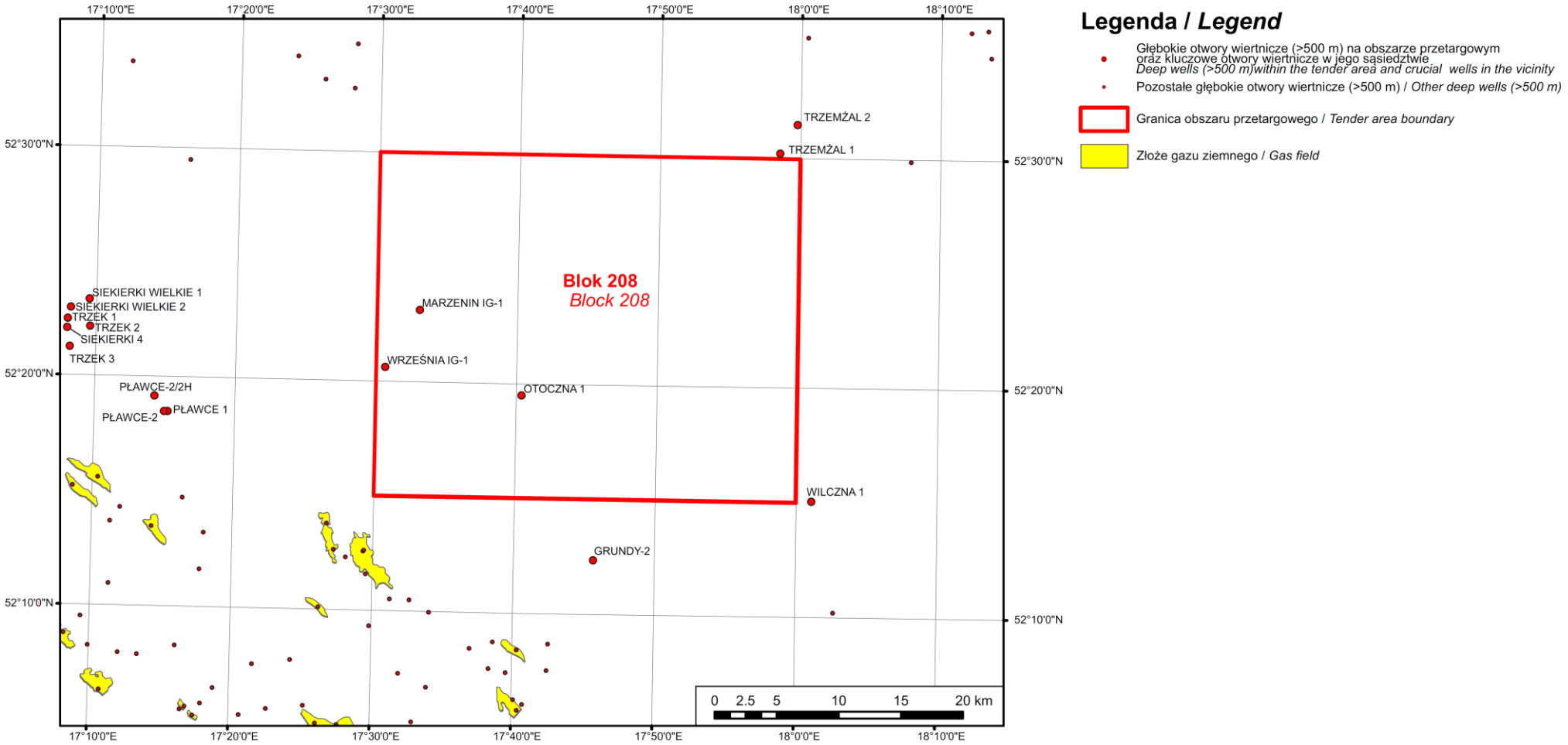

Fig. 2.4. Location of deep wells within the Block 208 and its vicinity as crucial for geological characteristics of the area in relation to oil and gas fields and other HC concessions.

Fig. 2.5. Location of the Block 208 tender area on the Geological map of Poland without Cenozoic deposits (Dadlez et al., 2000).

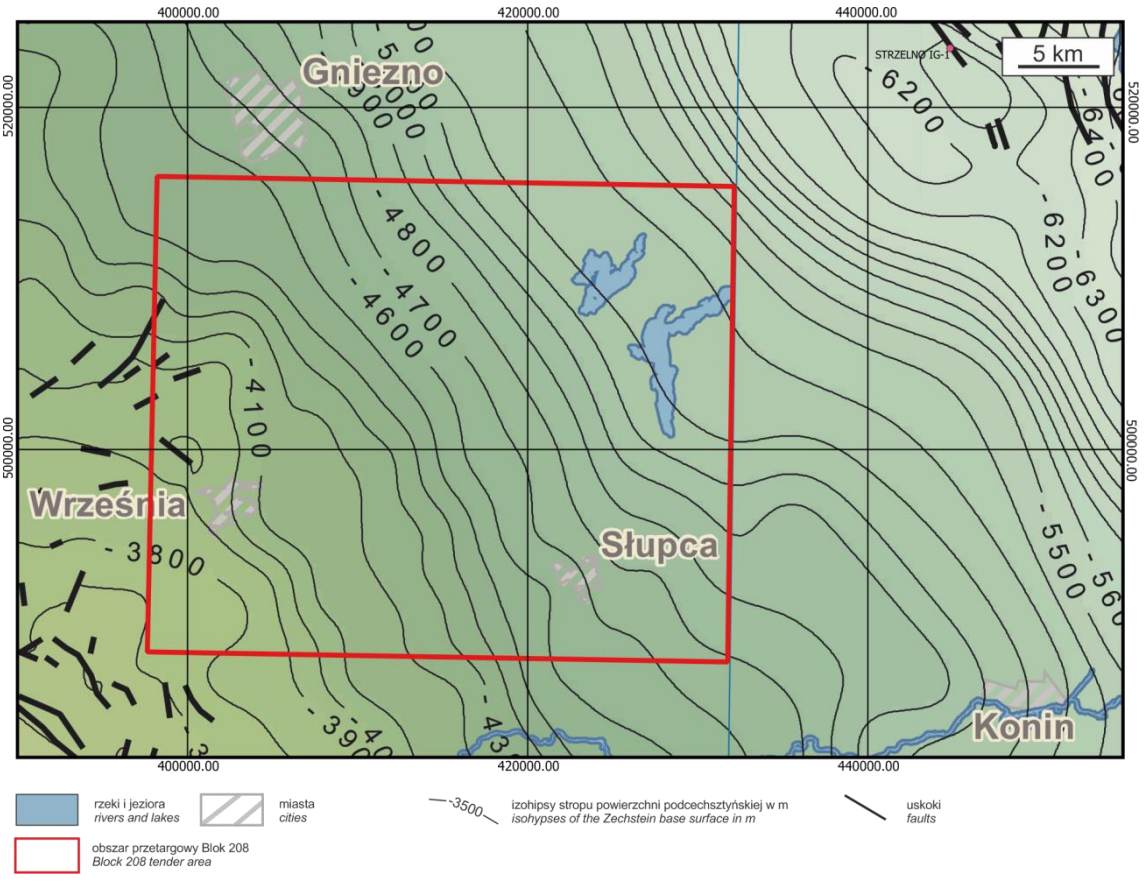

Fig. 2.6. Location of the Block 208 tender area on the structural map of the Zechstein base surface (Kudrewicz, 2007).

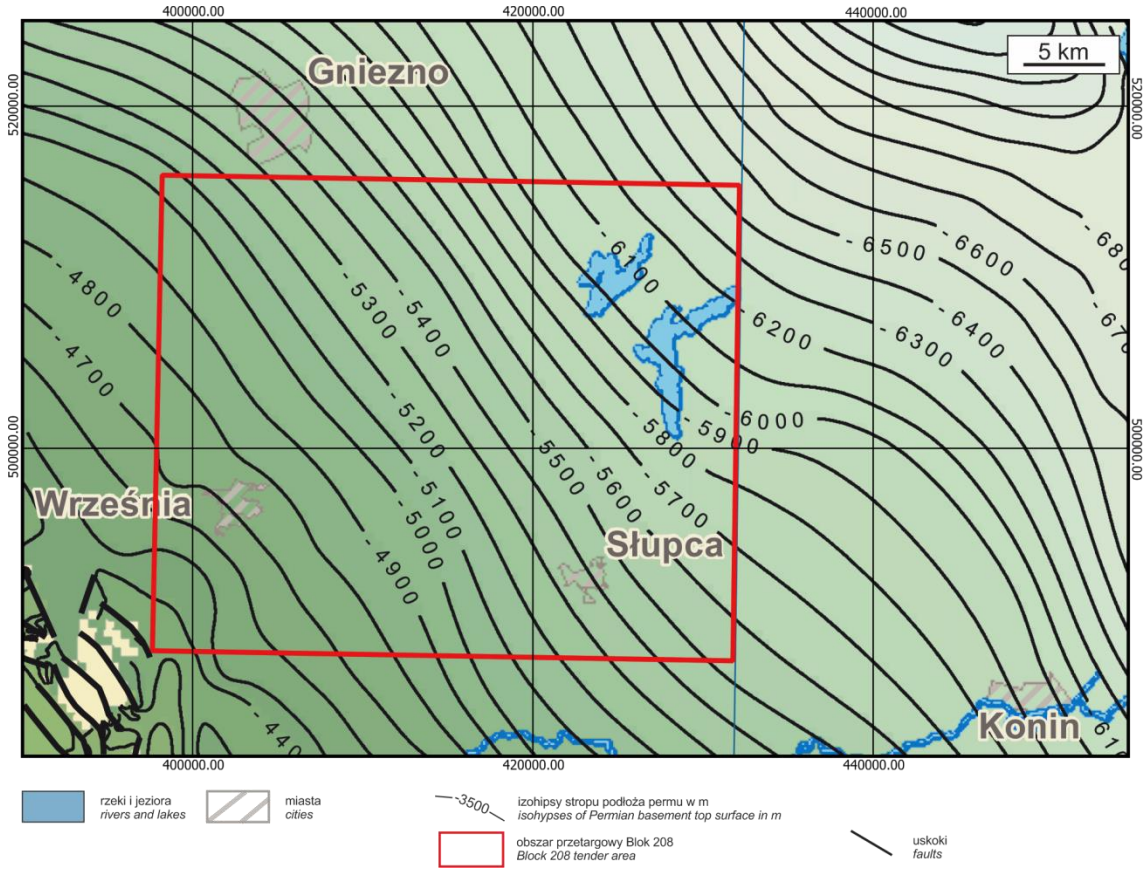

Fig. 2.7. Location of the Block 208 tender area on the structural map of the Permian basement top surface (Kudrewicz, 2007).

2.2. STRATIGRAPHY

2.2.1. CARBONIFEROUS

Distribution and thickness

The Carboniferous was recognized in 1 well – Września IG-1 – at depths 4889.5-5904.2 m. This well, however, did not pierce the unit. The Carboniferous deposits are supposed to occur in the whole tender area and in its vicinity; their total thickness may be of the order of 1–2 km (Żelaźniewicz et al., 2011).

Lithology and stratigraphy

According to the final report of the Września IG-1 well (Sokołowski et al., 1977), the following chronostratigraphic units were distinguished:

- Upper Visean: 4930.0–5904.2 m (974.2 m thickness),
- Lower Namurian(?): 4889.5–4930.0 m (40.5 m thickness).

The occurrence of the Upper Carboniferous (Pennsylvanian) in the Września IG-1 well was not confirmed (Sokołowski et al., 1977). However, palynological studies made by Parka and Ślusarczyk (1988) and Górecka-Nowak (2008) suggest that the upper part of the succession belongs to the Westphalian A or Westphalian D (Fig. 2.8).

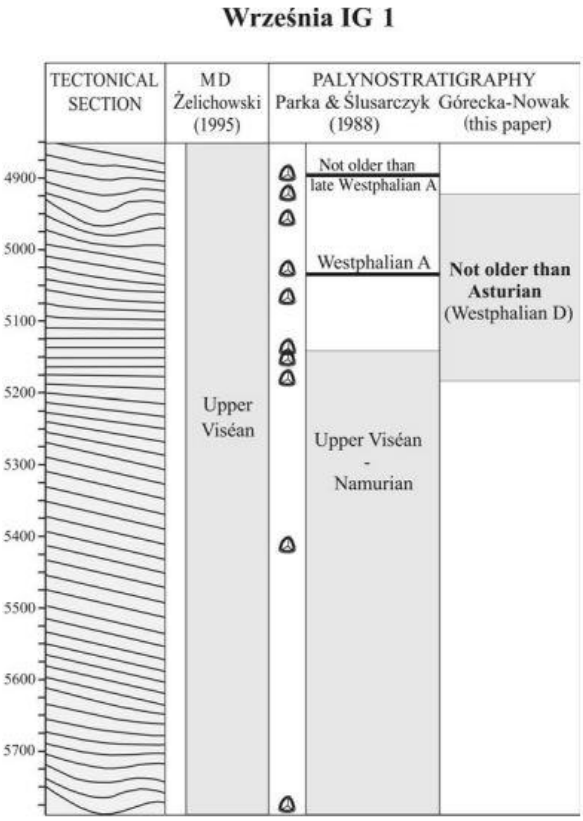

Fig. 2.8. Stratigraphy of the Carboniferous rocks in the Września IG-1 well. MD – dating based on macrofauna occurrences (Górecka-Nowak, 2008).

Petrography

The petrographic characteristics of the Carboniferous deposits are compiled basing on the final report of the Września IG-1 well (Sokołowski et al., 1977), the PGS project "Recognition of prospective zones for the occurrence of unconventional hydrocarbon deposits in Poland, stage I" (Podhalańska et al., 2016) and scientific publications (Krzemiński, 2005; Kozłowska and Kuberska, 2015; Sikorska-Jaworowska et al., 2016).

The Carboniferous sediments represent a package of sandy and silty rocks typical for the Fore-Sudetic Monocline. It is composed of three types of rocks: sandstones, siltstones and claystones.

Sandstones (Fig. 2.9A, B; Fig. 2.10A, B) are characterized by brown, cherry, and gray color. They represent fine- to medium-grained quartz, subarcose, and sublithic wackes and fine- to coarse-grained subarcose and sublithic arenites (Fig. 2.9A, B). The sandstones are characterized by a psammitic texture, slightly directional texture (parallel arrangement of organic matter, lamellae of micas or hematite) in the wackes and a disorder texture in the arenites. The sorting of the material is medium. The detrital material consists of sharp-edged and semi-mottled grains of mono- and polycrystalline quartz, feldspars, and rock fragments. The feldspars are represented by plagioclase-albite and in lesser amounts by potassium feldspars. In feldspar grains, the effects of the following processes are commonly observed: albitization, argillization, chloritization and carbonatization, less frequently dissolution. Lithoclasts mainly represent volcanic rocks, in addition to quartzites and metamorphic rocks (mostly quartz-schist shale). In lithoclasts the effects of argillization, chloritization and carbonatization processes are observed. The schists are represented by bent lamellae of muscovite and biotite, which is partly chloritized. Of the accessory minerals, zircon, tourmaline, rutile, anatase and pyroxene were observed. The main component of the cement is a clay matrix with quartz dust (Fig. 2.10A, B). The clay minerals include illite, chlorite, and illite/smectite mixed-pack minerals. Cement is formed by carbonate minerals (calcite, Fe-dolomite/ankerite, siderite), autigenic chlorite, autigenic quartz, hematite, and pyrite.

In the sandstones, the total porosity ranges from 0.40 to 4.86% and the effective porosity ranges from 0.05 to 3.65%. Permeability measurements indicate that some of the sandstones are impermeable, and some have permeability up to 3.5 mD.

The **siltstones** and **claystones** are dark to light brown and gray in color. These rocks show directional (laminated) texture. Their structure is pelitic, pelitic- aleuritic and pelitic-aleuritic-psamitic. Among the detrital material there are unmolded quartz grains, feldspars, mainly plagioclase, locally potassium feldspars and rock fragments. Apart, there are shaly minerals (muscovite and biotite, chloritized in places), linearly arranged organic matter and small intrusions of pyrite. The detrital material is interbedded in a clay-silica mass. Among the clay minerals, illite, illite/smectite mixed-pack minerals, and chlorite were distinguished. Carbonates (Fe-dolomite/ankerite) were observed in small amounts and occur as cement or vein fill.

In siltstones and claystones, the total porosity usually varies from 0.36 to 2.18% and the effective porosity from 0.14 to 1.52%. These rocks are either impermeable or characterized by permeability that reaches 0.17 mD.

The **Upper Visean** is developed as fine-grained, less frequently medium-grained (and very rarely coarse-grained sandstones with interbedding conglomerates) graywackes (these are mostly arkose wackes or lithic graywackes) of gray or dark gray color; as well as siltstones and claystones usually of dark gray, less frequently gray, or green-gray color (Sokołowski et al., 1977). Muscovite admixtures are common in sandstones and sandy siltstones, but no coal seams have been found. The matrix of sandstones is mostly clay with quartz grains. Sandstones often contain clasts of plutonic and volcanic rocks and quartz-schist shale and siltstone xenoliths.

In the **Lower Namurian** there is a significant share of fine-grained greywacke sandstones (quartz, arkose and lithic wackes) of grey through brown to cherry-brown and cherry-red color; there are also complexes of clayey-sandy and clayey-siltstones and claystone, of cherry-red through brown to grey or dark grey color (Sokołowski et al., 1977). The brown to cherry color of the clastic rocks is associated with the presence of hematite grains. Analogous to the Upper Carboniferous, the cement (matrix) of the sandstones is predominantly clayey, with quartz grains, and these rocks often contain clasts of plutonic and volcanic and fine clastic rocks.

Hydrocarbon potential

The Carboniferous sandstones in the Września IG-1 well are characterized by poor reservoir properties – their porosity and permeability may be mostly unsuitable for both conventional and unconventional (tight) gas accumulations (Kozłowska and Kuberska, 2015; Wójcicki et al., 2014).

The siltstones and claystones are characterized by thermal maturity of organic matter corresponding to gas window. However, the organic matter content is relatively low, generally not exceeding 1% wt. (Szpetnar-Skierniewska et al. 2015; Podhalańska et al., 2018), and thus not promising for the occurrence of shale gas deposits.

However, results from a single borehole cannot definitively rule out the prospectivity of the Carboniferous for the occurrence of tight gas in the area.

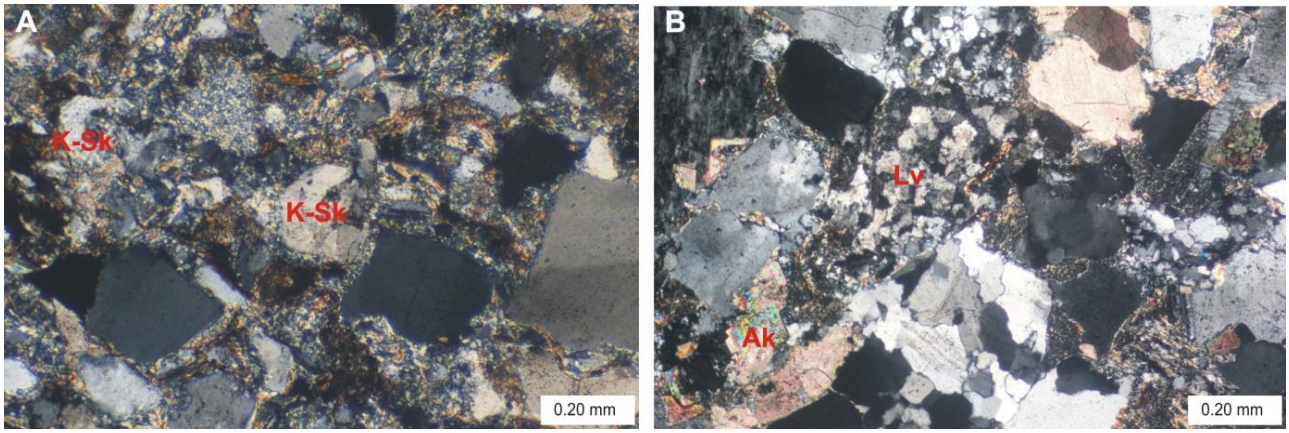

Fig. 2.9. Photographs with a polarizing microscope (PL). A. Sublithic/sublithic wackestone, fine-grained; visible grains of potassium feldspar (K-Sk). Września IG-1 well, depth 5622.2 m, crossed nicols. B. Sublithic arenite, medium-grained with ankerite cement (Ak); volcanic rock fragments (Lv). Września IG-1 well, depth 4994.1 m, crossed nicols.

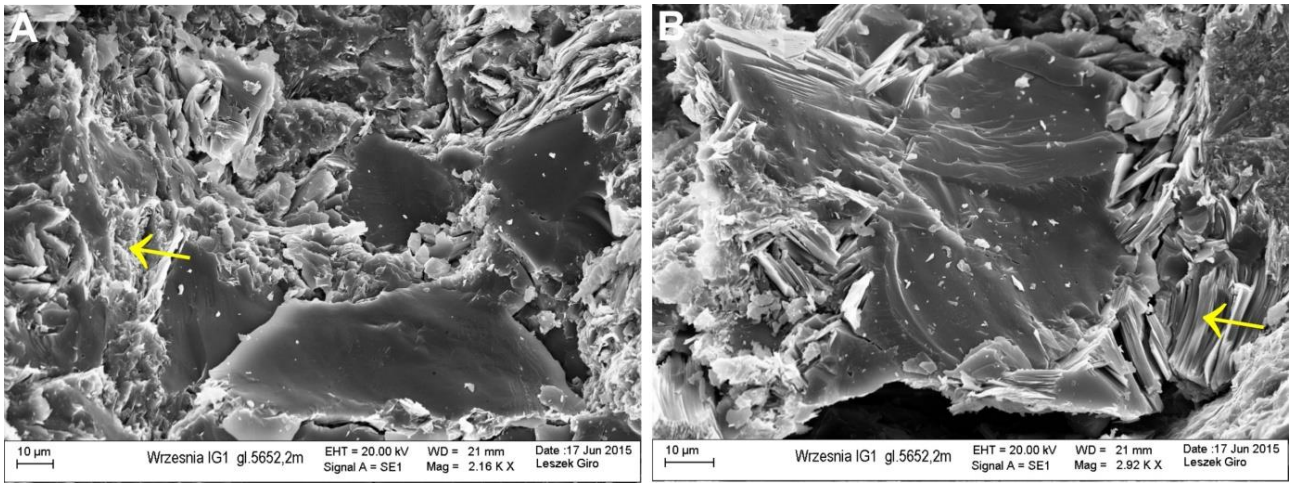

Fig. 2.10. Scanning electron microscope (SEI) photographs. A. Matrix (arrow) tightly filling the space between grains in a subarcose wacke. B. Matrix composed of shaly minerals (arrow). Images A and B are from the Września IG-1 well, depth 5652.2 m.

2.2.2. PERMIAN – ROTLIEGEND

Distribution and thickness

The Rotliegend rocks in the Block 208 tender area were recognized in the Września IG-1 well – at depths 4026.5–4889.5 m (Sokołowski et al., 1977). In addition, in the vicinity of the tender area, the Rotliegend has been recognized in the following wells:

- Grundy-2: 4240.0–5000.0 m,
- Kłecko-1: 4575.0–5200.0 m,
- Komorze 1: 3815.5–4305.0 m,
- Miłosław 1: 3695.0–3864.0 m,
- Miłosław 3: 3720.0–3787.0 m,
- Miłosław 4K: 3633.9–3726.7 m,
- Pławce-2: 3716.0–4202.0 m,
- Środa IG-3: 3522.0–3981.9 m,
- Środa Wielkopolska 4: 3568,0–3701.0 m,
- Środa Wielkopolska 5: 3540,3–3652.0 m,
- Środa Wielkopolska 6: 3707.5–3740.0 m,
- Trzek 1: 3655.0–3955.0 m.

Their location is illustrated in Fig. 2.4.

Lithology and stratigraphy

In the Września IG-1 well, the total thickness of the Rotliegend is 863 m. The Upper Rotliegend (Saxonian, 736 m thickness) is characterized by the predominance of sandstones, which are prospective for the occurrence of gas accumulations. The Lower Rotliegend (Autunian, 127 m thickness) is composed of conglomerates (agglomerate tuffites), which rest on red-brown Carboniferous siltstones (Sokołowski et al., 1977).

According to Pokorski (1981, 1988, 1997; Fig. 2.11), the Upper Rotliegend is represented by the Drawa and Noteć formations, and the Lower Rotliegend represents the Obrzycko Member of the Wielkopolska Volcanogenic Formation (Maliszewska and Pokorski, 1978).

Interpretation of the drill cores from the Września IG-1 well shows that the Rotliegend in this area is mainly built of aeolian sediments with subordinate contributions of fluvial (riverine) deposits. The Rotliegend consists of several horizons of pure dune sandstones intercalated with interdune sandstones. The occurrence of this type of aeolian sediments corresponds to relatively regular cycles of sedimentation associated with climatic changes from dry to wet and with the rate of subsidence and erosion of the area. In the uppermost part of the Rotliegend succession, the presence of more coarse-grained material is characteristic, which may indicate regional changes in sand supply during the sedimentation. Consequently, the porosity and permeability of the sandstones are rather good, in contrast to the neighboring areas – e.g., in the Siekierki-Trzek-Pławce area located to the west (Fig. 2.4), where thicker successions of the Zechstein Weissliegend (absent

in Września IG-1 well) also occur. Due to the hypothetical relatively high palaeorelief of the Września IG-1 area, aeolian sandstones predominate (Szpetnar-Skierniewska et al, 2015; Kiersnowski et al., 2020), although a predominance of aeolian sediments was also found in the Siekierki-Trzek-Pławce area. Generally, in the south-western and southern parts of the Block 208 tender area, aeolian sediments are present at the top of the Rotliegend (Fig. 2.12; Kiersnowski et al., 2020). In the central and south-eastern parts, sandstones and mudstones of the marginal playa-lake are found interlayered with aeolian sandstones. In contrast, the northern and north-eastern parts are postulated to contain playa-lake mudstones and sandstones, which are generally considered not prospective for the occurrence of natural gas accumulations.

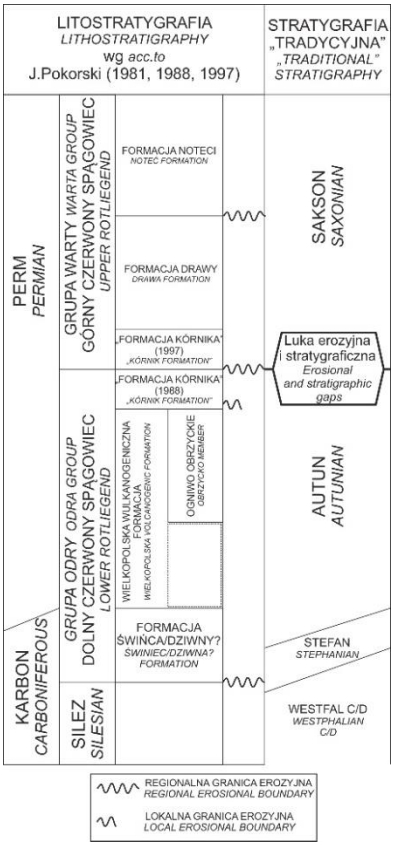

→Fig.2.11. Stratigraphic subdivision of the Rotliegend in the Polish part of the South Permian Basin (Kiersnowski in: Maliszewska et al., 2003).

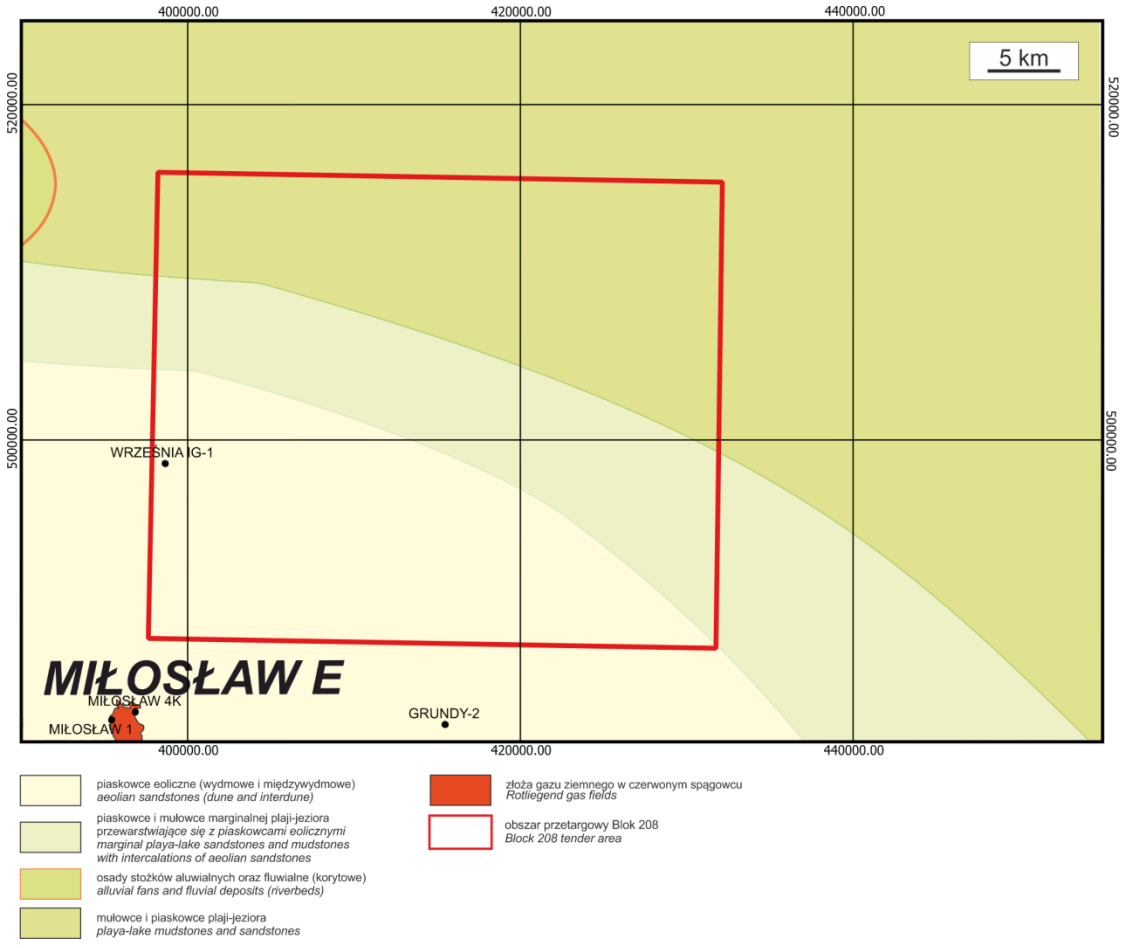

Fig. 2.12. Location of the Block 208 tender area on the facies-palaeogeographic map of the Upper Rotliegend (Kiersnowski et al., 2020) with wells drilling the Rotliegend rocks.

Petrography

Petrography of the Rotliegend deposits in the Block 208 tender area is derived from numerous scientific publications (Kuberska, 2001, 2004; Maliszewska, 1997; Maliszewska and Kuberska, 2008, 2009; Maliszewska et al., 1998, 2016) and from detailed analyses carried out in the Września IG-1 well (Maliszewska, 1997).

The Lower Rotliegend (Autunian) is represented by pyroclastic sediments admixed with terrigenous material. Agglomerate tuffites, sandstone tuffites and ash tuffites are distinguished.

The Upper Rotliegend (Saxonian) is developed as a series of lithic and sublithic sandstones, mostly fine-grained, often with interbedding of medium- and coarse-grained sandstones.

The Rotliegend **sandstones** are characterized by gray, pink, grayish-red or brown color. They are fine- and medium-grained rocks, sometimes coarse-grained. Their characteristic feature is their directional texture emphasized by the arrangement of laminae with coarser and finer grains. Due to the mineral composition of sandstones and the type of cement arenites were distinguished, very rarely wacky, lithic, locally sublithic. Nomenclature adopted the classification of Pettijohn et al. (1972).

The main components of **detrital material** in sandstones are mono- and polycrystalline quartz grains (27–58% by volume), occurring in the form of semi-mottled grains. Feldspars (5–16% by volume) are represented by grains of microcline, oligoclase, albite, microcline antipertite, and checkerboard albite. They occur in the form of tabular grains or are semi-rounded. They are partially kaolinitized, sericitized, or replaced by dolomite or quartz (Fig. 2.13A). Feldspathic autigenic rims were also observed on detrital grains (Fig. 2.13B). Among the lithoclasts, fragments of volcanic rocks, mainly rhyolites, are most abundant. Besides, there are fragments of quartz-mica crystalline schists, granitogneisses, composed of quartz and feldspars. In addition to the mentioned main components in sandstones there are micas (muscovite) and accessory minerals – zircon, tourmaline, hornblende, corundum, and andalusite. Also present are iron oxides in the form of detrital grains rimmed, sometimes with coatings of leucoxene or goethite.

The main components of the **cements** include iron oxides and hydroxides, allo- and autigenic clay minerals, carbonates, sulfates, quartz and autigenic feldspar. Iron oxides and hydroxides are common in the described sandstones, giving them a characteristic reddish color. They occur mostly in the form of dispersed pigment. The dispersed iron pigment, together with allogenic clay minerals, are part of the matrix-type cement and often form rims on detrital grains. The group of autigenic clay minerals includes illite (Fig. 2.13C), chlorite (Fig. 2.13D), and kaolinite. Individuals of autigenic illite occur as slats with numerous protrusions and as thin filaments, confining the pore space. Diagenetic illite is common in Lower Permian sediments in all depositional environments. Its crystallization was determined to be Early Cretaceous (Maliszewska and Kuberska, 2009), and crystallization temperatures under the assumptions of this study could range from 126–173°C. The autigenic chlorites found in the sandstones occur as rims on detrital grains or fill pore spaces to form fan-like forms. Chlorites forming rims can inhibit mechanical compaction in sediment (Rochewicz, 1980) and inhibit subsequent cementation – for example, with autigenic quartz (Hancock, 1978), but are not a common form found in sandstones from the Września IG-1 well. Fan forms have been described in Redstone sandstones in other boreholes (Kuberska, 2004) and have been classified as cements formed in later stages of diagenesis, at temperatures of 90–120°C (Aagaard et al., 2000).

Carbonate **cements** in the Rotliegend sediments are represented mainly by dolomite, with calcite in places. The dolomite occurs as fine rhombohedra (Fig. 2.13E), often showing a banded structure. The central parts of the rhombohedra are then composed of Mn/Fe-dolomite (yellow color of luminescence in CL), and the parts closer to the edges are Fe/Mn-dolomite (red color in CL). Crystallization temperatures of this mineral, given the results of oxygen isotope ratio determinations, may range from 60 to about 100°C, although slightly lower temperatures were more likely (Ku-

berska, 1999; Maliszewska et al., 2016). In places, Mn- or Mn/Fe-calcite co-occurs with dolomite, forming a pore cement composed of anhedral specimens.

Quartz cement (Fig. 2.13A) is commonly found in small amounts. Autigenic quartz forms regeneration rims on detrital grains or single euhedral crystals. In places, the presence of coarse crystalline quartz cement filling the pore spaces was noted. The sulfate cement is represented by anhydrite in the form of fine plaques, less frequently as a basic cement, and coarse crystalline barite (Fig. 2.13F). Regenerative feldspar rims were also included in the rock cements. These are K-feldspar composition rims brown in CL accreted on grains of potassium feldspar glowing blue/brown in CL.

Early **diagenesis** involved a set of physical and chemical processes occurring in a depositional environment and under shallow burial conditions. During this stage, processes that destroyed primary porosity outweighed those that could sustain it. Mechanical compaction was most important, causing an increase in the packing of detrital grains. This is illustrated by the counted grain contact ratio, which ranges from 2 to 4, mostly above 3, in the sandstones studied. In turn, porosity may have been partially protected by the stiffening of detrital grains by coating them with a clay-iron film. Early silica cements were also formed on detrital grains, observed as quartz syntaxial rims. At the stage of early diagenesis, processes of transformation of unstable rock components (feldspars, crumbs of volcanic rocks) may have begun. Crystallization of dolomite has also begun, with fine rhombohedra sometimes surrounding detrital grains.

The intermediate and late diagenesis is a continuation of the long-term stage of sediment burial and increase in the action of mechanical compaction, which at a depth of 3–4 km is replaced by chemical compaction and results in concave-convex and interlocking contacts. During the intermediate and late diagenesis, quartz, calcite, and sulfate cements were formed. The transformation of unstable components, especially volcanic glaze, into smectite group minerals continued. Under increasing temperature and pressure, the composition of smectite minerals evolved to form fibrous illite. While crystallization of fibrous illite destroyed the filtering capacity of sediments, crystallization of chlorite may have protected porosity and filtering capacity (Rochewicz, 1980).

Most of the studied sandstones are characterized by reservoir properties considered as medium or weak. Their porosity reaches about 16% by volume, mostly about 9%. According to Darłak et al. (1998) the porosity of sandstones decreases with depth. The permeability mostly oscillates near zero, sometimes it reaches a few-some mD, only exceptionally it reaches 200 mD. The microporous structure of pore spaces (Darłak et al., 1998) and the presence of diagenetic illite shall be deemed the reasons for low permeability in sandstones.

Hydrocarbon Potential

In the southwestern and southern part of the Block 208 tender area, aeolian sandstones are present in the topmost part of the Rotliegend succession. They are prospective for the occurrence of natural gas accumulation (Kiersnowski et al., 2020). Within the aeolian sandstone facies, there are numerous gas fields located to the south, south-west and west of the tender area (e.g., Miłosław and Komorze fields), where the source rocks are most probably Culm siltstones, while the sealing is provided by Zechstein evaporites. Porosities of aeolian sandstones drilled in the Września IG-1 well and in the vicinity are medium or low, while permeabilities oscillate close to zero, locally reaching several mD. Therefore, it is possible that in part of the area there are tight sands and thus tight gas accumulations in conventional traps, like those in the Siekierki-Trzek area to the west (Buniak et al., 2009; Kiersnowski et al., 2010). The conventional occurrence of gas accumulation in the area would depend on its history of burial, generation, expulsion, and migration. The results of interpretation of available seismic data indicate the presence of several small structural uplifts – potential traps for natural gas – in the south-western part of the considered area (Szpetnar-Skierniewska et al. 2015). In addition, hypothetical occurrence of ultra-deep continuous BCGS-type closed gas accumulations (at depths on the order of 5000 m; Wojcicki et al., 2014) is suggested in the eastern part of the Block 208 area.

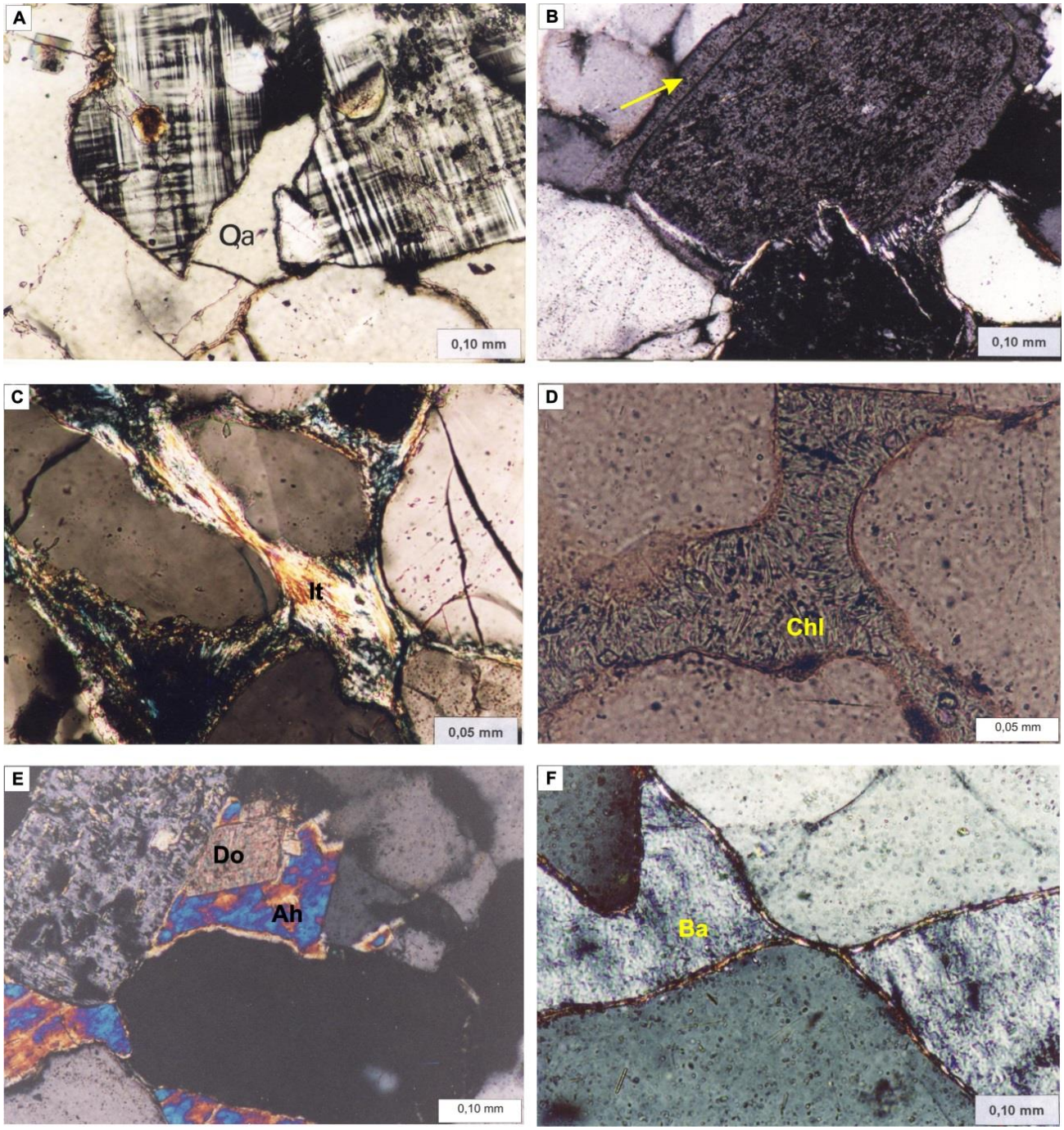

Fig. 2.13. Polarizing microscope images of rock fragments from the Września IG-1 well (from A. Maliszewska private archive). A. Microclinoid grain fragment (twin lattice) partially replaced by autigenic quartz (Qa); depth 4195.6 m; crossed nicols. B. K-feldspar grain fragment with regeneration rim (yellow arrow). The lower part of the grain shows interlocking contact with another feldspar; depth 4515.5 m; crossed nicols. C. Autigenic illite (It) in sandstone cement; depth 4651.0 m; crossed nicols. D. Coarse crystalline chlorite (Chl) in sandstone cement; depth 4116.3 m; no analyzer. E. Dolomite rhombohedra (Do) and anhydrite (Ah) in sandstone cement; depth 4558.5 m; crossed nicols. F. Fragment of barite-bonded arenite (Ba); also shows thin clay rims on surfaces of quartz grains; depth 4155.6 m; crossed nicols.

2.2.3. PERMIAN – ZECHSTEIN

Distribution and thickness

The Zechstein in the Block 208 tender area was drilled in the following wells:

- Września IG-1: 3125.0–4026.5 m (901.5 m thickness),
- Otoczna 1: 3260.0–3521.4 m (>261.4 m, not pierced).

The total thickness of the Zechstein succession in the Block 208 is ranging from 800 to 1300 m (Fig. 2.14; Tab. 2.1). The complete Zechstein succession was drilled only in the Września IG-1 well, where the thickness is 901.5 m. The second well – Otoczna-1 – drilled only the upper part of the Zechstein succession.

Lithology and stratigraphy

Four cyclothems – PZ1 to PZ4 – can be distinguished in the Zechstein succession in Poland (Wagner, 1994; Wagner and Peryt, 1997; Fig. 2.14) corresponding to the Werra, Strassfurt, Leine and Aller cyclothems of the German Basin (e.g. Richter-Bernburg, 1955). Most of the Zechstein sediments formed during transgressive-regressive carbonate-evaporite cycles (lower cyclothems PZl to PZ3 – Fig. 2.16), and only the uppermost part of the succession (cyclothems PZ4a to PZ4e – Fig. 2.17) during terrigenous-carbonate climate cycles associated with wet to dry climate fluctuations (Wagner and Peryt, 1997). During the carbonate deposition starting the first three cycles (PZ1–PZ3), three levels of carbonates were formed respectively: the Zechstein Limestone Ca1, Main Dolomite Ca2 and Platy Dolomite Ca3 (Figs 2.15–2.16). The carbonate sediments are separated by evaporates developed mainly in sulfate (anhydrite) and chloride (rock salt – halite) phases.

The lower part of the Zechstein in the Block 208 area can only be described based on the Września IG-1 well. The PZ1 cyclotheme thickness there is 254.0 m (Tab. 2.1). The Zechstein Limestone in this well is 2 m thick and according to description of the core included in the final well documentation (Sokołowski et al., 1977) it is developed mainly as gray calcareous dolomites and dolomitic limestones (upper part of the profile) with clay laminae and stylolites (lower part of the profile) containing numerous nodules of anhydrite. These rocks resemble the Ca1 sediments described in the nearby Grundy Górne IG-1 well (located outside the Block 208, about 10 km to the S of its southern boundary), where an approximately 2.5 m thick bipartite Ca1 succession was also found (Peryt, 1981). The rocks with a structure described as tubercular are perhaps, as in the Grundy Górne IG-1 well, oncolithic sediments. Sedimentation of the Zechstein Limestone in this area occurred in a sublittoral environment of the open sea (Peryt and Ważny, 1978; Peryt, 1981). The overlying evaporites – Lower and Upper Anhydrite interlayered with Oldest Halite reach a thickness of about 250 m (see Tab. 2.1).

The PZ2 cyclotheme in the Block 208 are approximately 400 m thick (Fig. 2.14) The Września IG-1 well reported 355 m (Tab. 2.1). The Main Dolomite Ca2 drilled in this well is only 3.5 m thick and is developed as dark gray dolomites densely horizontally laminated with clayey material (Sokolowski et al., 1977). These are sediments of the basin plain. Such formations occupy practically the whole discussed area. Only on its southern edges (in a very small area in the central part of the Block 208) slightly thicker (about 10 m) slope deposits may occur (Fig. 2.18). In the nearby Grundy-2 well, located less than 5 km south of the boundary of the discussed area, the Main Dolomite with thickness of 31 m was found (Gościk et al., 2010). Based on the interpretation of seismic surveys, it was indicated that small zones of increased Ca2 thickness ("reefs") may exist in the tender area (Szpetnar-Skierniewska et al., 2015). The lying above evaporitic succession comprises mainly the Basal Anhydrite and Older Halite, as well as the Older Potash 8 m thick.

The PZ3 cyclotheme has thicknesses in the range of 200–300 m (Fig. 2.14). The Września IG-1 well found 182.5 m and the Otoczna-1 – 164.4 m (Tab. 2.1; Wróbel and Szewc, 1977). The sedimentation of the PZ3 cyclotheme begins with the Gray Pelite with a thickness of 2 m. Higher, there are the Main Anhydrite (42.5 m in the Września IG-1 well)

and Younger Halite (138 m in the Września IG-1 well and 154 m in the Otoczna 1 well.

The PZ4 cyclotheme has thickness from less than 100 to more than 300 m (Fig. 2.14; in wells see Tab. 2.1). The lowest part of the succession is represented by Lower Red Pelite of thickness 13.5 m and higher there is the Lower Youngest Halite (70–80 m thick). The Top Terrigenous Series occur in both Września IG-1 and Otoczna 1 wells (25.0 and 12.5 m in thickness, respectively), completing the Zechstein succession at the top.

Hydrocarbon Potential

It is possible, considering the results of seismic interpretation, that small zones of increased Main Dolomite thickness ("reefs") occur in the Block 208 tender area, most likely in its southern and southwestern parts. In these zones, the Main Dolomite could play a role both of the source and reservoir rocks for possible conventional oil and gas accumulations (Szpetnar-Skierniewska et al. 2015). However, the 2D seismic surveys available in the area is not enough to identify such small structures and conduction of the 3D seismic surveys is required.

The thickness of the Main Dolomite in the Block 208 tender area is relatively low. On the other hand, this thickness is considerably higher in wells adjacent to the tender area from the south, situated in the Main Dolomite carbonate platform as the area prospective for occurrence of hydrocarbon deposits (the closest to the tender area is the Buk oil and gas field, situated about 70 km to the west).

Lithostratigraphy		Depth (thickness) [m]	
		Września IG-1	**Otoczna 1**
Cyclothem PZ4		**110.0**	**97.0**
Reval Formation [Pzt]	Top Terrigenous Series	3125.0–3150.0 (25.0)	3260.0–3272.5 (12.5)
Na4b2	Top Youngest Halite		3272.5–3357.0 (84.5)
T4b2	Upper Red Pelite – upper part		
Na4b1	Intrastratal Halite		
T4b1	Upper Red Pelite – lower part		
A4a2	Upper Pegmatite Anhydrite		
Na4a	Youngest Halite	3150.0–3221.0 (71.5)	
A4a1	Lower Pegmatite Anhydrite		
T4a	Lower Red Pelite	3221.0–3235.0 (13.5)	
Cyclothem PZ3		**182.5**	**>164.4**
A3r	Top Anhydrite		3357.0–3360.0 (3.0)
Na3	Younger Halite	3235.0–3373.0 (138.0)	3360.0–3514.0 (154.0)
A3	Main Anhydrite	3373.0–3415.5 (42.5)	3514.0–1643. (>7.4)
T3	Grey Pelite	3415.5–3417.5 (2)	
Cyclothem PZ2		**355.0**	
A2r	Screening Anhydrite	3417.5–3419.0 (1.5)	
Na2r	Screening Older Halite	3419.0–3420.5 (1.5)	
K2	Older Potash	3420.5–3428.5 (8.0)	
Na2	Older Halite	3428.5–3766.5 (338.0)	
A2	Basal Anhydrite	3766.5–3769.0 (2.5)	
Ca2	**Main Dolomite**	**3769.0–3772.5 (3.5)**	
Cyclothem PZ1		**254.0**	
A1g	Upper Anhydrite	3772.5–3811.0 (38.5)	
Na1	Oldest Halite	3811.0–3978.0 (167.0)	
A1d	Lower Anhydrite	3978.0–4022.5 (44.5)	
Ca1 + T1	Zechstein Limestone and Copper Shale	4022.5–4026.5 (4.0)	
Total thickness of Zechstein		**901.5**	

Tab. 2.1. Zechstein lithostratigraphy in the Block 208 tender area according to data from wells.

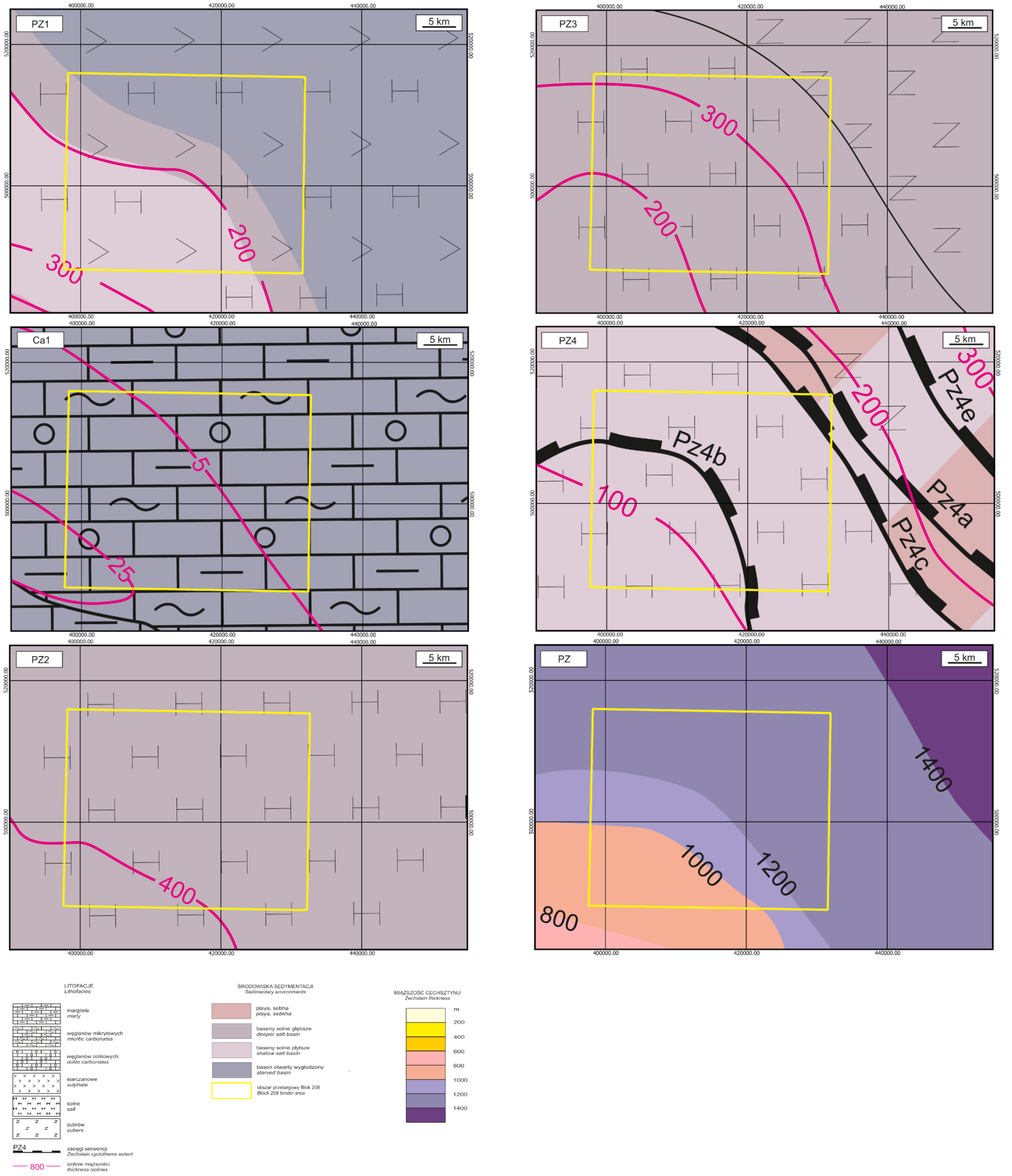

Fig. 2.14. Paleogeography and thickness of the Zechstein deposits in the Block 208 area (according to Wagner, 1998).

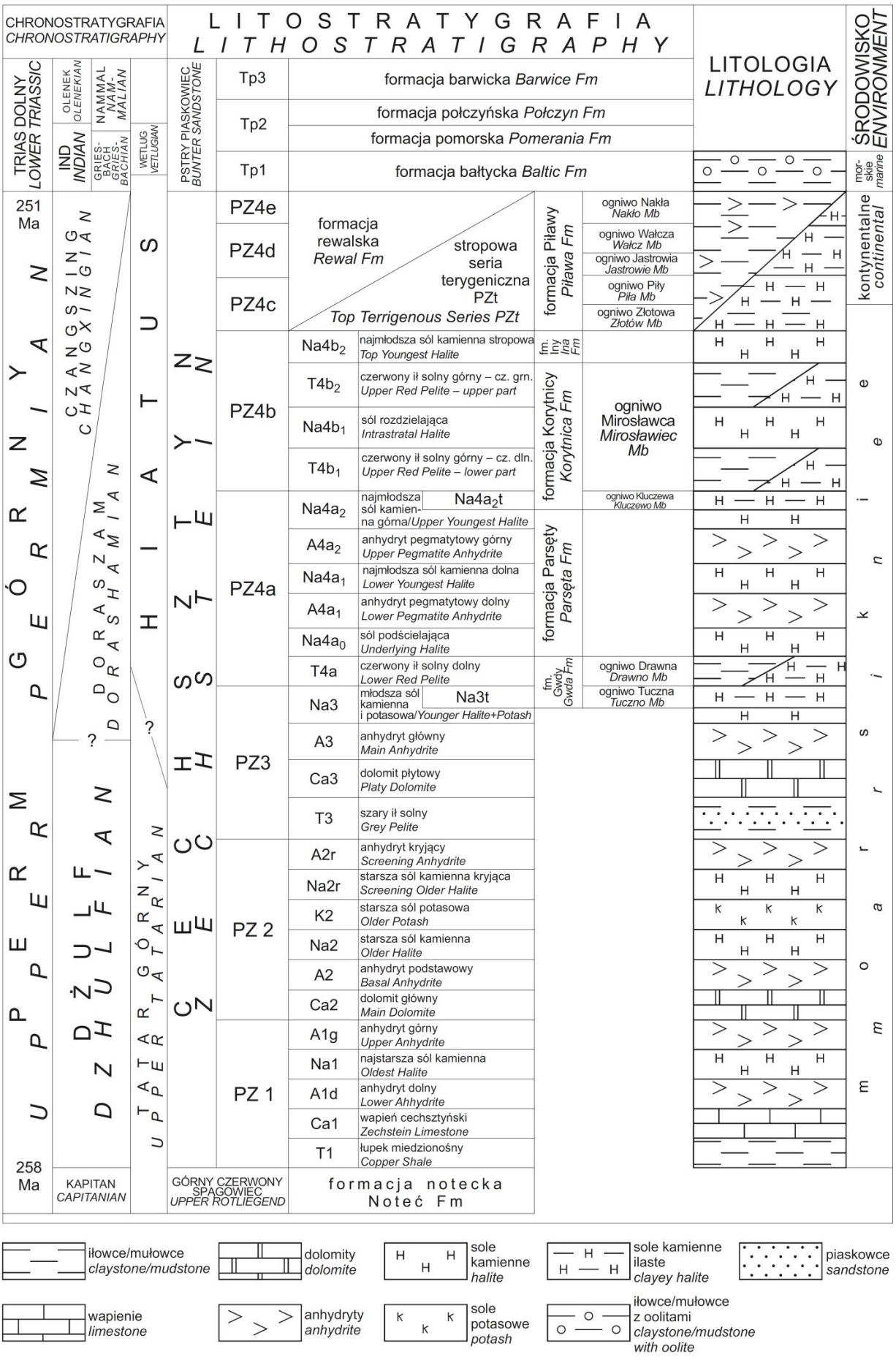

Fig. 2.15. Stratigraphy of the Zechstein in the Polish Zechstein Basin (Wagner and Peryt, 1997).

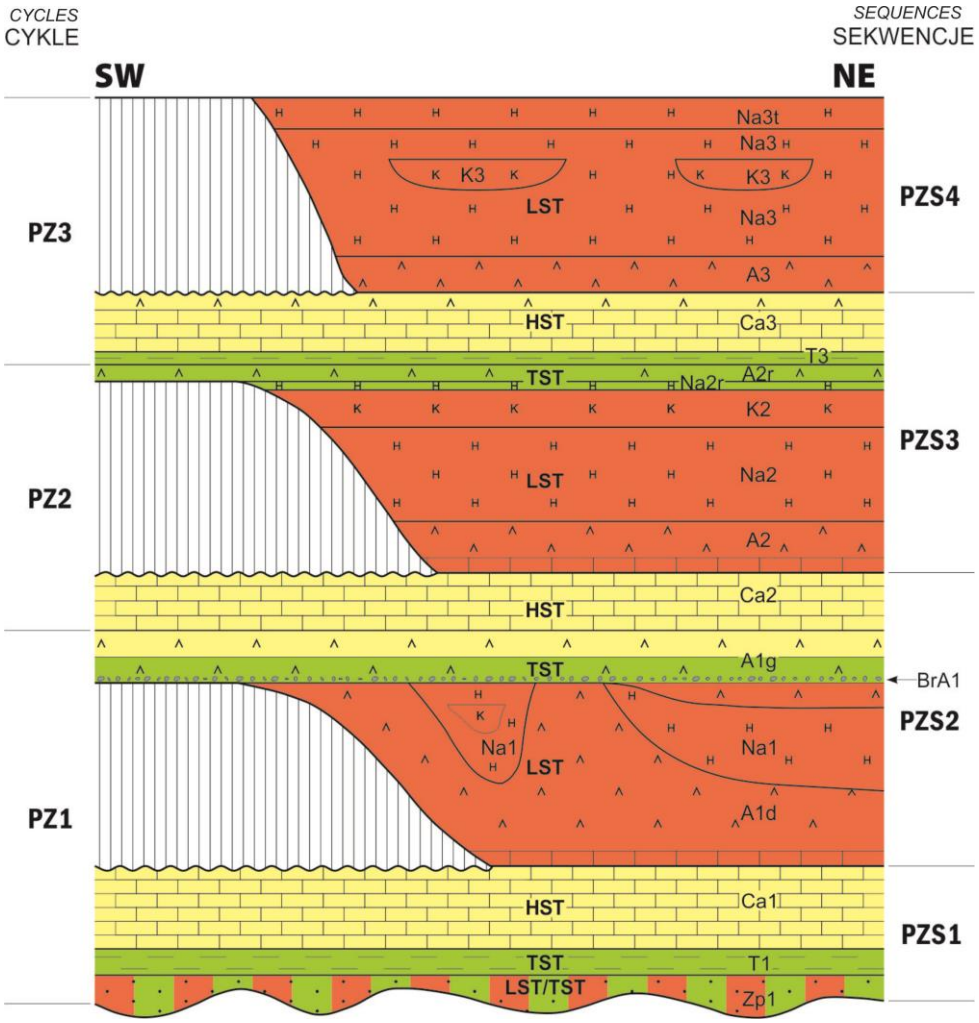

Fig. 2.16. Zechstein chronostratigraphy and depositional sequences – PZ1– PZ3 cyclothems (Wagner and Peryt, 1997).

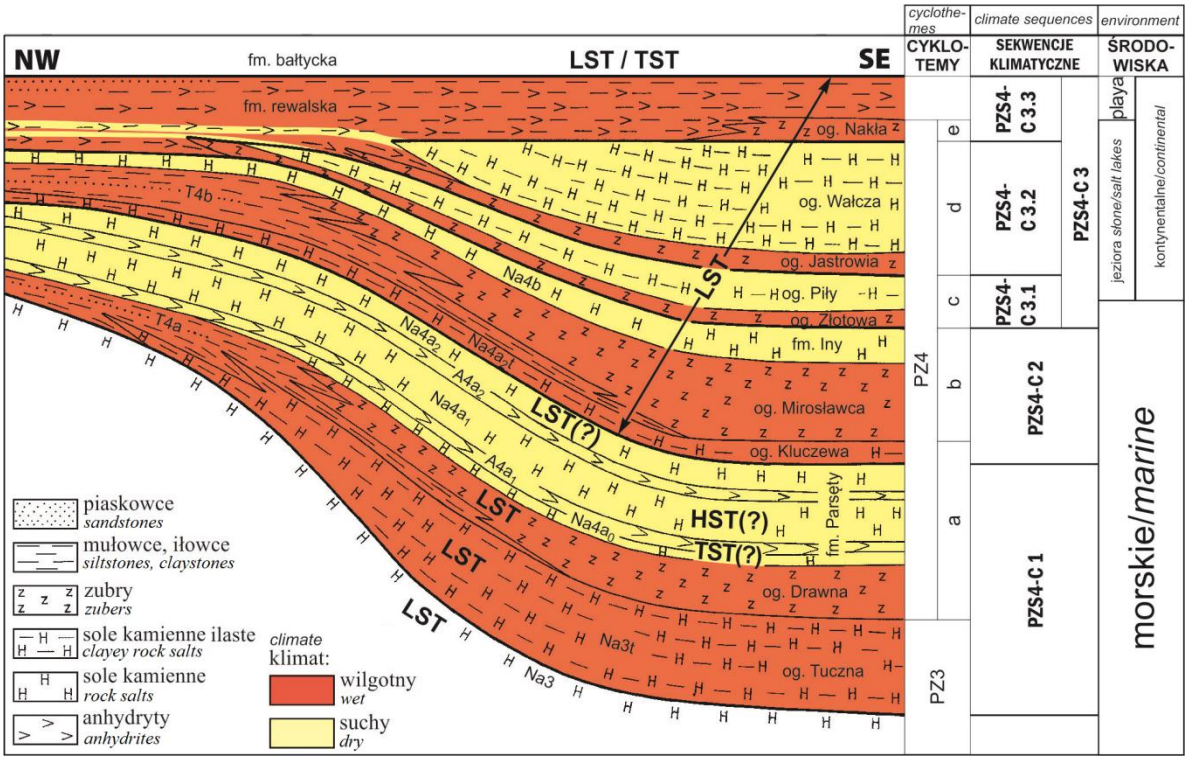

Fig. 2.17. Climatic depositional sequences of the Zechstein PZ4 cyclothem (Wagner and Peryt, 1997).

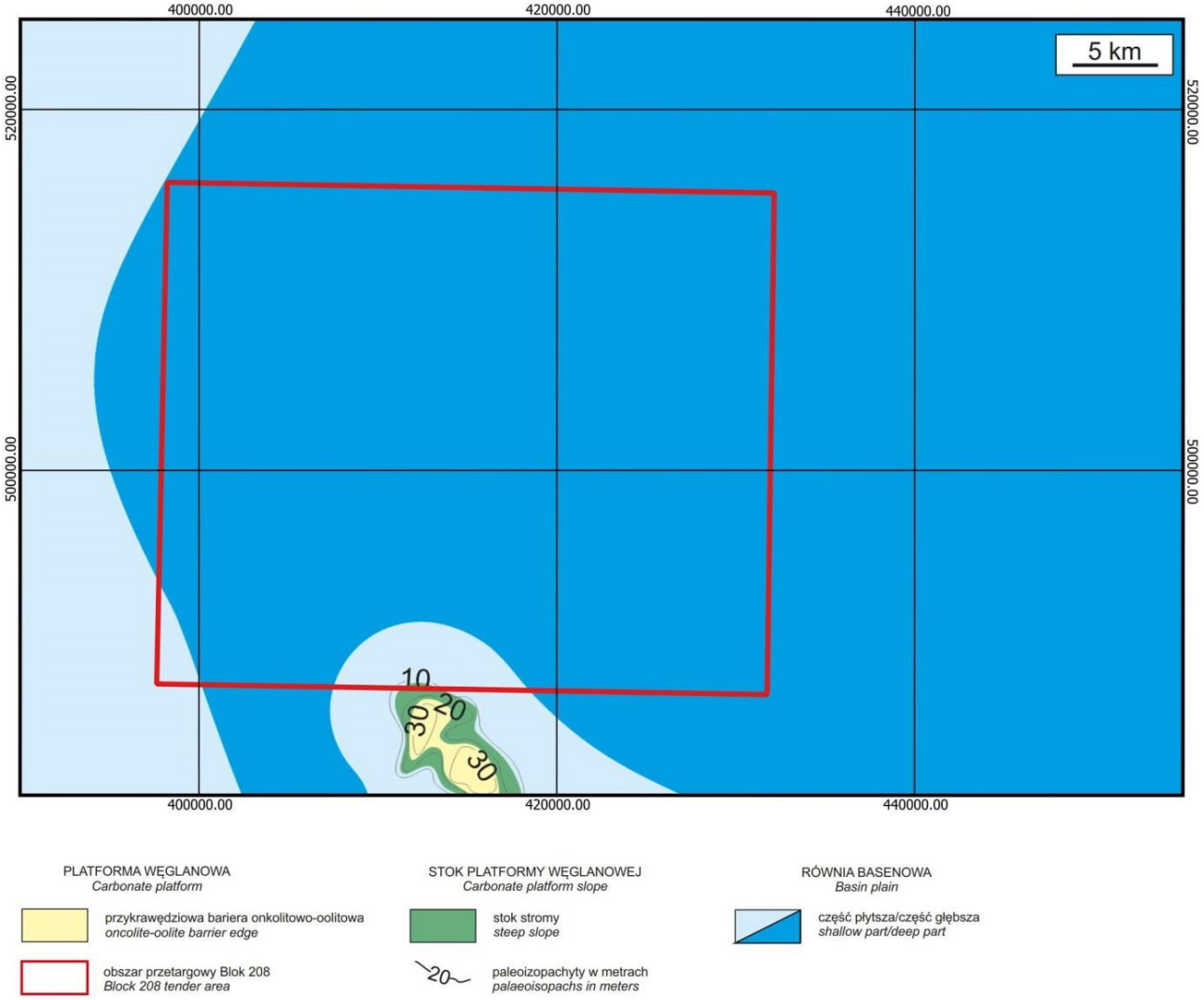

Fig. 2.18. Paleogeography of the Main Dolomite (Ca2) within and around the Block 208 tender area (Wagner, 2012).

2.2.4. TRIASSIC

Distribution and thickness

The Triassic succession was recognized in 2 wells within the tender area:

- Otoczna 1: 1387.0–3260.0 m,
- Września IG-1: 1339.0–3125.0 m.

The Triassic thickness is 1786.0–1873.0 m.

Lithology and stratigraphy

Three main lithostratigraphic units are defined and identified within the Triassic succession in the tender area. In stratigraphic order (from base to top) these are:

Bunter Sandstone (748.5–812.0 m thick):

- Otoczna 1: 2448.5–3260.0 m,
- Września IG-1: 2376.5–3125.0 m;

Muschelkalk (246.0–274.0 m thick):

- Otoczna 1: 2202.5–2448.5 m,
- Września IG-1: 2102.5–2376.5 m;

Keuper (763.5–815.5 m thick):

- Otoczna 1: 1387.0–2202.5 m,
- Września IG-1: 1339.0–2102.5 m.

In the **Lower Bunter Sandstone** there are claystones and shales of different colors (most commonly chocolate or red brown) with anhydrite and mudstone crumbs and intercalations of sandstones and limestones. The total thickness of the Lower Bunter Sandstone is 330–340 m. Above, the Middle Bunter Sandstone is developed as diversely colored clays, sandstones and limestones of the total thick-

ness of 320–350 m. In the uppermost part of the succession, the **Röt** was identified, comprising mudstones and claystones with intercalations of limestones, dolomites, anhydrites, and sandstones. The total thickness of the Röt succession is 100–120 m.

The **Muschelkalk** (Middle Triassic) comprises, in the lower part, a succession of limestones and marly limestones, marls, and subordinately gray claystones and steel-gray shales. The total thickness is about 160 m. In the middle part the dolomites, fine crystalline gray limestones, marly limestones, gray claystone marls, steel-gray shales, and anhydrites predominates. Its total thickness is 50–60 m. The upper part of the Muschelkalk includes limestones, claystones with limestones and dark claystones 40–50 m thick.

The **Keuper** (Upper Triassic) includes the **Sulechów Beds** in the lower part, developed as muddy sandstones, mudstones, siltstones and claystones, most often brownish-cherry or brownish-violet in color, and in general mudstones and claystones (identified only in the Września IG-1 well). The thickness of the beds is about 16.5 m. Higher, the **Lower Gypsum Beds** (Lower Carnian) occurs, built of dark gray or chocolate claystones with intercalations of anhydrites and clayey dolomites and gypsum nodules (thickness of 30.0–150.0 m). Above, the **Reed Sandstone** (Stuttgart Formation) appears, developed as claystones, fine-grained sandstones with mudstone intercalations, and silty claystones, reaching the thickness of 39–76 m. The **Upper Gypsum Beds** (Upper Carnian), comprise intercalations of claystones and anhydrites, and reach the thickness of 140–160 m. In the uppermost part of the Triassic succession, the **Zbąszynek and Jarkowo Beds** (Norian, 280 m thick) were identified. Tey are composed of multicolor (mostly brownish-red) claystones with interbedding of mudstones and silty claystones. The succession is completed by the **Wielichowskie Beds**, classified as the Rhaetian, built of mostly dark grey claystones with interbedding of mudstones and sandstones and spherulitic siderites. The thickness of these beds is 45–47 m.

2.2.5. JURASSIC

Distribution and thickness

The Jurassic in the Block 208 area was recognized in 3 wells:

- Marzenin IG-1: 291.2–500.0 m,
- Otoczna 1: 267.0–1387.0 m,
- Września IG-1: 210.0–1339.0 m.

The thickness of the Jurassic in the Września IG-1 and Otoczna 1 wells is from 1120.0 to 1129.0 m, respectively, whereas in the Marzenin IG-1 only the Upper Jurassic with thickness of 207.5 m was drilled. The Jurassic occurs throughout the tender area and its surroundings (Dayczak-Calikowska and Moryc, 1988).

Lithology and stratigraphy

The Jurassic succession in the Block 208 tender area is subdivided into:

Lower Jurassic (335.5–359.0 m thick):

- Otoczna 1: 1051.5–1387.0 m,
- Września IG-1: 980.0–1339.0 m;

Middle Jurassic (105.0–112.5 m):

- Otoczna 1: 939.0–1051.5 m,
- Września IG-1: 875.0–980.0 m;

Upper Jurassic (665.0–672.0 m):

- Marzenin IG-1: 291.2–500.0 m (not pierced)
- Otoczna 1: 267.0–939.0 m,
- Września IG-1: 210.0–875.0 m.

The Lower Jurassic (Liassic) in the SW part of the tender area, where all three wells were drilled, is almost completely developed. However, data from the Trzemżal 1 and 2 wells, located in the NE vicinity, indicate a significant reduction in the thickness of the Lower Jurassic, in the extreme case to about 40 m. The Lower Jurassic is probably represented here only by the Pliensbachian sandstones. In the SW part, a succession from the Hettangian to the Upper Toarcian has been found, which corresponds to the Zagaje, Ostrowiec, Łobez, Komorowo, Ciechocinek and

Borucice formations (Pieńkowski, 2004). **The Ostrowiec** and **Zagaje Formations** comprise fine-grained sandstones (medium-grained in the upper part), sometimes clayey, mostly light gray, intercalated with dark gray mudstones. In the Września IG-1 well, the recorded thickness of the Zagaje Formation was 134 m, whereas in the Otoczna 1 – only 101 m. The **Łobez Formation** is developed as grey sandy claystones, light grey fine-grained sandstones and claystones. In the Września IG-1 well its total thickness is 35 m, while in the Otoczna 1 it reaches 34 m. **The Komorowo Formation** in the Września IG-1 well reaches the thickness of 76 m and is developed as fine- and medium-grained sandstones, light gray, intercalated with mudstones and, in the upper part, sandy claystones. In the Otoczna 1 well, the thickness of this formation reaches 90 m and it is dominated by sandstones. The **Ciechocinek Formation** comprises gray greenish claystones with interbedding of sandstones and siltstones, and light gray fine-grained sandstones. In the Września IG-1 well the thickness of this formation is 77 m, whereas in the Otoczna 1 well – 74.5 m. The Lower Jurassic succession is completed by the **Borucice Formation** with the thickness of 36–37 m, developed as fine-grained sandstones, locally muddy, light gray, weakly compacted.

The Middle Jurassic (Doggerian) includes, in the Block 208 case, the Upper Bajocian to the Callovian succession. The **Upper Bajocian** is developed as dark grey claystones and muddy claystones with biodetritus (Września IG-1) or as mudstones and claystones (Otoczna 1). The **Bathonian** is composed of dark grey calcareous mudstones and muddy claystones containing remains of fossils, and higher – mudstones and fine-grained sandstones with interbedding of sandy marls. The total thickness is 87.5 m. The Middle Jurassic succession is completed by the **Callovian** sediments with the thickness of only 1.5 m. In the Września IG-1 well they are developed as grey, greyish green and light grey muddy marls.

The Upper Jurassic (Malmian) is generally completely developed in the tender area, comprising succession ranging from the Oxfordian to the Tithonian. The **Oxfordian**, with a total thickness of about 165 m, begins with clayey-marly sediments representing the Łyna Formation (Dembowska, 1979). Higher, there are cream-gray limestones, dark-gray mudstones, then nodular limestones, sponge limestones with marly and clayey intercalations, and compact, massive limestones with sponge remains. The **Lower Kimmeridgian** in the Września IG-1 well is composed of marly and clayey limestones, gray marly limestones, and marls, as well as limestones, in places with detritus of bivalvia shells. The total thickness is 334.5 m. In the Otoczna 1 well (thickness slightly lower, exact value not determined), dark gray and gray mudstones with admixture of limestone occur in the Lower Kimmeridgian. The **Upper Kimmeridgian** is developed as shale-marly series with marl and mudstone intercalations, marly mudstones and muddy limestones in the Września IG-1 well (total thickness 91 m) and gray mudstones in the Otoczna 1 well. They represent lower part of the Pałuki Formation. In the Marzenin IG-1 well only lummachelles in the bottom part and black claystones and green-grey marls in the upper part were drilled. The **Tithonian** in the Września IG-1 well comprises clayey-marly sediments, then marly shales and marly mudstones with skeletal remains, muddy marls with inserts of limestones (upper part of the Pałuki Formation) and limestones, in places oolitic (Kcynia Formation). In the Otoczna 1 well there are grey, sometimes lighter, very sandy mudstones (Pałuki Formation) and limestones (Kcynia Formation) of the total thickness over 44 m.

2.2.6. CRETACEOUS

Distribution and thickness

Within the tender area, the Cretaceous strata were identified in 115 wells, at depths of the order of tens, rarely a hundred of meters. Only 3 wells pierced the Cretaceous:

- Marzenin IG-1: 133.7–291.2 m,
- Otoczna 1: 105.0–267.0 m,
- Września IG-1: 82.0–210.0 m.

However, the Trzemżal 1 and Trzemżal 2 wells, located in the NE vicinity, the Cretaceous occurs at depths of 99.0–1303.5 m and 125.0–1476.0 m, respectively, while the Wilczna 1 well, located near the SE corner of the area, penetrates the Cretaceous at depths of 40.0–921.5 m. The Cretaceous occurs throughout the tender area, while the thickness of Cretaceous, especially the Upper Cretaceous increases generally to NE, (Jaskowiak-Schoeneichowa, 1977; Marek, 1977).

Lithology and stratigraphy

In the Block 208 tender area the Cretaceous is divided into the Lower and Upper series:
Lower Cretaceous (77.5–112.0 thick):

- Marzenin IG-1: 204.1–291.2 m,
- Otoczna 1: 155.0–267.0 m,
- Września IG-1: 132.5–210.0 m;

Upper Cretaceous (50.0–70.4 m thick):

- Marzenin IG-1: 133.7–204.1 m,
- Otoczna 1: 105.0–155.0 m,
- Września IG-1: 82.0–132.5 m.

In the Trzemżal 1 and Trzemżal 2 wells, the thickness of the Lower Cretaceous is 146.0–147.0 m, while the thickness of the Upper Cretaceous is 1057.5–1205.0 m. In the Wilczna 1 well, the Lower Cretaceous has thickness of 142.5 m and the Upper Cretaceous ha thickness of 739.0 m.

The Lower Cretaceous includes succession ranging from the Hauterivian, locally the Upper Valanginian, to the Upper Albian. The Lower Cretaceous begins with the **Wloclawek Formation** (about 10 m thick), the lower part of which is developed as sandy, fine- and coarse-grained sediments, with crumbs or intercalations of siltstones, rarely claystones, whereas the upper part, comprising the Gniewków and Żychlin Members (Lower and Upper Hauterivian) is a series of claystones and mudstones with fucoids passing upwards into fine- to coarse-grained sandstones with inserts of siderites. Above, the **Mogilno Formation** (Barremian – Middle Albian) occurs, whose lowest part is built mostly of fine- to coarse-grained sandstones, the middle part of dark or black claystones, while the highest part of fine- to coarse-grained sandstones with admixtures of gravels. The total thickness of the formation is 60–90 m. The Lower Cretaceous succession is completed by the Upper Albian of several meters thick, which includes a thin layer of grey-green quartz-glauconitic sandstones with phosphate concretions, passing upward into sandy marls and marls with bivalves and belemnites.

The Upper Cretaceous, which is not divided into lithostratigraphic units, comprises the Cenomanian and Turonian sediments. Near the eastern and north-eastern edges of the tender area, younger stages (Coniacian, Santonian and Campanian) also appear. In the Cenomanian (thickness usually of a dozen meters) the succession is composed of limestones and marly limestones. The Turonian, on the other hand, comprises marly limestones in the lower part, and marls and opokas in the upper part, similarly to the lowest Coniacian (if the latter is present; complexes of Turonian, or Turonian and the lowest Coniacian reach the thickness of several dozen to one hundred and several dozen meters). The Upper Coniacian, Santonian and Campanian are built of opokas, marls, and locally gaizes.

2.2.7. CENOZOIC

Distribution and thickness

The Cenozoic sediments have been recognized in 119 wells (deep and shallow) located within the tender area. The thickness of the Cenozoic sediments in the analyzed wells is of the order of tens to hundreds of meters, reaching a maximum of 194.1 m. It is represented by clastic Paleogene, Neogene and Quaternary sediments.

The Paleogene sediments occur in the whole tender area, except for its south-eastern part, and are represented by sands, silts, and clays (less frequently by mudstones and claystones), locally carbonaceous. These deposits are included to the Oligocene. In the north-eastern part of the area these deposits occur together with similarly developed Lower Miocene sediments.

The Neogene sediments, with the total thickness of several tens of meters, occur in the whole tender area and include sands, lignite, clays, silts and locally gravels (Middle Miocene), colored clays with intercalations of sandstones and silts of the Upper Miocene (in the north-eastern part of the area), and clays, silts, and sands of the Upper Miocene – Pliocene in the remaining part, including locally lignite at the bottom of the Upper Miocene.

The Quaternary sediments have varied thickness, from several to over a hundred meters and include mainly Pleistocene glacial deposits. The Holocene deposits (fluvial sands and silts, fluvisols, muds, peats and gyttjas and locally humus sands and lake silts and clays) most often have 2–3 m thickness.

Because Cenozoic deposits have no importance in terms of petroleum palys, they are not characterized in detail here. Instead, information on their hydrogeological significance can be found in Section 2.3.

2.3. HYDROGEOLOGY

The Block 208 tender area is located in two water regions: the Warta region and a small fragment of the Noteć region. Within the discussed area, there are two main groundwater reservoirs: the Neogene-Paleogene Inowrocław-Gniezno (MGB No. 143) and a fragment of the Quaternary Wielkopolska Fossil Valley (MGB No. 144) – Fig. 2.19.

Within the Block 208 tender area, three aquifers were recognized: Quaternary, Neogene-Paleogene and Cretaceous. The Quaternary and Neogene-Paleogene aquifers are recognized as useable, while the Cretaceous has a subordinate meaning. In the Quaternary aquifer, two water bearing horizons are distinguished: the subsurface water level and the middle, located deeper, between clay layers.

The subsurface water level occurs mainly in sands and gravels of river valleys and moraines. Its thickness is up to 15 m. Locally, it can connect with the level of Miocene sands or with the Quaternary inter-clay level to form the main usable aquifer.
The middle inter-clay level (of the Wielkopolska Fossil Valley) is formed by sandy river sediments of the Mazovian Interglacial with a thickness of up to 32 m and the water table is subartesian. The groundwater hazard degree of the main usable aquifer in the tender area is low and very low, which results from the presence of clays above the aquifer (Fig. 2.20). The largest water supplies exploiting the waters of this level are Żydowo-Cielimowo (water intake for Gniezno) and Witkowo.

The Neogene-Paleogene aquifer is formed mainly by the Miocene sands with depths reaching up to several dozen of meters. It occurs at depths from about 40 m to over 150 m. The water table is confined. Locally, it connects with the Oligocene sand layer to form an integrated water circulation system. Due to the very good isolation, the degree of threat to the usable water level is generally very low and in the south-eastern part of Block 208 – low (Fig. 2.20).

The largest water supplies exploiting this water level are the communal multi-well water supply system in Września and the municipal water supply for the town of Słupca.

The Cretaceous aquifer has been identified in the eastern part of Block 208, where it remains in hydraulic contact with the Quaternary inter-valley level forming the Quaternary-Cretaceous water bearing horizon and in the south-eastern part, where it contacts Miocene aquifers or forms a separate aquifer of less importance. In that case, water bearing zones are associated with the Upper Cretaceous weathered and cracked limestones and marls; and weathered sandstones. They occurs at a depth of about 50 to over 130 m b.g.l., and their thickness ranges from a few to over 70 m. The water table is generally confined, mostly subartesian or, less frequently, artesian.

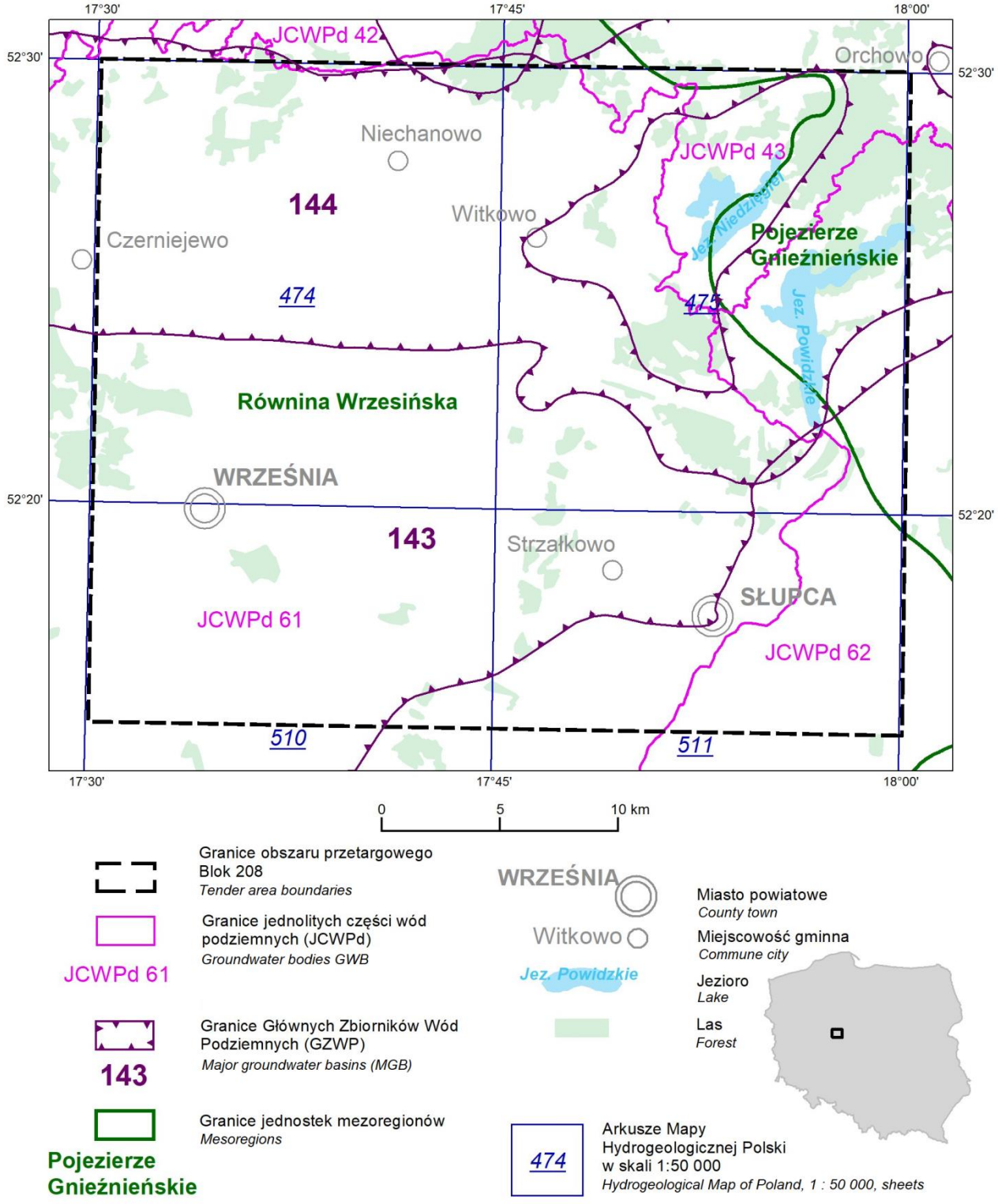

Fig. 2.19. Location of the Block 208 tender area in relation to physico-geographic units, Major Groundwater Basins (MGB) and Groundwater Bodies (GBW).

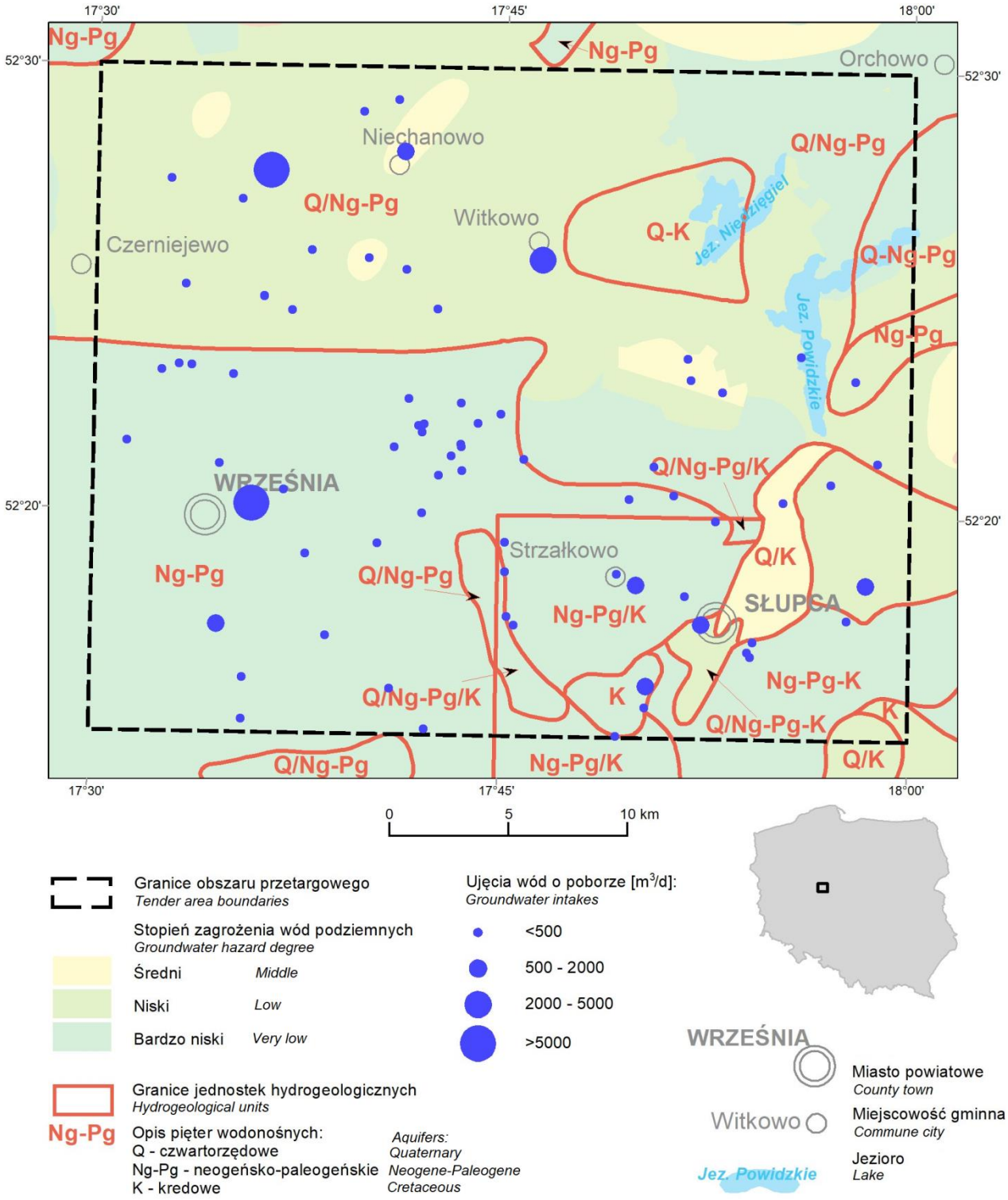

Fig. 2.20. Location of the Block 208 tender area in relation to hydrogeological units

3. PETROLEUM PLAY
3.1. GENERAL CHARACTERISTICS

The petroleum play is defined as the set of geological and petroleum processes leading to the formation of a hydrocarbon field. The petroleum play includes source rocks, reservoir rocks, and seal rocks. In addition, an essential element of the petroleum play in conventional accumulations is a trap, which, due to its structural, stratigraphic, lithological and tectonic features, creates a place of accumulation of hydrocarbons. The existence of a petroleum play and the formation of a hydrocarbon reservoir require a set of processes located in space, as well as in geological time, consisting of generation, expulsion, migration and accumulation of hydrocarbons and formation of a reservoir trap. The temporal interrelationships between the mentioned elements and processes of the petroleum play allow the formation of oil and gas fields.

The geology and tectonic of the Block 208 tender area, as well as geochemical parameters, and results of petrophysical studies in individual lithostratigraphic units, allow to distinguish two separate petroleum plays:

- unconventional petroleum play, represented by the Lower Permian Rotliegend tight sandstones and Carboniferous sandstones and shales,
- conventional petroleum play developed in the Zechstein Main Dolomite rocks.

The Carboniferous – Lower Permian play includes the Lower and Upper (?) Carboniferous siltstones and claystones (shales) as source rocks. These rocks could play a role, at the same time, of unconventional reservoir rocks for shale gas accumulation. However, a relatively low content of organic matter in the Lower and Upper (?) Carboniferous shales rather excludes this possibility (Szpetnar-Skierniewska et al. 2015; Podhalańska et al., 2018). A similar conclusion is suggested by current concepts of gas generation, expulsion, and migration for this region (Botor et al., 2013) indicating that most of the gaseous hydrocarbons generated there have already undergone expulsion and migration. Available data on the properties of the Carboniferous sandstones do not support the possibility that tight gas accumulations may exist in these rocks (Kozłowska and Kuberska, 2015), but it cannot be completely excluded. On the other hand, the primary reservoir unconventional rock, because we are talking about tight sandstones, would be the Upper Rotliegend rocks (Buniak et al., 2009; Kiersnowski et al., 2010). The aeolian sandstones, occurring in south-western and southern part of the Block 208 area, in the topmost part of the Rotliegend, are prospective for the tight gas occurrence in conventional traps, similarly to the Siekierki-Trzek area located to the west of the Block 208. The Carboniferous – Lower Permian petroleum play is sealed by the PZ1 Zechstein evaporites.

Additional target for gas exploration could be related to the sandstones of the so called deep Rotliegend, where a possible existence of BCGS (Basin Centered Gas System) is assumed. In here, the gas is sealed by so called water block connected with capillary system (Kiersnowski et al., 2010).

The increased thickness of the Main Dolomite (Szpetnar-Skierniewska et al. 2015) are postulated to occur, most likely, in the southern and southwestern parts of the area. The conventional petroleum play in the Main Dolomite is sealed from the base and top by the Zechstein PZ1 and PZ2 evaporites.

3.2. SOURCE ROCKS

Carboniferous fine-grained clastic rocks

For the numerous conventional gas fields in the Upper Rotliegend in the Polish Permian Basin, including those fields located to the S and SW of the tender area, the source rocks are believed to be Carboniferous in age (Botor et al., 2013; Karnkowski, 1993). These sediments, formed as siltstones and claystones, are characterized by a wide distribution and significant thickness in the southwestern and southern parts of the Variscan Externides, as well as by high thermal maturity, mostly corresponding to thermogenic gas generation (Fig. 3.1; Botor et al., 2013). Only in the extreme SW part of the Fore-Sudetic Monocline the maturity is lower, while in the extreme SE part overmature rocks are present (Poprawa et al., 2005), but both zones are far from the tender area.

The Carboniferous siltstones and claystones in the Września IG-1 well show a directional (laminated) texture, and their structure is pelitic, pelitic-aleuritic and pelitic-aleuritic-psamitic. In addition to detrital material, they contain micas (muscovite and biotite, chloritized in places), linearly arranged organic matter, and small intrusions of pyrite. The detrital material is interbedded in a clay-silica mass. Among the clay minerals, illite, interstratified minerals of the illite/smectite group, and chlorite are distinguished. (Sokołowski et al., 1977; Podhalańska et al., 2016; Krzemiński, 2005; Kozłowska and Kuberska, 2015; Sikorska-Jaworowska et al., 2016).

According to the report of Szpetnar-Skierniewska et al. (2015), the total organic carbon content TOC for the Carboniferous is 0.3–0.7% wt. These rocks are characterized by the presence of type III kerogen. Three complexes differing in average values of this parameter were identified in the Carboniferous of the Września IG-1 well (Tab. 3.1). It should be noted that these are average values of complexes comprising both silty and clayey and sandy sediments, while in the Carboniferous succession the sandy formations have slightly larger total thickness than silty and clayey ones, especially. Thus, the actual TOC values in Carboniferous siltstones and claystones may be significantly higher than the averaged values for individual complexes given in Tab. 3.1 (i.e., they may reach up to 1% wt. in complex C, and even exceed this value in complex B). Based on such assumptions, as well as considering available data on temperature distribution and thermal maturity of organic matter in the vitrinite reflectance scale (Wagner et al., 2008; Botor et al., 2013), 1-D modeling of hydrocarbon generation processes was performed for the Września IG-1 well (Szpetnar-Skierniewska et al., 2015). As a result of modeling, values of vitrinite reflectance R_o in the range of 1.6–3.1% were obtained for the Carboniferous rocks, thus corresponding to the dry gas window. Analogical modeling was performed in the project "Recognition of prospective zones for the occurrence of unconventional hydrocarbon deposits in Poland, stage II". (Podhalańska et al., 2018), where vitrinite reflectance R_o values were obtained in the range of 2.2–3.4% and thus also in the dry gas window.

Lithological complex	Depth interval [m]	TOC [% wt.]
A	4889–5033	0.30
B	5033–5124	0.96
C	5124–5904	0.70

Tab. 3.1. TOC – total organic carbon contents assumed for hydrocarbon generation modeling in the Września IG-1 well (Szpetnar-Skierniewska et al., 2015).

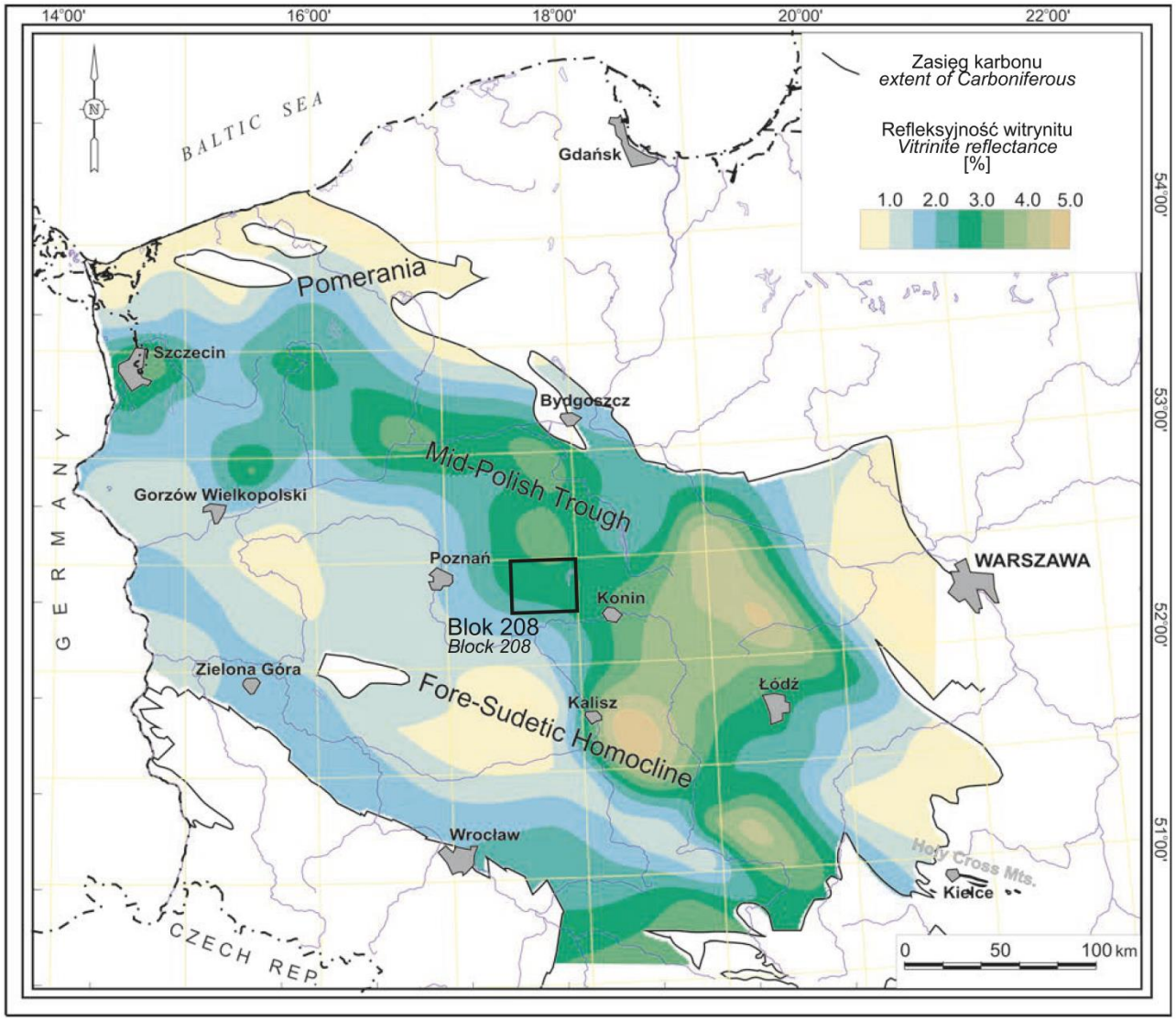

Fig. 3.1. Present-day maturity of organic matter in vitrinite reflectance scale in the Carboniferous of the Polish Permian Basin (Botor et al., 2013).

Main Dolomite
mudstones, bindstones, packstones, grainstones

Similarly to hydrocarbon fields documented in the western part of the Polish Permian Basin (the closest of which is the Buk oil and gas field located about 70 km from the tender area), the role of potential source rocks in the Main Dolomite in the tender area could be played by the shallow-water carbonate platform sediments, generally of the inner and outer barrier slopes, and to a lesser extent of the platform plain and barrier zone elevations (Wagner, 2012; Kotarba et al., 2020). Currently, the source rocks within the Main Dolomite are believed to be of microbial (algal) origin (Kotarba and Wagner, 2007), which can occur in two varieties: (1) compact – complexes associated with microbial-algal structures and mudstone layers, (2) dispersed – forming laminae that stabilize granular sediments (Słowakiewicz and Gąsiewicz, 2013; Słowakiewicz et al., 2016).

Within the Block 208 tender area, there are no the Main Dolomite carbonate platforms. Only in the extreme southern part of the area the basin plain is shallowing. However, just south of the area boundary, there is an oncolite-oolite edge barrier (Fig. 2.18) occurring as an isolated carbonate microplatform. Within this barrier, the Grundy-2 well was drilled, in which the Main Dolomite reaches a thickness of over 30 m (Gościk et al., 2010; Wagner, 2012). The Main Dolomite sediments are developed there in the lower part as clayey dolomites, anhydritized dolomites and anhydrites, while in the upper part – as porous carbonate granular sediments (grainstones, packstones). Microbial lamination is present throughout the entire succession, and in the lower part, in addition, microbial structures of the thrombolite type also occur (Chruścińska and Wiśniewska, 2018). There are no rocks found there that could be classified as source rocks (Gościk et al., 2010) – the TOC values obtained from the RockEval laboratory analyses on core samples are very low, rarely exceeding 0.1% wt., while thermal maturity analyses in the vitrinite reflectance scale R_o give values corresponding to dry gas window or overmature rocks.

In the Września IG-1 wells, the Main Dolomite sediments with thickness of 3.5 m were drilled and no source rock was found there. There are basin plain sediments developed as dark grey dolomites densely horizontally laminated with clayey material (Sokołowski et al., 1977).

In the southern and southwestern parts of the tender area, it is postulated (Szpetnar-Skierniewska et al., 2015) that small zones of increased thickness of the Main Dolomite, or "reefs" – isolated carbonate microplatforms, occur within small local uplifts. Such zones would, hypothetically, be surrounded by slope sediments including source rocks.

3.3. RESERVOIR ROCKS – CONVENTIONAL PLAY

Main Dolomite
grainstones and packstones?

Thickness:

Main Dolomite ~10–30 m, generally increasing toward the SW and decreasing toward the NE, probably greater in local uplifts/isolated carbonate microplatforms.

Top depth:

~3769.0 m in the Września IG-1 well.

Information on reservoir properties of the Main Dolomite in the tender area is basically not available. In the Września IG-1 well the Main Dolomite was not tested and analyzed. Only weak hydrocarbon shows were observed during drilling. The only information on reservoir properties characterizing the Main Dolomite came from the Grundy-2 well, located about 5 km to the south of the tender area, in which maximum and average (helium) porosities being relatively high in grainstones and packstones.

3.4. SEAL ROCKS

The conventional petroleum play developed in the Main Dolomite horizon is an independent system, hydrodynamically sealed from the top and base by the Zechstein evaporites of cyclotheme PZ2 (Stassfurt) and PZ1 (Werra). The latter horizon also acts as a seal for the unconventional Carboniferous – Lower Permian petroleum play.

The top sealing horizon for the Main Dolomite reaches the thickness of 400 m (Fig. 2.13). It is developed as anhydrites, halites, and potash salts. In the Września IG-1 well this complex reaches 351.5 m thickness (Tab. 2.1). Higher in the succession, the PZ3 and PZ4 cyclothems form an additional seal, which, together with PZ4 terrigenous series, reaches 292.5 m.

The seal for the Upper Rotliegend tight sandstones (belonging to the unconventional Carboniferous – Lower Permian petroleum play) is formed by a complex of Zechstein evaporates belonging to the PZ1 cyclothem. Their thickness reaches ~250 m in the Września IG-1 well (Tab. 2.1).

3.5. UNCONVENTIONAL PLAY

Upper Rotliegend
aeolian tight sandstones

Thickness:

~736 m in the Września IG-1 well.

Top depth:

~4026.5 m in the Września IG-1 well.

The unconventional petroleum play in the Block 208 tender area is represented by Lower Permian Rotliegend tight sandstones. They have significant thickness, probably hundreds of meters. Possibly, also Carboniferous tight sandstones of undetermined total thickness (the sandstones may be several meters thick packages separated by other clastic rocks, mostly of smaller fractions – Sokołowski et al., 1977) should be considered in this play. The source rocks here are Carboniferous siltstones and claystones (shales).

The unconventional play in the tender area can be recognized only in the Września IG-1 well. To the south-west and further south and west of the Block 208 area, several conventional natural gas deposits in the Rotliegend sandstones were recognized and documented (e.g., Kromolice S, Kromolice, Środa Wielkopolska, Winna Góra, Miłosław, Miłosław E, Lisewo, Komorze fields). Some of these deposits occur at depths of up to 4000 m below the sea level and are therefore characterized by low permeability, of the order of a few mD, but are classified as conven-

tional (subconventional?) deposits. On the other hand, west of the tender area, in the Siekierki-Trzek-Pławce zone, tight gas accumulations in conventional traps have been recognized, but not yet formally documented (Buniak et al., 2009; Kiersnowski et al., 2010).

Consequently, tight gas is postulated to occur in the Rotliegend aeolian sandstones (Kiersnowski et al., 2020), in conventional traps, most likely in the southern and southwestern parts of the tender area, where the depths of this deposits would be suitable for the occurrence of tight sandstones. According to Szpetnar-Skierniewska et al. (2015), several structural uplifts, framed by dislocation zones, have been recognized at the top of the Rotliegend, mostly 1–3 km in size, which could be traps for the accumulation of hydrocarbons, in our case (hypothetically) – tight gas.

In general, the basic criteria for the occurrence of tight gas (Wójcicki et al., 2014) concern reservoir properties, i.e., permeability below 0.1 mD and total porosity on the order of a few percent (not less than 3%, preferably more than 5%). While the porosity values of the Rotliegend sandstones in the vicinity of the tender area and in the Września IG-1 well (Darłak et al., 1998; Sokołowski et al., 1977) generally meet the relevant criteria (porosity sometimes exceeding 10%), we do not have a precise understanding of the permeability distribution in the Rotliegend sediments in the tender area. Available information from the Września IG-1 well suggest that permeabilities of sandstones usually oscillate close to zero, more rarely reaching several to dozen mD. It should be considered that the description of sandstones as impermeable rocks (or with permeability close to zero) meant that their permeability values were below the measurement accuracy in 1977. In contrast, the permeabilities of typical tight sandstones can be on the order of hundreds of nD (Wójcicki et al., 2014), or thousands of times less than the measurement accuracy in 70s.

The Carboniferous rocks are characterized by lower porosities, but some sandstone packages meet the criteria (i.e. they reach total porosities of 3–5%), while permeabilities oscillate mostly near zero, rarely reaching several mD, only in one case 10 mD. The question of whether tight sandstones are present there remains unsolved. However, the occurrence of Carboniferous source rocks (Carboniferous siltstones and claystones) in the area under consideration and its vicinity should not raise any doubts – this is discussed in the subsection on source rocks.

Considering the petrophysical properties of the Carboniferous siltstones and claystones in the Września IG-1 well, their total porosity generally ranges from 0.36 to 2.18%, whereas their effective porosity – from 0.14 to 1.52%, which is relatively low. These rocks are either impermeable or have low permeability of up to 0.17 mD. It should be mentioned here (again) that the statement that most of the samples of siltstones and claystones are impermeable meant that the values of their permeability were below the measurement accuracy of the equipment used at that time. However, for one sample the permeability value was determined as low (0.17 mD).

An excellent seal of the Carboniferous – Lower Permian unconventional petroleum play, is provided by the Zechstein PZ1 cyclotheme evaporates (~250 m thick in the Września IG-1 well).

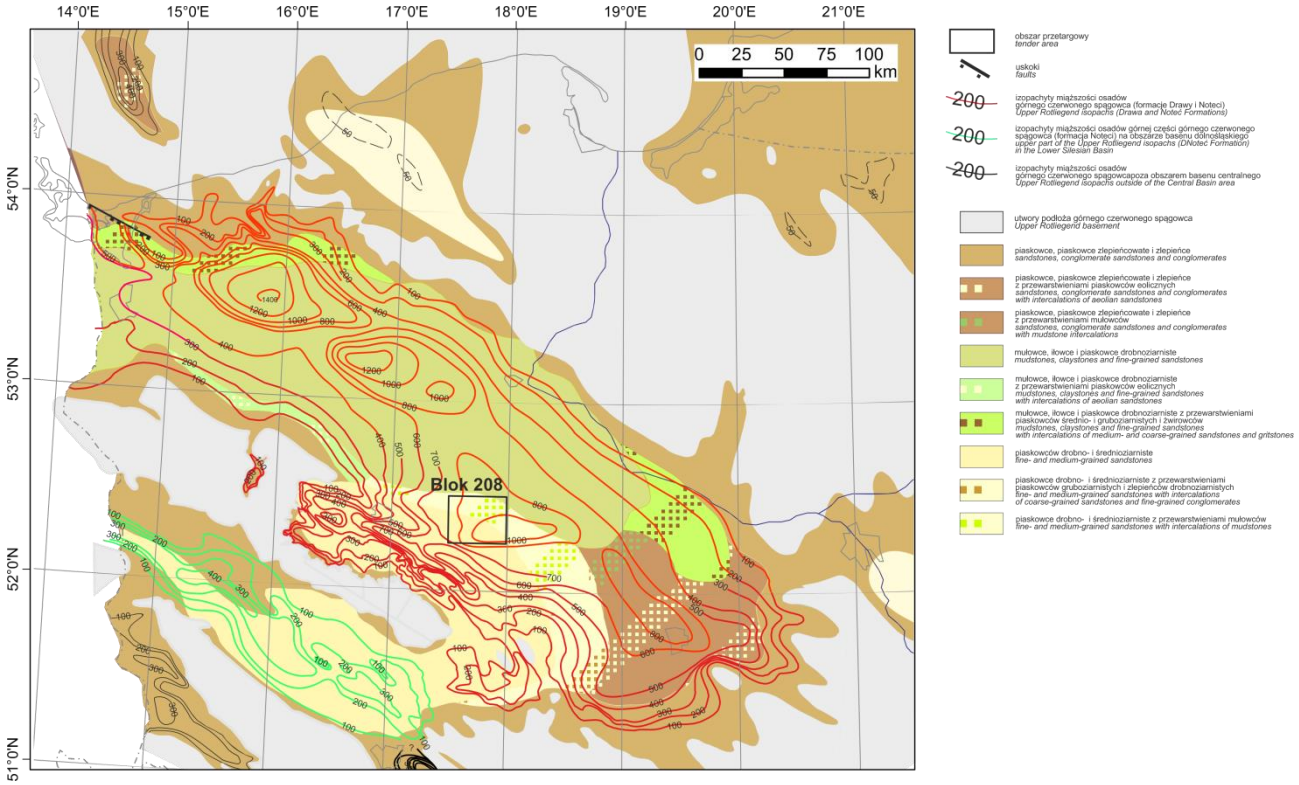

Fig. 3.2. The Upper Rotliegend thickness and facies in Poland (Kiersnowski, in: Wagner et al., 2008).

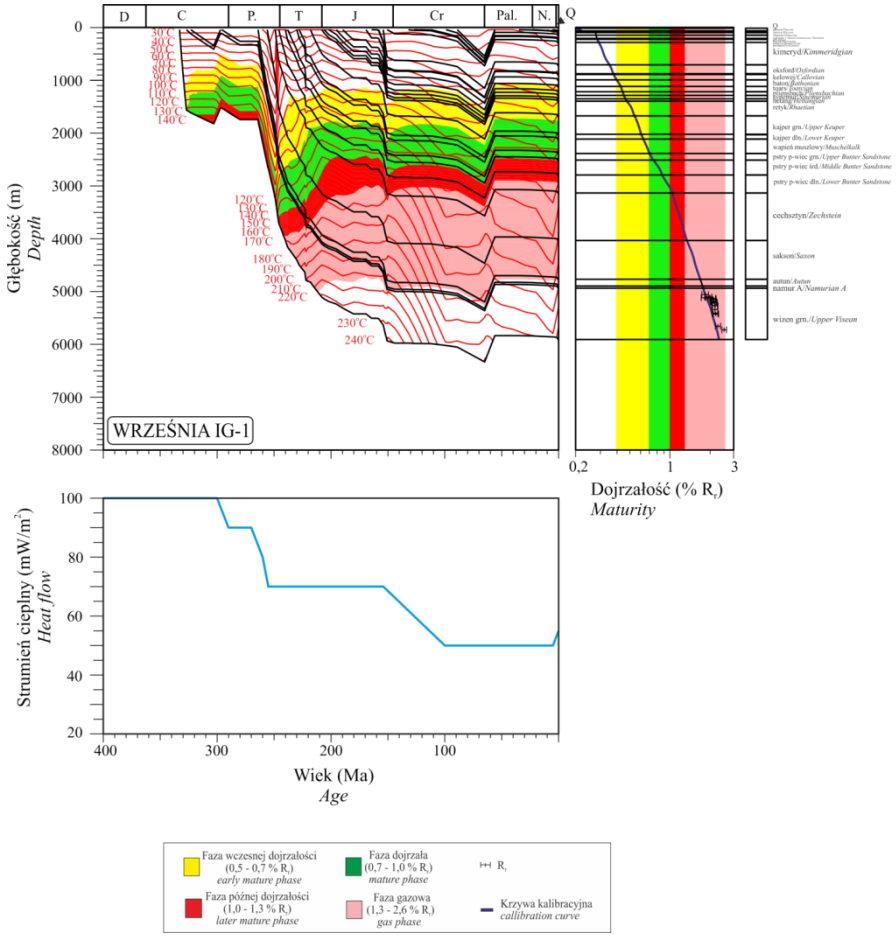

Fig. 3.3. Development of thermal maturity of the Carboniferous source rocks in the Września IG-1 well (after Wagner et al., 2008).

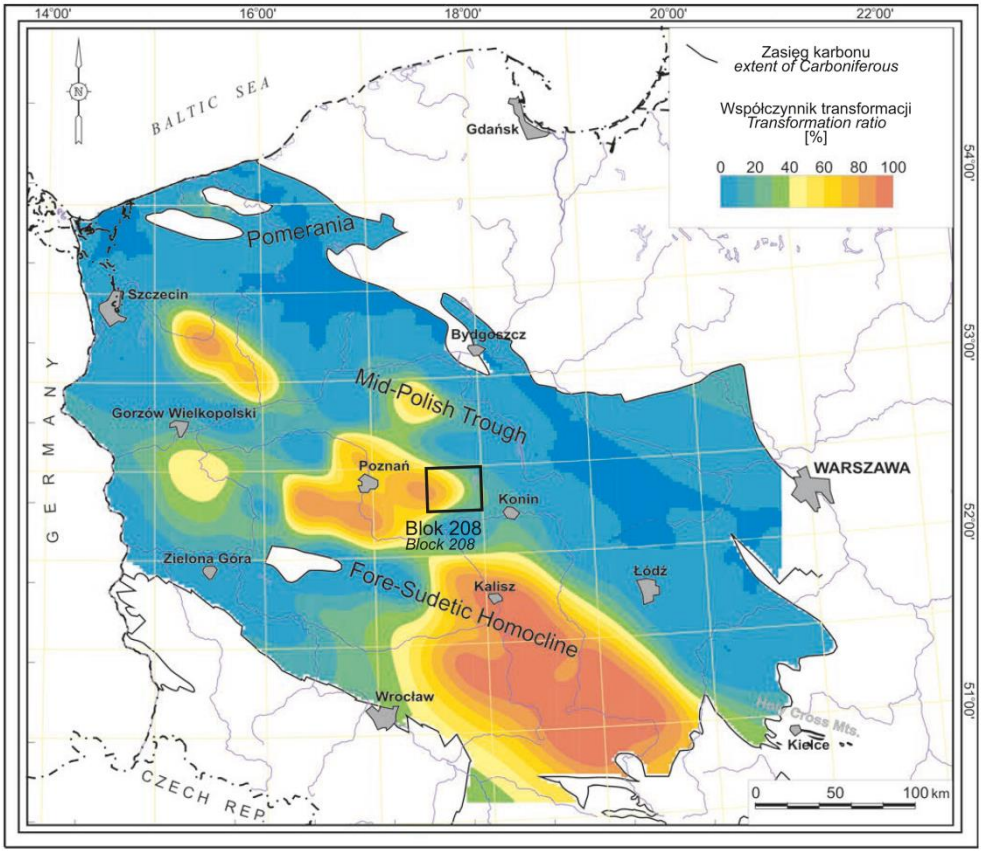

Fig. 3.4. Kerogen transformation ratio of the Carboniferous source rocks in the Polish basin calculated for the end of the Carboniferous (Botor et al., 2013).

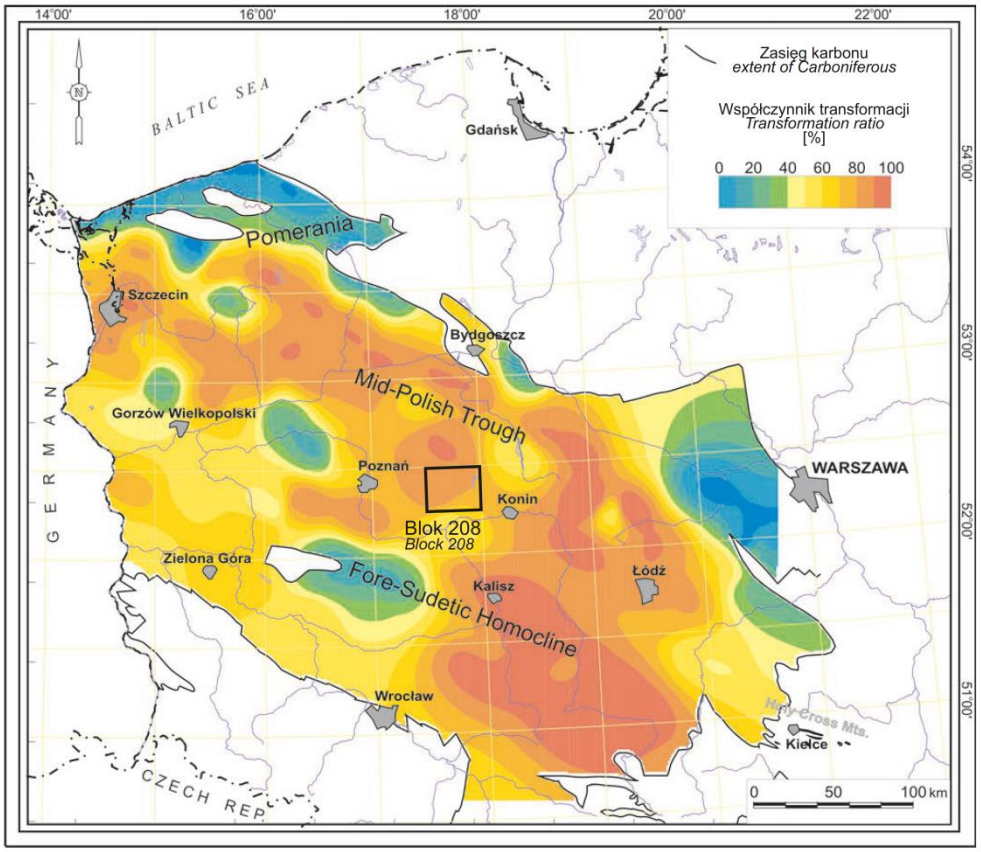

Fig. 3.5. Kerogen transformation ratio of the Carboniferous source rocks in the Polish basin calculated for the end of the Triassic (Botor et al., 2013).

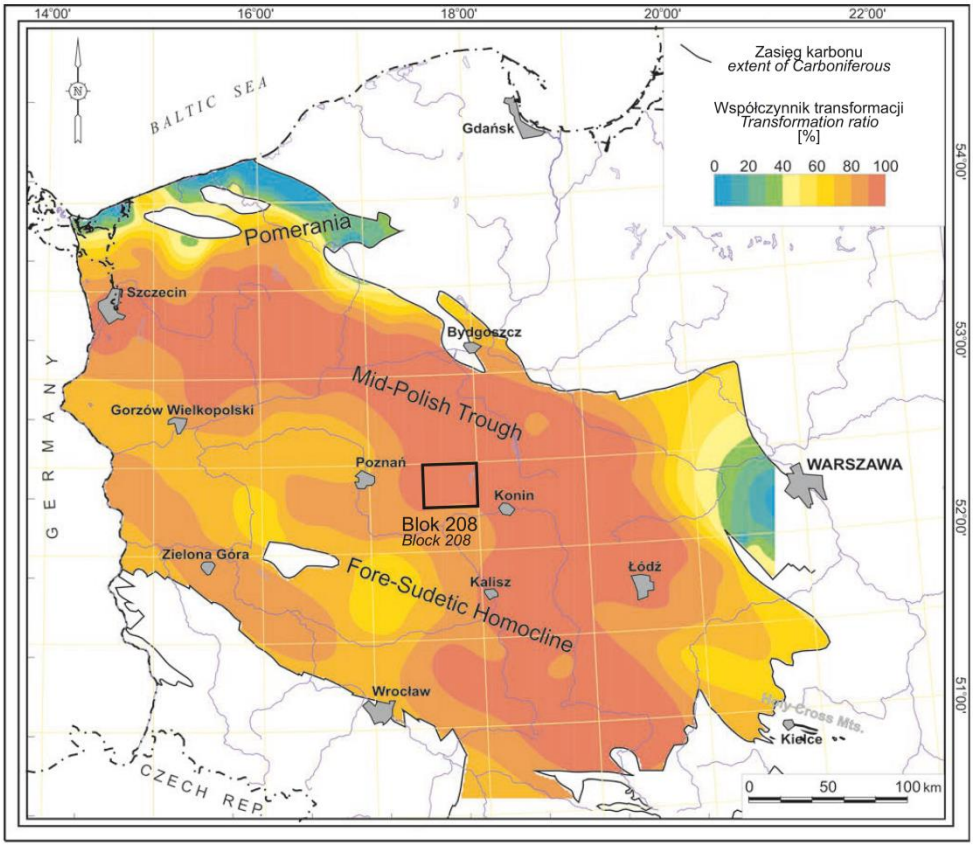

Fig. 3.6. Kerogen transformation ratio of the Carboniferous source rocks in the Polish basin calculated for the end of the Cretaceous (Botor et al., 2013).

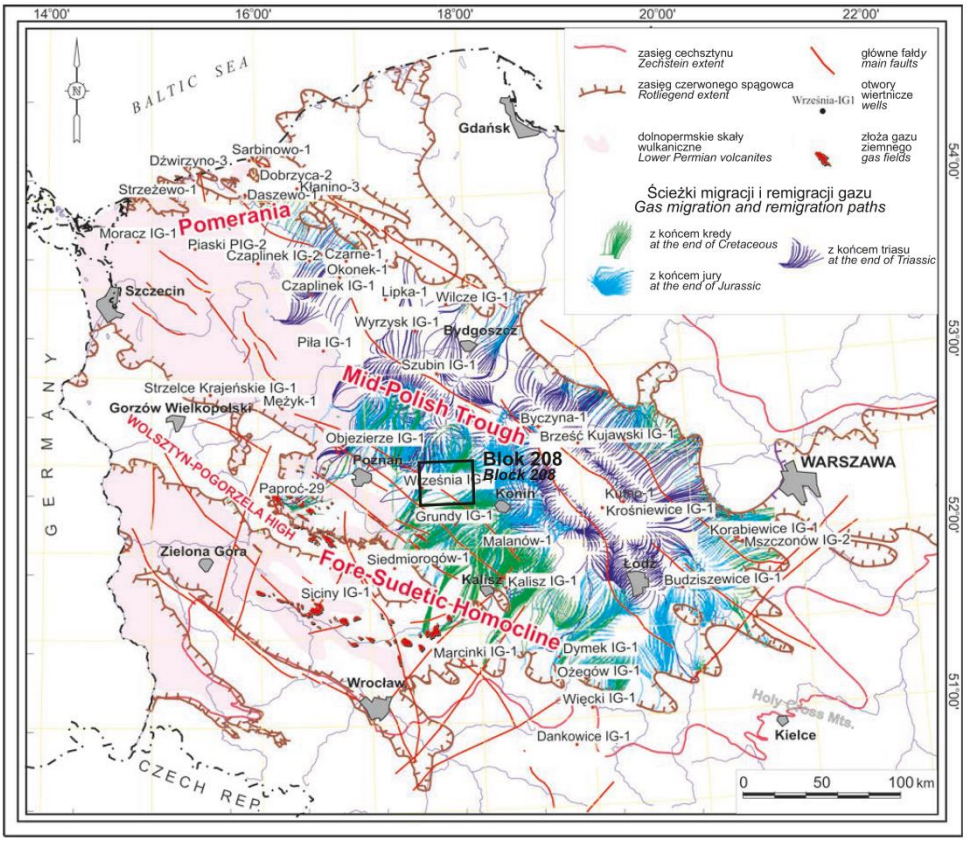

Fig. 3.7. Gas migration paths at the top of the Upper Rotliegend reservoir rocks in the Polish basin (Botor et al., 2013; Maćkowski et al., 2008).

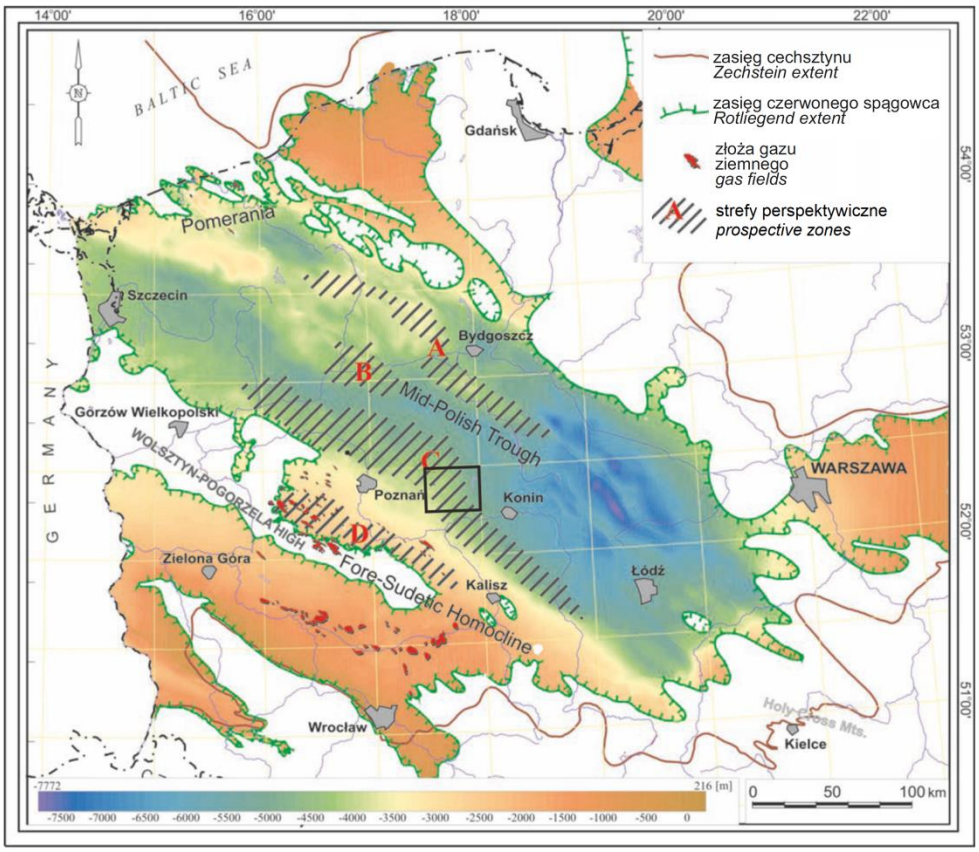

Fig. 3.8. Prospective zones for gas accumulations in the topmost part of the Rotliegend in Poland (Burzewski et al., 2009; Górecki et al., 2011; Botor et al., 2013).

3.6. GENERATION, MIGRATION, ACCUMULATION AND HYDROCARBON TRAPS

Carboniferous – Lower Permian petroleum play

Source rocks: Lower and Upper Carboniferous siltstones and claystones (shales).
Reservoir rocks: Carboniferous sandstones (tight), Upper Rotliegend aeolian sandstones (tight) and possible sub-conventional reservoirs.
Seal rocks: PZ1 evaporites.
Overburden rocks: (about 4000–4500 m thick): Zechstein PZ2, PZ3 and PZ4 cyclothems and the Mesozoic-Cenozoic succession.
Shape and size of traps: structural and tectonic. According to Szpetnar-Skierniewska et al. (2015), numerous dislocation zones are observed, most often with NW-SE direction (i.e., perpendicular to the direction of the regional dipping of the Rotliegend horizon), less often close to latitudinal or meridional, framing or crossing local structural uplifts of the size 1–3 km. The map was developed based on the interpretation of the 2D seismic survey completed in 2011 and reprocessed archival profiles.
Age and mechanism of formation of traps: The paleorelief of the Early Permian deposits, as well as the terminating phases of the Variscan Orogeny formed the primary traps. It can be mentioned here that between the Września IG-1 well and the Pławce 1 well, a N-S-direction synsedimentary fault was probably active during the sedimentation of the Rotliegend and Weissliegend deposits. As a result, the Września limb was 130–180 m higher in the Permian than it is today (Szpetnar-Skierniewska et al., 2015). However, the formation of the traps, as well as the dominant directions of dislocations framing them, should be linked to successive phases of the Alpine Orogeny. These processes may have initiated during the Old Kimmeridgian tectonic deformations with the strike-slip tectonics of sub-Permian basement, through the Young Kimmeridgian and Laramide transformation (Maćkowski and Reicher, 2008). The final formation of the geometry of the structures and their tectonic closures took place in the later stages of the Alpine tectonic evolution, during the Young Kimmeridgian and Laramide phases, and because of this structural reconstruction, some of the reservoirs may have been dismantled and the released hydrocarbons may have migrated and filled traps located in a higher position or simply dispersed. It is also possible that during this youngest, compressional stage of tectonic deformation, an unfavorable leveling of trap amplitudes at the top of the Rotliegend may have occurred (Maćkowski and Reicher, 2008).
Age and mechanism of hydrocarbon generation, expulsion, migration, and accumulation: Hydrocarbon generation in the Block 208 started at the end of the Carboniferous (Wagner et al., 2008; Botor et al, 2013; Karcz, in: Podhalańska et al., 2018; Szpetnar-Skierniewska et al., 2015), when the deepest parts of the Carboniferous succession entered the oil window. The rate of the subsidence and burial accelerated markedly in the Permian – the late Paleozoic stage of basin development in this region contributed to the accumulation of a 1200–2800 m sedimentary cover – and became rapid with the onset of the Triassic. With the beginning of the Middle Triassic, the rate of subsidence slowed, but continued until the end of the Middle Jurassic. The shallowest parts of the Carboniferous entered the oil window in the Middle Triassic. In contrast, the condensate (wet gas) window was reached by the deepest parts of the Carboniferous in the Late Permian, while the shallowest in the Late Triassic. Dry gas generation began during the Triassic – with the beginning of the Triassic in the deepest parts of the Carboniferous, and in the shallowest parts with the end of the Triassic. The Late Jurassic was marked by further tectonic movements, causing further rapid burial of Carboniferous strata (Wagner et al., 2008; Botor et al., 2013; Karcz, in: Podhalańska et al., 2018; Szpetnar-Skierniewska et al., 2015; Fig. 3.3).

Expulsion of hydrocarbons began, according to Botor et al. (2013), at the end of the Carboniferous and continued until the end of the Late Jurassic and the beginning of the Early Cretaceous, interrupted by the Kimmeridgian orogenic movements. During the late Carboniferous, the degree of kerogen

transformation in the Carboniferous strata within the tender area ranged from about 20% in the NE and SE margins of the area to about 80% in the western part of the area (Fig. 3.4), where, moreover, according to Burzewski et al. (2009), the generation potential of Carboniferous rocks was relatively high. In contrast, at the end of the Triassic, the degree ranged from 60% near the southern edge of the area to more than 90% in the northern and northwestern parts (Fig. 3.5). On the other hand, with the end of the Cretaceous, the kerogen transformation degree in Carboniferous formations within the tender area was over 90% (Fig. 3.6).

Gas migration processes may have started most likely at the end of the Triassic from the uppermost parts of the Carboniferous, due to the low permeability of the Carboniferous complexes. If, on the other hand, there were open fault zones in the Carboniferous reaching the deepest parts of this complex, then gas migration could have occurred even at the end of the Permian (Szpetnar-Skierniewska et al., 2015). In general, however, it can be assumed that migration lasted from the end of the Triassic to the end of the Cretaceous (Botor et al., 2013; Fig. 3.7). The natural gas accumulations, that were a product of this migration, may have persisted in much of the Block 208 tender area, except in its northeastern and extreme eastern parts (Fig. 3.8).

A summary of the characteristics of the Carboniferous – Lower Permian petroleum system is shown in Fig. 3.9.

Main Dolomite petroleum play

Source rocks: mudstones, bindstones, packstones, grainstones.
Reservoir rocks: dolomitized grainstones and packstones?
Seal rocks: PZ2 evapotites from the top, PZ1 evaporates from the base.
Overburden rocks (over 3000 m thick): remaining Zechstein cyclothems (PZ3, PZ4), Mesozoic and Cenozoic successions.
Shape and size of traps: structural, lithological, mixed. In the southern and southwestern part of the Block 208 tender area, it is postulated (Szpetnar-Skierniewska et al., 2015) that small zones of increased thickness of the Main Dolomite, or "reefs" in a form of isolated carbonate microplatforms, occur within small local structural uplifts. Such zones, comprising reservoir rocks of dolomitized grainstones and packstones would be surrounded on their slopes by sediments comprising source rocks.
Age and mechanism of trap formation: the postulated traps are probably associated with paleogeography of the Main Dolomite. Presumably, some of these traps may be original if they have not been deformed by later tectonic movements (compare to Kotarba et al., 2000).
Age and mechanism of hydrocarbon generation, expulsion, migration, and accumulation: The first stage of hydrocarbon generation from the Main Dolomite began in the Late Permian. At this stage, autochthonous gas was generated, whose composition is dominated by methane. The formation of autochthonous gas is associated with microbial activity of bacteria transforming organic matter (Kotarba et al., 2000).

The main stage of hydrocarbon generation in the tender area should be associated with the entry of the Ca2 rocks into the oil window. In addition to organic matter enriched source rocks and good reservoir properties and sealing, increased subsidence and high heat flow were very important factors for hydrocarbon generation. It was assumed after Dadlez et al. (1995) that the magnitude of heat flow was highest in the Late Permian and Early Triassic. It cooled throughout the Mesozoic until it reached temperatures near modern by the end of the Cretaceous. Increased subsidence began in the Permian and continued into the Early, Middle, and Late Triassic. As a result, the Main Dolomite rocks that were buried above 1500 m became heated with temperatures exceeding 80°C, entering the initial stage of the oil window (Kosakowski and Wróbel, 2010). However, due to the regional paleogeographic setting of the Main Dolomite, determined by the diverse paleorelief, the Triassic entry of source rocks into the oil window stage mainly affected basinal facies (Pletsch et al., 2010). The greatest burial of the Main Dolomite rocks occurred in the Jurassic. The main stage of hydrocarbon generation also was in this period. Due to the rela-

tively high heat flow that occurred in this part of the Permian basin, the basin plain source rocks may have already exhausted their generation potential in the Late Triassic (Pletsch et al., 2010).

The expulsion of hydrocarbons from the Zechstein source rocks probably started in the Early Triassic and lasted till the end of Late Jurassic and beginning of the Early Cretaceous, interrupted by the Kimmeridgian orogenic movements. Calculations based on 1D modeling indicate the kerogen transformation degree for the area of the Silesian-Sudetic carbonate platform is above 98% (Kosakowski and Wróbel, 2010).

Extrapolating the results of 2D modeling made for the western part of the Fore-Sudetic area (Kosakowski and Wróbel, 2010), it can be assumed that the process of hydrocarbon migration started and continued at a similar time as the generation process. In the Block 208 tender area, the hydrocarbon migration occurred already in the Early Triassic, which continued until the Late Jurassic and still occurred in the Late Cretaceous.

According to Kotarba and Wagner (2007), the process of hydrocarbon generation in the western part of the Fore-Sudetic area (where zones encompassing basin plain facies may be an analogue for the situation in the considered tender area) occurred in two pathways. In the case of the first pathway, the generation process was a one-step process. It involved a continuous and progressive phase of transformation of organic matter, whose hydrocarbon potential was exhausted at the end of the Triassic. The second pathway is characterized by two stages of hydrocarbon generation. The first, during which 80 to 90% of the hydrocarbon mass was generated from kerogen, lasted until the end to Late Jurassic. For the remainder part, generation already took place during the post-Cretaceous period. Consequently, oil accumulations in traps were formed at the turn of the Triassic and Jurassic periods, gas saturation took place at the end of the Late Jurassic, and final gas generation occurred in the Paleogene and Neogene. Geological and geochemical studies indicate that migration of hydrocarbons from the source rock to the reservoir rock may have occurred in these cases over a range of at most a dozen kilometers (Kotarba and Wagner, 2007).

A summary of the characteristics of the Main Dolomite petroleum play is shown in Fig. 3.9.

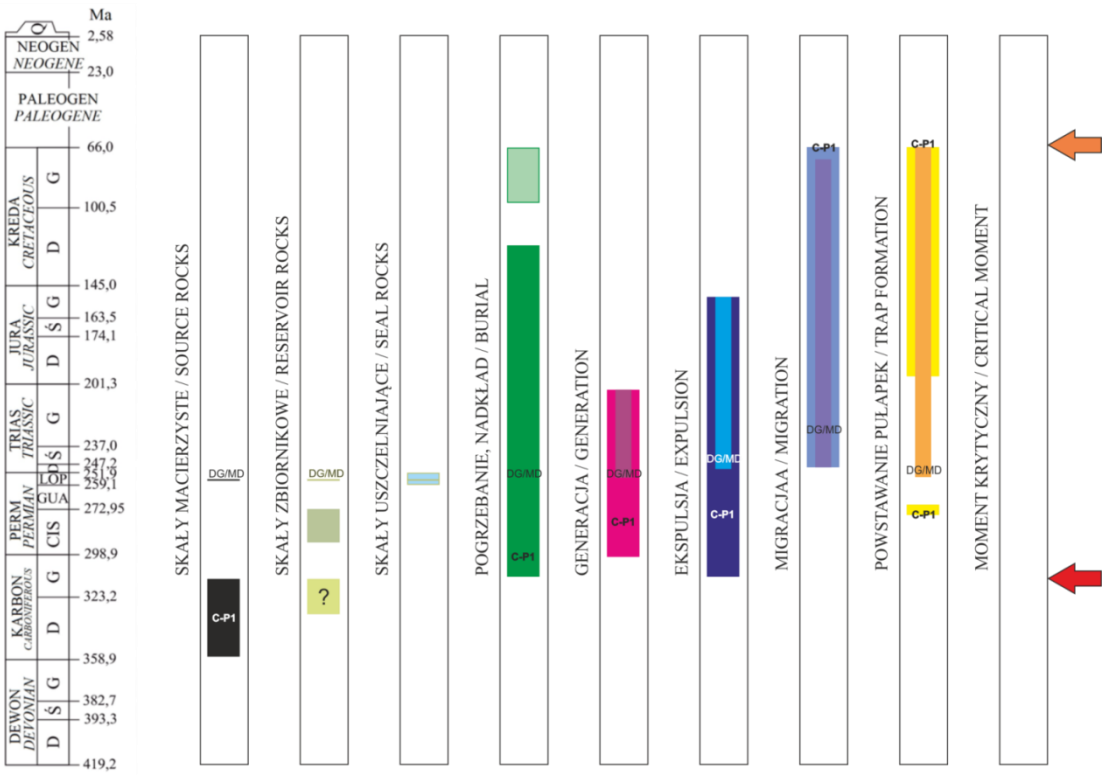

Fig. 3.9. Petroleum plays in the Block 208 tender area.

4. HYDROCARBON FIELDS

Three hydrocarbon fields have been documented in the close neighborhood of the Block 208 tender area (Fig. 4.1). These are:

- Miłosław natural gas field (GZ 19299; Figs 4.2–4.3, Tab. 4.1);
- Miłosław E natural gas field (GZ 18606; Figs 4.4–4.5, Tab. 4.2);
- Komorze natural gas field (GZ 17085; Fig. 4.6, Tab. 4.3).

A little further there is also the Winna Góra natural gas field (GZ14324; Fig. 4.1).

All of the above-mentioned fields are documented in the Rotliegend horizon. The first three were selected as the closest and potential analogues for future oil and gas exploration in the Block 208 tender area. However, information about the Winna Góra deposit will be available in the DATA ROOM in the National Geological Archive during 6th tender round.

→ **Fig. 4.1.** Hydrocarbon fields in the neighborhood of the Blok 208 tender area.

Obszary wytypowane
do postępowania przetargowego na koncesje
na poszukiwanie i rozpoznawanie
złóż węglowodorów oraz wydobywanie
węglowodorów ze złóż (VI runda przetargowa)

Areas selected to the tender procedure
for concessions for hydrocarbons fields prospection
and exploration and for hydrocarbons production
from fields (6th tender round)

Blok 208

0 2,5 5 10 km

Układ współrzędnych / *Coordinate system: PL-1992*

Objaśnienia / Legend

- obszary wytypowane do przetargu
  areas selected to the tender procedure
- złoża węglowodorów
  hydrocarbon fields
- obszary górnicze wyznaczone dla złóż węglowodorów
  mining areas assigned for hydrocarbon fields
- granice gmin
  commune border
- granice powiatów
  county border

Współrzędne punktów wyznaczających granice obszaru przetargowego, ukł. wsp. PL-1992
Coordinates determining the borders of tender area, coordinate system PL-1992

Nr punktu / *Point No*	X	Y
1	487578,09	431753,89
2	488166,79	397632,46
3	515963,52	398208,96
4	515376,16	432138,19

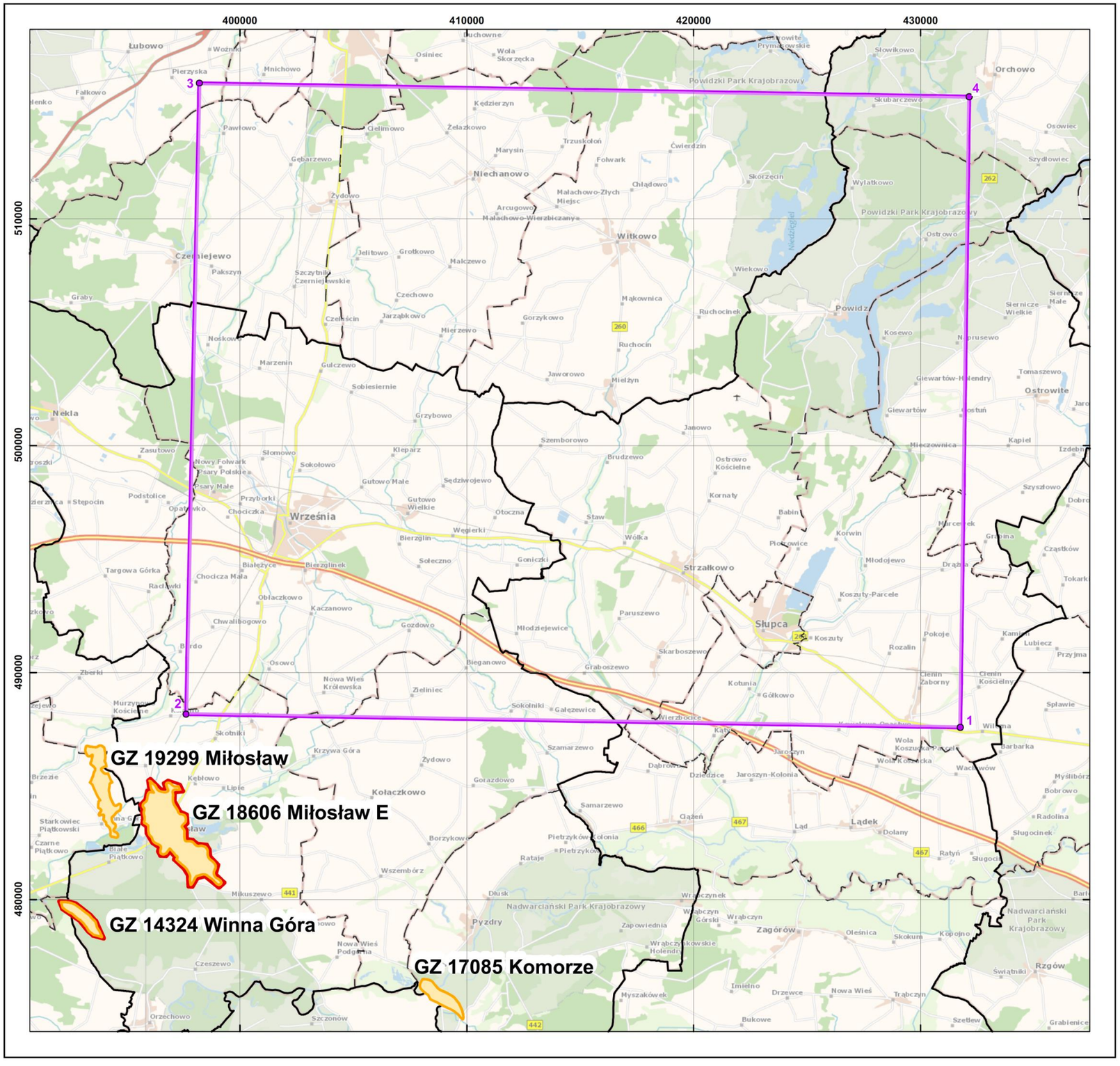

Udokumentowane złoża kopalin, obszary i tereny górnicze:
Państwowy Instytut Geologiczny - Państwowy Instytut Badawczy
System Gospodarki i Ochrony Bogactw Mineralnych Polski MIDAS

Podkład topograficzny: Główny Urząd Geodezji i Kartografii
Mapa podkładowa BDOO i BDOT10k (usługa WMTS)

Documented field, mining areas and mining counties:
Polish Geological Institute - National Research Institute
System of Management and Protection of Mineral Resources
in Poland MIDAS

Topographic background: Head Office of Geodesy and Cartography
Background maps of BDOO and BDOT10k (WMTS service)

Miłosław natural gas field

The total field acreage: 236.3 ha
Depth: from 3,958.5 m to 4,058.0 m
Stratigraphy: Permian – Rotliegend
Resources:

- The primary exploitable anticipated economic resources (as of 2017):
  202.00 MCM of natural gas in cat. C
- The exploitable anticipated economic resources as of 31 XII 2022:
  127.01 MCM of natural gas in cat. C
- The economic resources in place as of 31 XII 2022:
  117.82 MCM of the natural gas economic resources in place in cat. C
  211.19 MCM of the natural gas sub-economic resources in place in cat. C
- The production in 2022:
  13.24 MCM of natural gas in cat. C

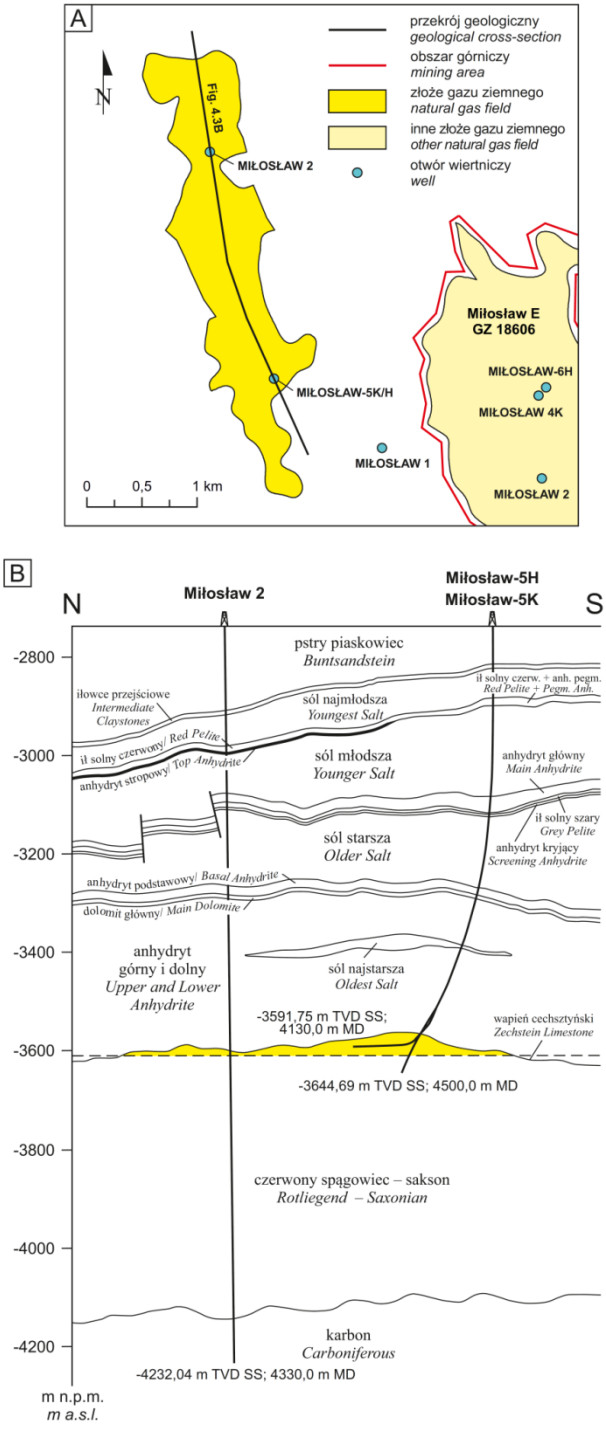

Fig. 4.2. A. Location of wells drilling the Miłosław natural gas field and its vicinity (CGDB, 2023). **B.** Geological cross-section through the Miłosław natural gas field (Chruścińska and Czajka, 2018).

Parameter	Minimum value	Maximum value	Average value	Unit	Comments
current pressure	---------	---------	40.820	MPa	
primary reservoir pressure	---------	---------	40.820	MPa	at the depth of -3,587 m TVDSS
depth of underlying water	---------	-3,609.060	---------	m	TVDSS
effective reservoir thickness	---------	---------	8.010	m	average from the map of effective thickness
porosity	---------	---------	12.980	%	
permeability	---------	---------	1.100	mD	average for effective thickness in Miłosław-5K well
reservoir temperature	---------	---------	136.370	°C	at the depth of -3,587 m TVDSS
production conditions	---------	---------	---------	–	volumetric
hydrocarbons saturation factor	---------	---------	66.000	%	
production factor	---------	---------	0.500	–	
absolute efficiency V_{abs}	---------	249.000	---------	m^3/min	on the basis of efficiency measure in Miłosław-5H well
permitted efficiency V_{dozw}	---------	80.000	---------	m^3/min	proposed, on the basis of production projection
quality parameters of natural gas (main raw material)					
Parameter	**Minimum value**	**Maximum value**	**Average value**	**Unit**	**Comments**
combustion heat	31.880	34.200	32.760	MJ/m^3	
Wobbe index	---------	---------	39.740	MJ/m^3	
calorific value	28.730	31.490	29.900	MJ/m^3	
C_2H_6	0.102	0.235	0.163	% v/v	
CH_4	79.620	85.540	82.000	% v/v	
CO_2	1.284	1.347	1.313	% v/v	
He content	0.089	0.210	0.128	% v/v	
Hg content	29.857	44.246	37.273	$\mu g/m^3$	
N_2 content	13.520	18.700	17.110	% v/v	
H_2S	0.000	0.000	0.000	% v/v	
hydrocarbons content	---------	---------	82.170	% v/v	
heavy hydrocarbons C_{3+} content	0.001	0.012	0.003	% v/v	

Tab. 4.1. Parameters of Miłosław natural gas field and quality parameters of the raw material (the MIDAS Database, 2021 according to Chruścińska and Czajka, 2018).

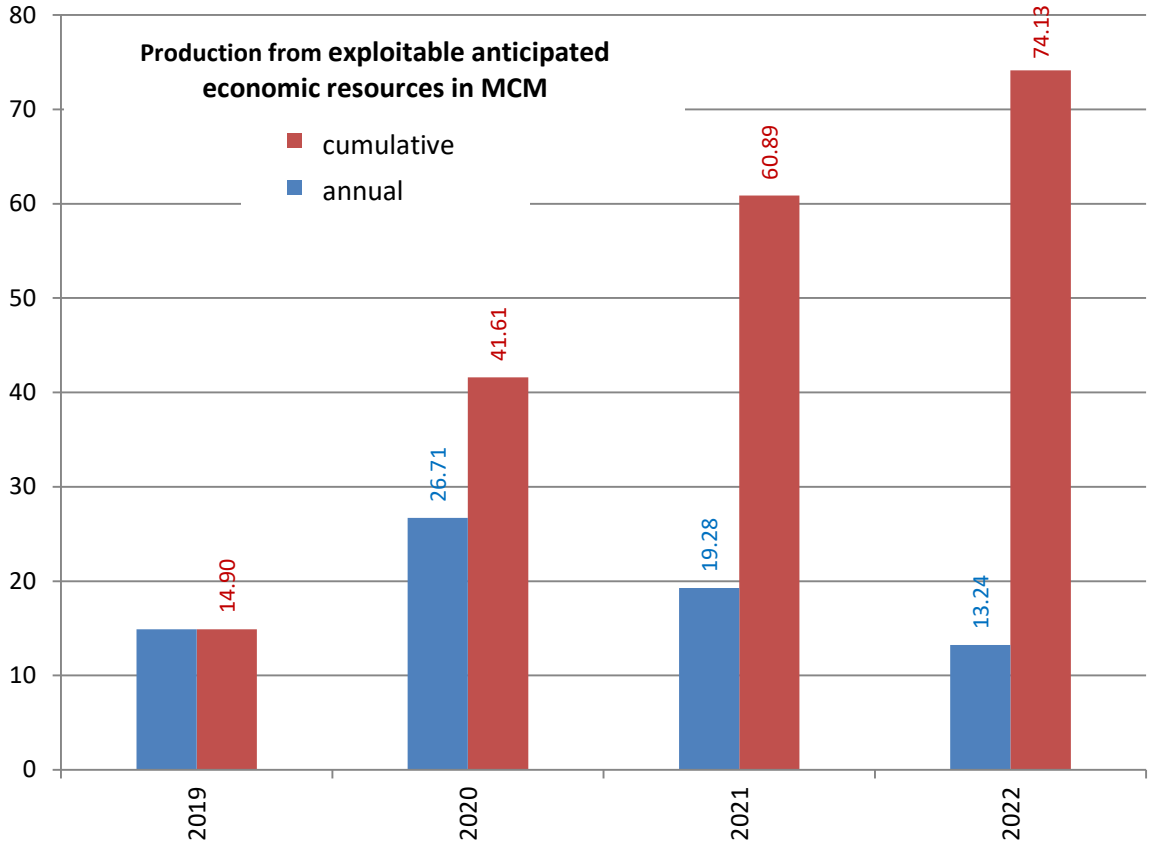

Fig. 4.3. Graph of natural gas production from Miłosław field (MIDAS, 2022).

Miłosław E natural gas field

The total field acreage: 586.8 ha
Depth: from 3,633.86 m to 3,690.0 m
Stratigraphy: Permian – Rotliegend
Resources:

- The primary exploitable anticipated economic resources (as of 2015):
  926.64 MCM of natural gas in cat. C
- The exploitable anticipated economic resources as of 31 XII 2022:
  792.96 MCM of natural gas in cat. C
- The economic resources in place as of 31 XII 2022:
  791.51 MCM of the natural gas economic resources in place in cat. C
  361.81 MCM of the natural gas sub-economic resources in place in cat. C
- The production in 2022:
  20.42 MCM of natural gas in cat. C

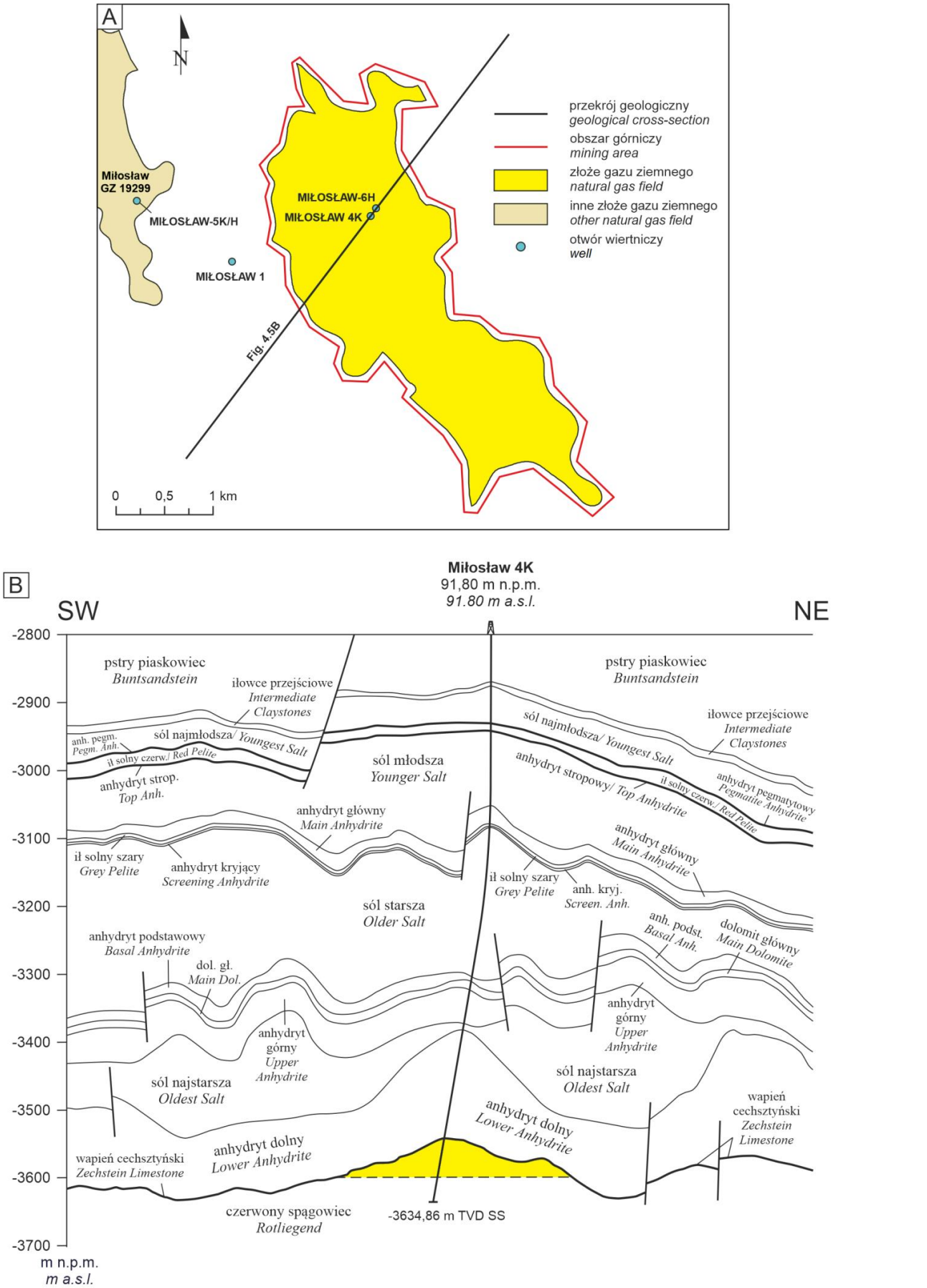

Fig. 4.4. A. Location of the wells drilling the Miłosław E natural gas field and its vicinity (CGDB, 2023). **B.** Geological cross-section through Miłosław E natural gas field (Chruścińska, 2016).

Parameter	Minimum value	Maximum value	Average value	Unit	Comments
current pressure	---------	---------	42.030	MPa	
primary reservoir pressure	---------	---------	42.030	MPa	at the depth of -3,542.08 m TVDSS
depth of underlying water	---------	3,690.000	---------	m	TVD
depth of underlying water	---------	-3,598.200	---------	m	TVDSS
effective reservoir thickness	---------	---------	13.010	m	
effective porosity	---------	---------	10.040	%	average from the map of effective thickness
permeability	---------	---------	13.220	mD	average in Miłosław 4K well
reservoir temperature	---------	---------	133.000	°C	at the depth of -3,542.08 m TVDSS
production conditions	---------	---------	---------	–	volumetric
hydrocarbons saturation factor	---------	---------	67.060	%	
production factor	---------	---------	0.720	–	
absolute efficiency V_{abs}	---------	146.000	---------	m^3/min	
permitted efficiency V_{dozw}	---------	50.000	---------	m^3/min	
quality parameters of natural gas (main raw material)					
Parameter	**Minimum value**	**Maximum value**	**Average value**	**Unit**	**Comments**
combustion heat	31.581	31.688	31.612	MJ/m^3	
density	---------	---------	0.647	–	relative
density	---------	---------	0.836	kg/m^3	
Wobbe index	---------	---------	39.307	MJ/m^3	
calorific value	28.463	28.557	28.490	MJ/m^3	
C_2H_6	0.212	0.213	0.213	% v/v	
CH_4	78.910	79.140	78.980	% v/v	
CO_2	0.841	1.175	1.119	% v/v	
He	0.121	0.122	0.121	% v/v	
Hg	0.771	0.813	0.797	$\mu g/m^3$	
N_2	19.510	19.570	19.540	% v/v	
H_2S	0.000	0.000	0.000	% v/v	
heavy hydrocarbons C_{3+} content	0.000	0.000	0.000	% v/v	

Tab. 4.2. Parameters of Miłosław E natural gas field and quality parameters of the raw material (MIDAS, 2022).

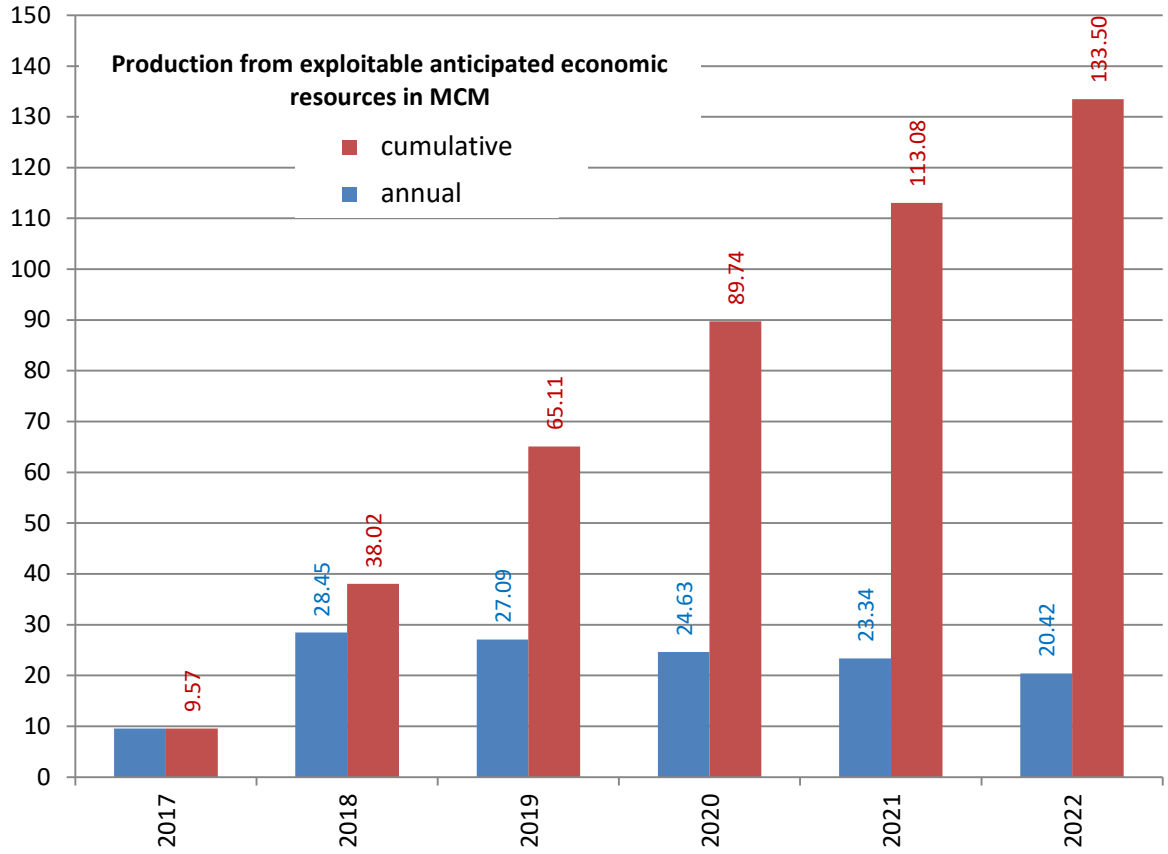

Fig. 4.5. Graph of natural gas production from Miłosław E field (MIDAS, 2022).

Komorze natural gas field

The total field acreage: 116.0 ha
Depth: from 3,972.2 m to 4,009.5 m
Stratigraphy: Permian – Rotliegend
Resources:

- The primary exploitable anticipated economic resources (as of 2015):
  340.20 MCM of natural gas in cat. C
- The exploitable anticipated economic resources as of 31 XII 2022:
  340.05 MCM of natural gas in cat. C
- The economic resources in place as of 31 XII 2022:
  lack of resources
- The production in 2022:
  lack of production

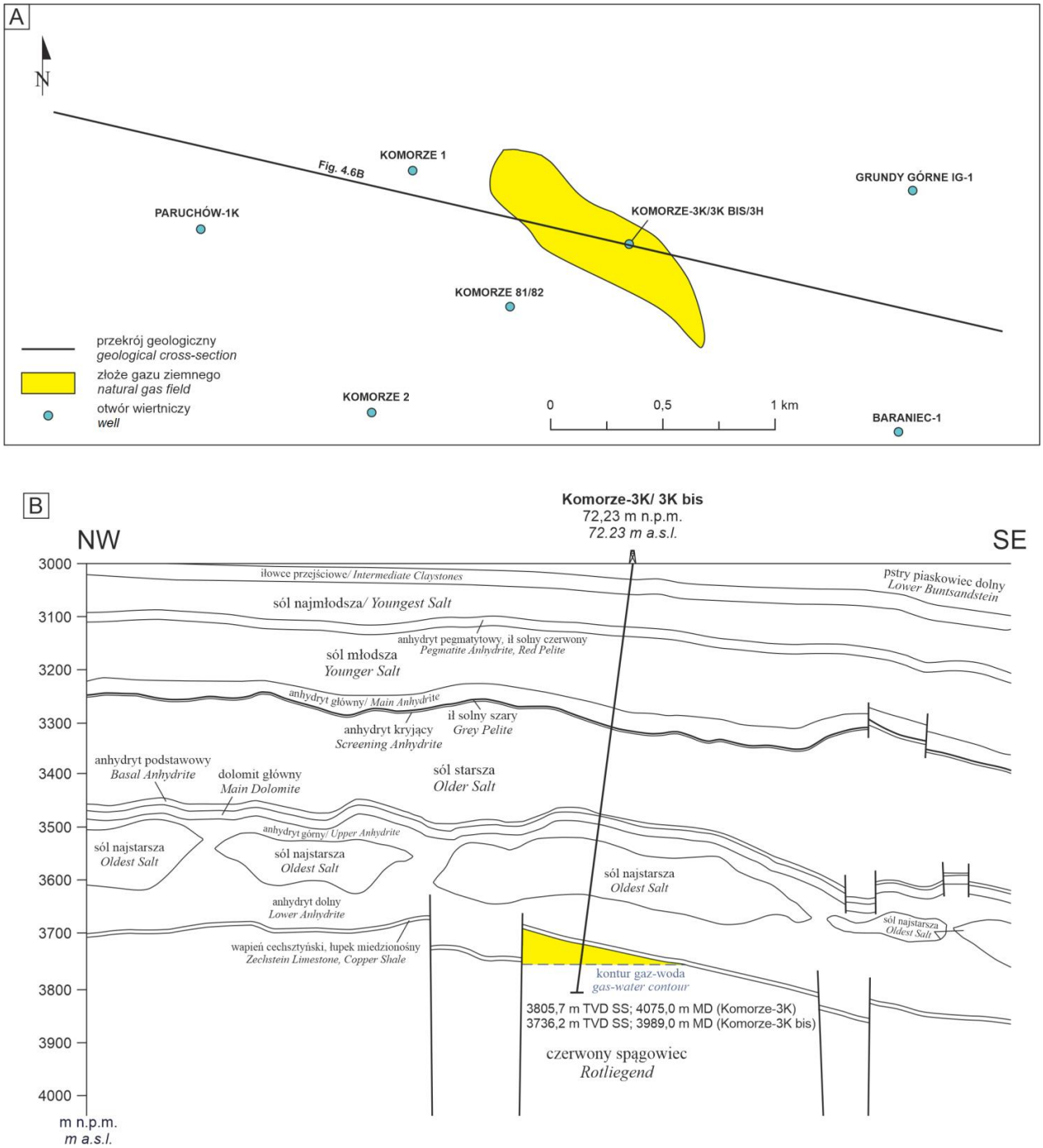

Fig. 4.6. A. Location of the wells drilling the Komorze natural gas field and its vicinity (CGDB, 2023). **B.** Geological cross-section through Komorze natural gas field (Chruścińska, 2014).

Parameter	Minimum value	Maximum value	Average value	Unit	Comments
primary reservoir pressure	---------	---------	41.320	MPa	at the depth of 3,791.4 m TVD
depth of underlying water	---------	4,009.500	---------	m	MD
depth of underlying water	---------	-3,751.000	---------	m	TVDSS
effective reservoir thickness	---------	---------	19.700	m	average from the map of effective thickness
porosity	---------	---------	12.700	%	average from the map of effective thickness
permeability	---------	---------	1.950	mD	average from reservoir series
mineralization degree of formation water	---------	---------	---------	g/l	not stated
reservoir temperature	---------	---------	133.120	°C	at the depth of 3,791.4 m TVD
reservoir temperature	---------	---------	406.270	°K	at the depth of 3,791.4 m TVD
chemical type of formation water	---------	---------	---------	–	infiltrator, type not stated
production conditions	---------	---------	---------	–	volumetric
hydrocarbons saturation factor	---------	---------	0.790	–	
production factor	---------	---------	0.600	–	
absolute efficiency V_{abs}	---------	---------	31.000	m^3/min	
permitted efficiency V_{dozw}	---------	24.000	---------	m^3/min	
water exponent	---------	---------	28.220	g/m^3	
quality parameters of natural gas (main raw material)					
Parameter	**Minimum value**	**Maximum value**	**Average value**	**Unit**	**Comments**
combustion heat	29.150	29.240	29.190	MJ/m^3	
calorific value	26.270	26.350	26.300	MJ/m^3	
C_2H_6 content	0.193	0.204	0.198	% v/v	
CH_4 content	72.800	73.040	72.910	% v/v	
carbon dioxide content	1.265	1.434	1.360	% v/v	
He content	0.149	0.152	0.151	% v/v	
Hg content	17.411	21.768	19.724	$\mu g/m^3$	
N_2 content	25.160	25.630	25.410	% v/v	
sulfur content	---------	---------	---------	% v/v	not applicable
hydrogen sulfide content	---------	---------	---------	% v/v	not applicable
heavy hydrocarbons C_{3+} content	---------	---------	---------	% v/v	<0,001 % v/v

Tab. 4.3. Parameters of Komorze natural gas field and quality parameters of the raw material (MIDAS, 2022).

5. WELLS

The following wells deeper than 500 m MD and reaching the prospective intervals were drilled in the Block 208 tender area:

Well name	Year	Owner	Depth [m]	Stratigraphy at the bottom
OTOCZNA 1	1976	State Treasury	3521.4	Upper Permian
WRZEŚNIA IG-1	1976	State Treasury	5904.2	Carboniferous

Właściciel informacji geologicznej
OTOCZNA 1
1976
Skarb
Państwa
Głębokość [m]
3521,4
Stratygrafia na dnie
perm górny

WRZEŚNIA IG-1
1976
Skarb
Państwa
5904,2
karbon

Location of the above-mentioned wells is presented in Fig. 5.1. Their general characteristics are shortly summarized in Tab. 5.1. The Września IG-1 well is illustrated in Fig. 5.2 as an example.

The original data from the wells, which belong to the State Treasury, are collected in the DATA ROOM and will be available at the Polish Geological Institute – National Research Institute in Warsaw during the 6th tender round.

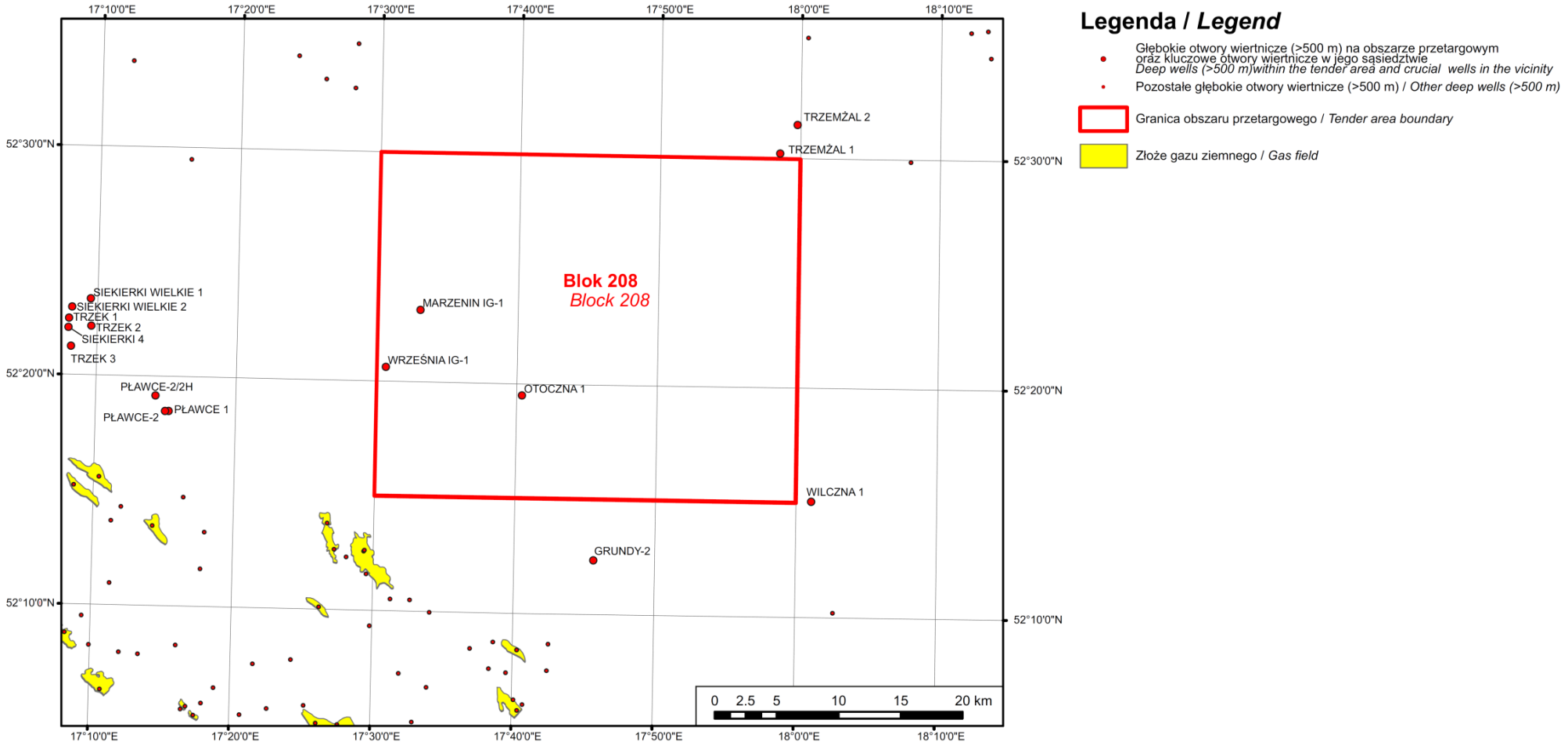

Fig. 5.1. Deep wells (>500 m MD) located within the Block 208 tender area and in its close neighborhood.

STRATIGRAPHY	Otoczna 1 top – bottom [m]		Września IG-1 top – bottom [m]		Marzenin IG-1 top – bottom [m]	
CENOZOIC	0.0	105.0	0.0	82.0	0.0	133.7
CRETACEOUS	105.0	267.0	82.0	210.0	133.7	291.2
JURASSIC	267.0	1 387.0	210.0	1 339.0	291.2	500.0
TRIASSIC	1 387.0	3 260.0	1 339.0	3 125.0		
PERMIAN	3 260.0	3 521.4	3 125.0	4 889.5		
Top Terrigenous Series PZt	3 260.0	3 272.5	3 125.0	3 150.0		
Upper Youngest Halite Na4a2			3 150.0	3 157.0		
Upper Pegmatite Anhydrite A4a2			3 157.0	3 159.0		
Lower Youngest HaliteNa4a1	3 272.5	3 357.00	3 159.0	3 221.0		
Red Pelite T4a			3 221.0	3 235.0		
Top Anhydrite A3r	3 357.0	3 360.00				
Younger Halite Na3r	3 360.0	3 514.00	3 235.0	3 277.5		
Younger Potash K3			3 277.5	3 294.0		
Younger Halite Na3			3 294.0	3 373.0		
Main Anhydrite A3	3 514.0	3 521.40	3 373.0	3 415.5		
Grey Pelite T3			3 415.5	3 417.5		
Screening Anhydrite A2r			3 417.5	3 419.0		
Screening Older Halite Na2r			3 419.0	3 420.5		
Older Potash K2			3 420.5	3 428.5		
Older Halite Na2			3 428.5	3 766.5		
Basal Anhydrite A2			3 766.5	3 769.0		
Main Dolomite Ca2			3 769.0	3 772.5		
Upper Anhydrite A1g			3 772.5	3 811.0		
Upper Oldest Halite Na1g			3 811.0	3 941.0		
Middle Anhydrite A1s						
Lower Oldest Halite Na1d						
Lower Anhydrite A1d			3 941.0	4 022.5		
Zechstein Limestone Ca1			4 022.5	4 024.5		
Weissliegend			4 024.5	4 026.5		
Upper Rotliegend			4 026.5	4 762.5		
Lower Rotliegend			4 762.5	4 889.5		
CARBONIFEROUS			4 889.5	5 904.2		

Tab. 5.1. Summary of stratigraphy with indication of prospective horizons for gas accumulations in the wells located within the Block 208 tender area.

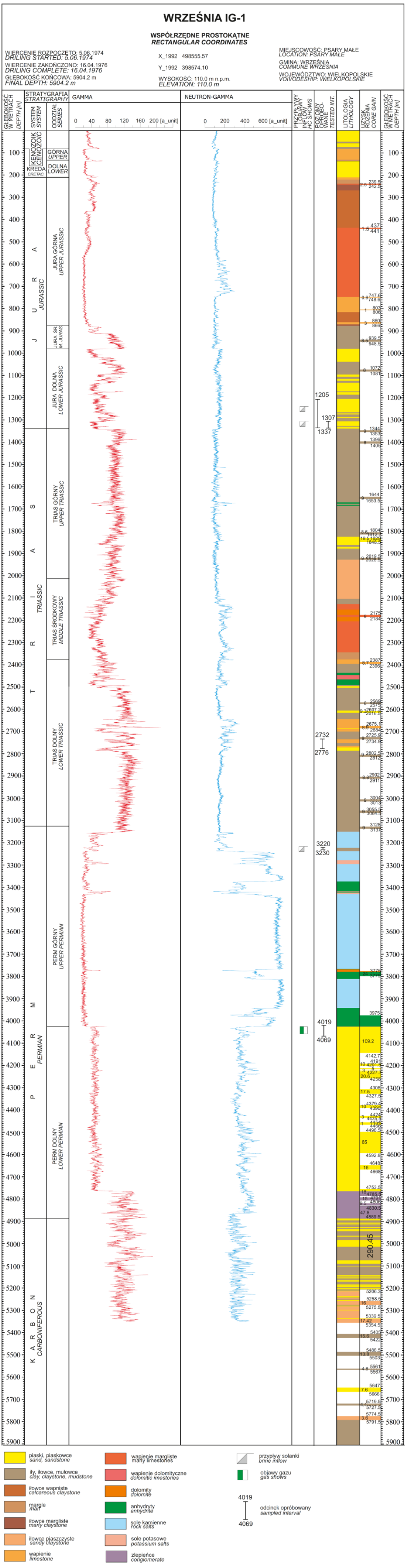

Fig. 5.2. Września IG-1 well lithology, stratigraphy and geophysics (Sokołowski et al., 1977).

6. SEISMIC SURVEYS

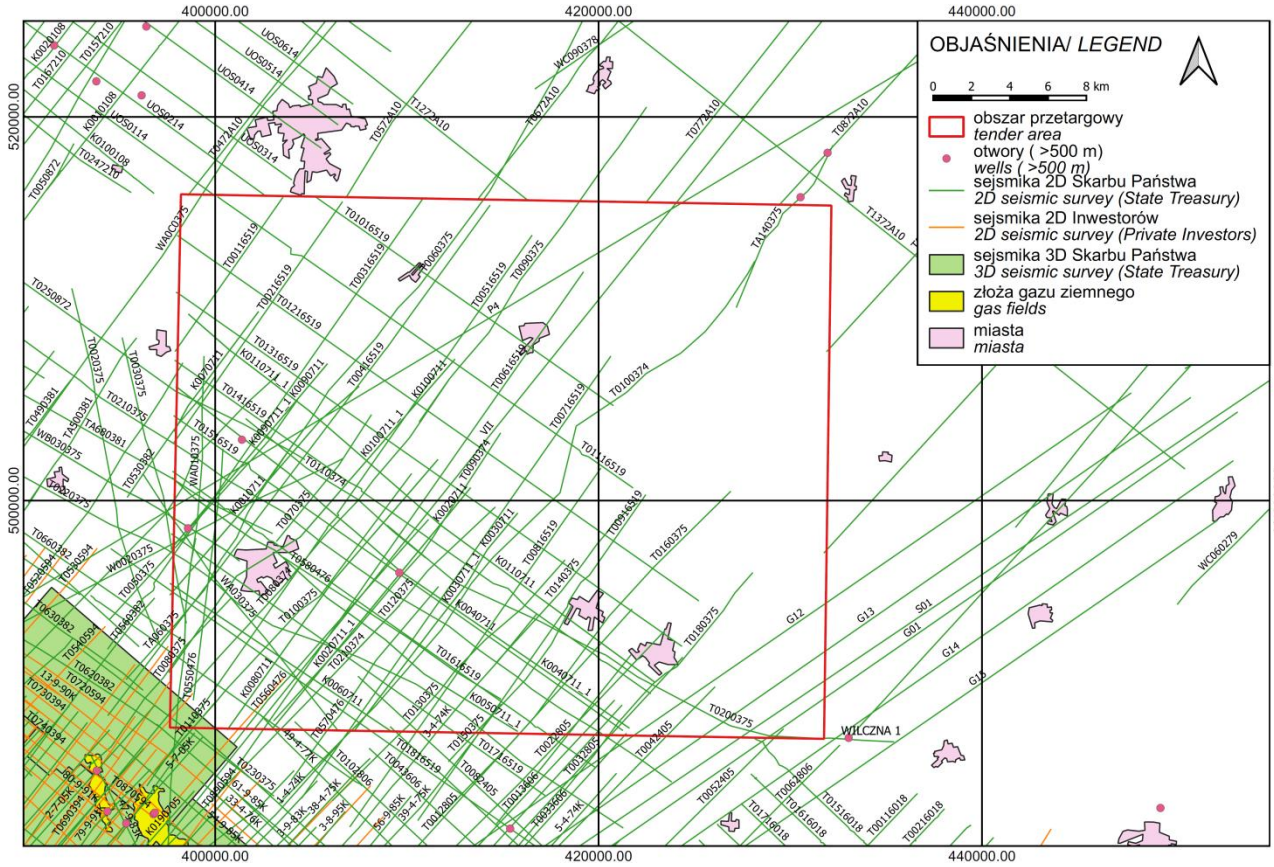

Fig. 6.1. Seismic survey within and in the neighborhood of the Block 208 tender area (CGDB, 2023).

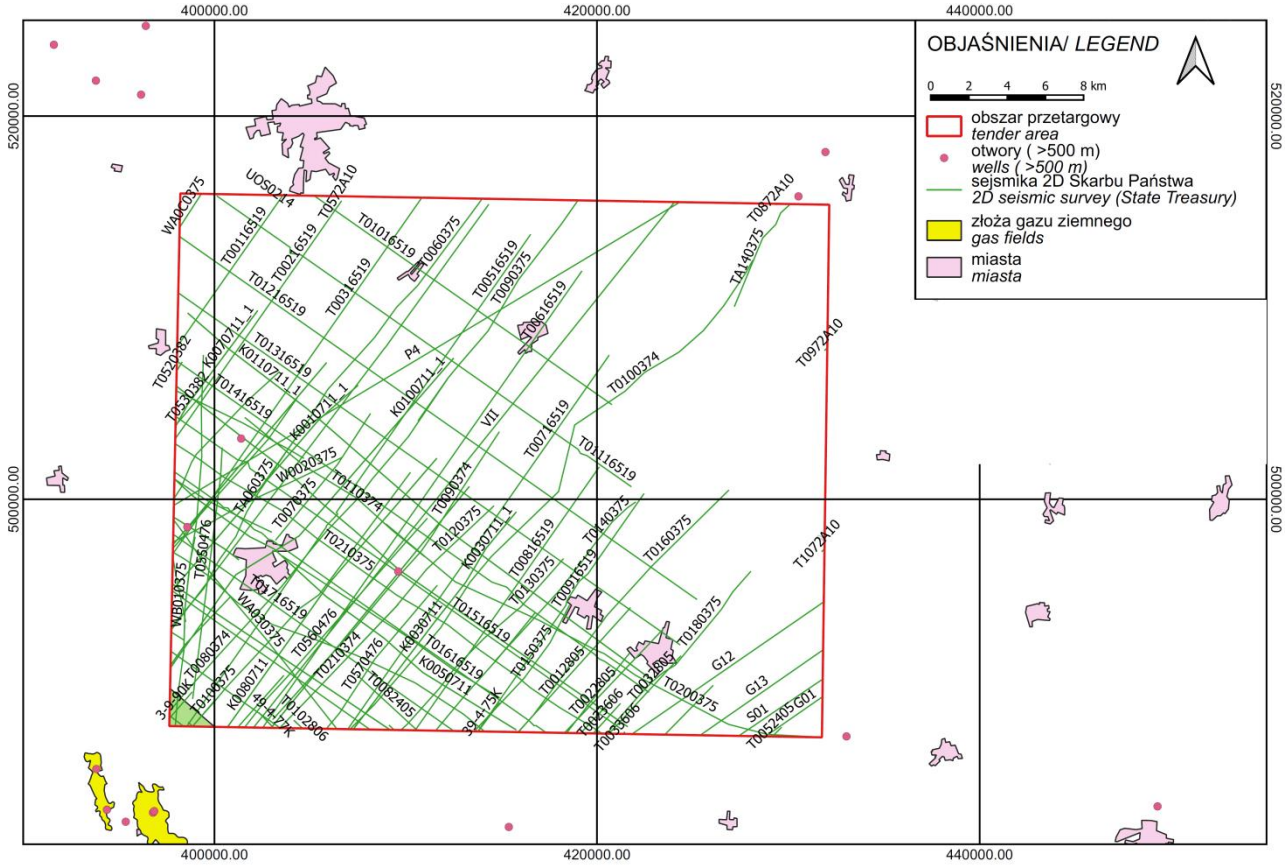

Fig. 6.2. Seismic survey within the Block 208 tender area (CGDB, 2023).

LINE NAME	YEAR	PROJECT	CONCESSIONS (after 2001)	OWNER	LENGTH [km]
3-4-74K	1974	Jarocin-Kalisz		State Treasury	8.05
T0080374	1974	Środa-Września		State Treasury	22.61
T0090374	1974	Środa-Września		State Treasury	19.13
T0100374	1974	Środa-Września		State Treasury	33.00
T0110374	1974	Środa-Września		State Treasury	11.84
T0210374	1974	Środa-Września		State Treasury	8.94
T0030375	1975	Września-Słupca-Kłecko		State Treasury	3.43
T0040375	1975	Września-Słupca-Kłecko		State Treasury	8.71
T0050375	1975	Września-Słupca-Kłecko		State Treasury	10.15
T0060375	1975	Września-Słupca-Kłecko		State Treasury	19.05
T0070375	1975	Września-Słupca-Kłecko		State Treasury	8.22
T0080375	1975	Września-Słupca-Kłecko		State Treasury	4.76
T0090375	1975	Września-Słupca-Kłecko		State Treasury	14.23
T0100375	1975	Września-Słupca-Kłecko		State Treasury	17.53
T0120375	1975	Września-Słupca-Kłecko		State Treasury	11.15
T0130375	1975	Września-Słupca-Kłecko		State Treasury	12.35
T0140375	1975	Września-Słupca-Kłecko		State Treasury	11.03
T0150375	1975	Września-Słupca-Kłecko		State Treasury	8.30
T0160375	1975	Września-Słupca-Kłecko		State Treasury	16.77
T0170375	1975	Września-Słupca-Kłecko		State Treasury	5.29
T0180375	1975	Września-Słupca-Kłecko		State Treasury	11.35
T0200375	1975	Września-Słupca-Kłecko		State Treasury	25.79
T0210375	1975	Września-Słupca-Kłecko		State Treasury	27.02
T0220375	1975	Września-Słupca-Kłecko		State Treasury	18.97
TA060375	1975	Września-Słupca-Kłecko		State Treasury	12.34
TA140375	1975	Września-Słupca-Kłecko		State Treasury	6.18
W0020375	1975	Września		State Treasury	9.86
W0030375	1975	Września		State Treasury	4.05
WA010375	1975	Września		State Treasury	19.43
WA030375	1975	Września		State Treasury	13.88
WA0C0375	1975	Profile Regionalne		State Treasury	2.09
WB010375	1975	Września		State Treasury	6.04
WB030375	1975	Września		State Treasury	4.05
T0550476	1976	Czarnków-Poznań-Strzelno		State Treasury	13.16
T0560476	1976	Czarnków-Poznań-Strzelno		State Treasury	14.49
T0570476	1976	Czarnków-Poznań-Strzelno		State Treasury	9.46
T0580476	1976	Czarnków-Poznań-Strzelno		State Treasury	13.51
TA680381	1981	Poznań-Września		State Treasury	5.79
T0530382	1982	Poznań-Września		State Treasury	3.34
5-9-90K	1990	Miłosław-Solec		ORLEN S.A.	3.59
T0012805	2005	Grundy	Projekt badań sejsmicznych 2D dla rejonu GRUNDY	State Treasury	8.73
T0022805	2005	Grundy		State Treasury	7.46
T0032805	2005	Grundy		State Treasury	5.51
T0042405	2005	Grundy		State Treasury	3.58
T0082405	2005	Grundy		State Treasury	4.25
T0013606	2006	Lubinia		State Treasury	2.44
T0023606	2006	Lubinia		State Treasury	2.08
K0010711	2011	Blok 208	5/03/9 Blok 208	State Treasury	14.46
K0020711	2011	Blok 208		State Treasury	16.23
K0030711	2011	Blok 208		State Treasury	14.18
K0040711	2011	Blok 208		State Treasury	29.57
K0050711	2011	Blok 208		State Treasury	22.22
K0060711	2011	Blok 208		State Treasury	13.71
K0070711	2011	Blok 208		State Treasury	7.42
K0080711	2011	Blok 208		State Treasury	17.79
K0090711	2011	Blok 208		State Treasury	12.41
K0100711	2011	Blok 208		State Treasury	22.11
K0110711	2011	Blok 208		State Treasury	30.94
T00116519	2019	Września-Witkowo 2D	Częściowo na obszarze koncesji 18/99/p Pyzdry i 32/96/p Kórnik-Środa	State Treasury	9.59
T00216519	2019	Września-Witkowo 2D		State Treasury	15.14
T00316519	2019	Września-Witkowo 2D		State Treasury	22.63
T00416519	2019	Września-Witkowo 2D		State Treasury	27.71
T00516519	2019	Września-Witkowo 2D		State Treasury	31.44
T00616519	2019	Września-Witkowo 2D		State Treasury	29.09
T00716519	2019	Września-Witkowo 2D		State Treasury	23.82

T00816519	2019	Września-Witkowo 2D		State Treasury	16.76
T00916519	2019	Września-Witkowo 2D		State Treasury	15.18
T01016519	2019	Września-Witkowo 2D		State Treasury	18.92
T01116519	2019	Września-Witkowo 2D		State Treasury	26.66
T01216519	2019	Września-Witkowo 2D		State Treasury	33.03
T01316519	2019	Września-Witkowo 2D		State Treasury	32.02
T01416519	2019	Września-Witkowo 2D		State Treasury	30.26
T01516519	2019	Września-Witkowo 2D		State Treasury	28.52
T01616519	2019	Września-Witkowo 2D		State Treasury	23.83
T01716519	2019	Września-Witkowo 2D		State Treasury	17.91
T01816519	2019	Września-Witkowo 2D		State Treasury	12.64
T01916519	2019	Września-Witkowo 2D		State Treasury	6.98
				State Treasury	1132.56
				ORLEN S.A.	3.59

Tab. 6.1. 2D seismic surveys (lines longer than 2 km) within the Block 208 tender area.

NAME	YEAR	CONCESSIONS (after 2001)	OWNER	ACREAGE [km^2]
Miłosław 3D	2012	32/96/p Kórnik-Środa 18/99/p Pyzdry 4/03/p Blok 207 4/03/p Blok 208	State Treasury	2,33

Tab. 6.2. 3D seismic surveys within the Block 208 tender area.

7. GRAVIMETRY, MAGNETOMETRY AND MAGNETOTELLURICS

7.1. GRAVIMETRY

There are 1492 data points of semidetailed gravimetric survey within the Block 208 tender area (Fig. 7.1). The surveys were collected as part of two projects. Most of the tender area is covered with Mogilno-Konin-Uniejów survey (Reczek, 1967) collected with a point density ca. 2 stations/km^2. Remaining part of the area (south-west corner) is covered with the Gorzów-Jarocin survey (Duda and Kruk, 1973) with a point density ca. 2.5 stations/km^2. The latest survey – Zgorzelec-Wiżajny (Ostrowski et al., 2007) was collected with 2 km step.

There is no detailed survey within the Block 208 tender area, but a few surveys were collected in its close neighborhood (Fig. 7.1). Usually they were focused on brown coal exploration (Reczek, 1963; Łaszczyńska et al., 1982; Iciek, 1989; Wasiak, 1990; Ostrowska and Pisuła, 1991), and only one of them is focused on the Mogilno salt diapir Mogilno (Soćko, 1982).

Królikowski and Petecki (1995) proposed a division of Poland into several gravity regions. Thus, the Block 208 tender area is placed within the Szczecin-Mogilno-Miechów Low (Fig. 7.2) witch source is defined indefinitely. Most researchers assume the dominant role of the crystalline basement in its formation. The influence of the Variscan Orogeny is also not excluded.

Band-pass filtering of Bouguer anomalies map for the depth range from 2 km to 50 km (Fig. 7.3; Szpetnar-Skierniewska et al., 2015) shows a NNW-SSE fault, separating two gravimetric anomalies, which may be associated with elevation of Carboniferous formations (SW part of the Block 208 tender area, Fig. 7.3). In addition, these anomalies also coincide with the increased thickness of anhydrite, which may suggest that the fault was also active during Zechstein sedimentation.

7.2. MAGNETOMETRY

A ground, semidetailed survey of the total magnetic field intensity was conducted in the Block 208 tender area (Kosobudzka and Paprocki, 1997). The survey has an average density of 2 stations/km^2. All data are available in the CGDB (2023). There are1607 data points within the tender area.

An image of magnetic anomalies presented on Fig. 7.5 is taken from magnetic map of Poland (Petecki and Rosowiecka, 2017). The map is divided into several regions with different magnetic characteristic. The Block 208 tender area is located within the Central and Western Poland domain (CWPd), which is limited by Szczecin-Stargard Szczeciński-Piła-Inowrocław gradient zone (Petecki, 2008). This domain is a vast magnetic low in which there are no strong anomalies of regional importance. The absence of magnetic anomalies in this domain suggests either consistently lower magnetization of the basement rocks in comparison to the neighboring magnetic domains, or a smooth top of the basement at a great depth.

7.3. MAGNETOTELLURICS

Within Block 208 tender area there is a segment of Zgorzelec-Wiżajny regional profile (Ostrowski et al, 2007; Fig. 7.6). 2D inversion results are presented on Fig. 7.7. The measurement step of 4 km does not allow for a detailed analysis of sub-Zechstein structures or tracing the continuity of some resistance horizons, i.e. in the area of advanced salt tectonics.

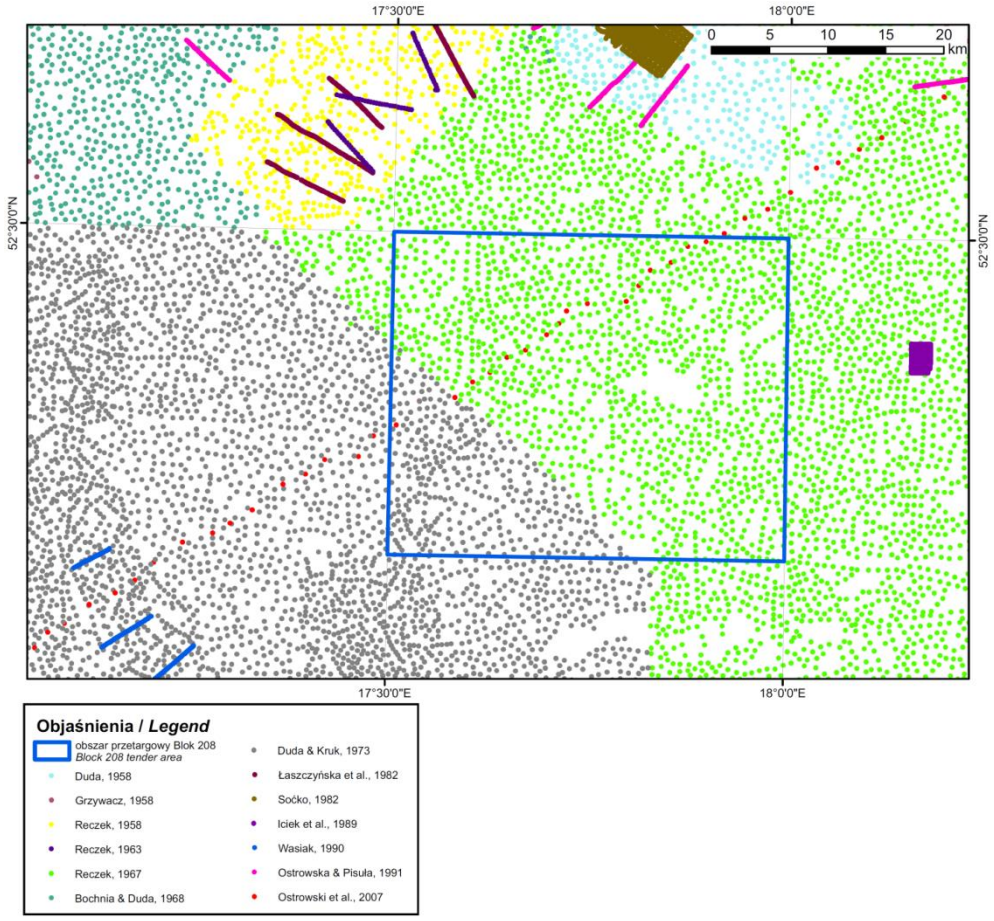

Fig. 7.1. Distribution of gravimetric measurements in the Block 208 tender area (based on CGDB, 2023).

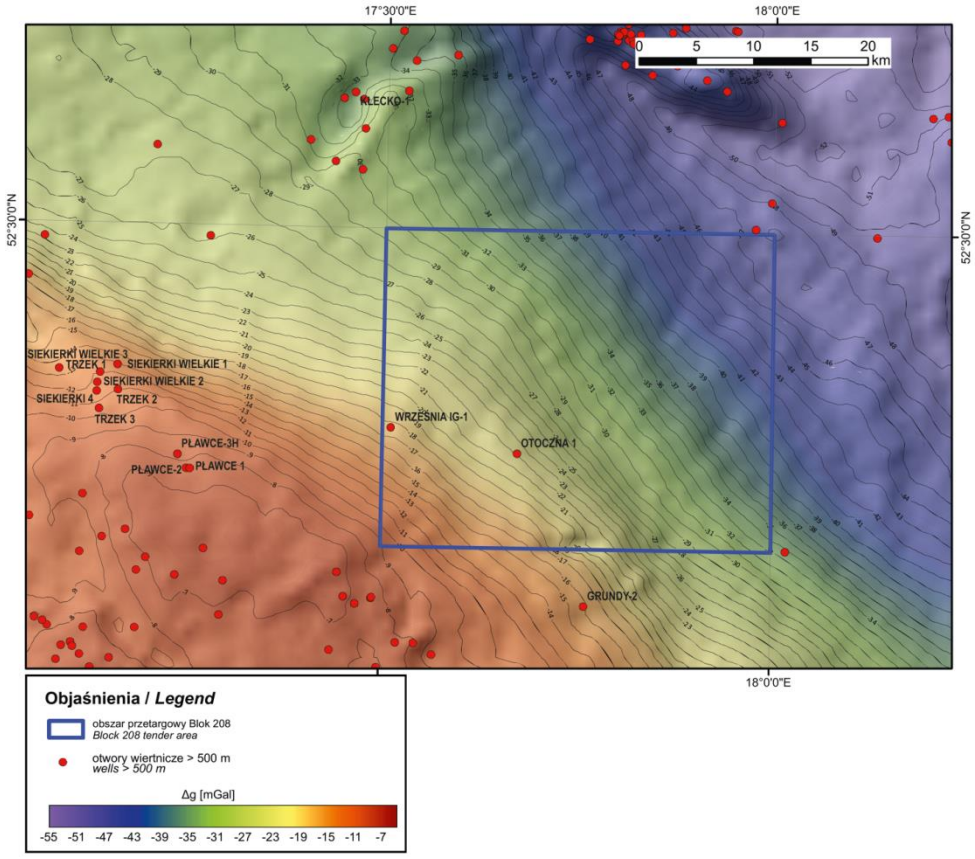

Fig. 7.2. Location of the Block 208 tender area in the Bouguer gravity anomaly map of Poland.

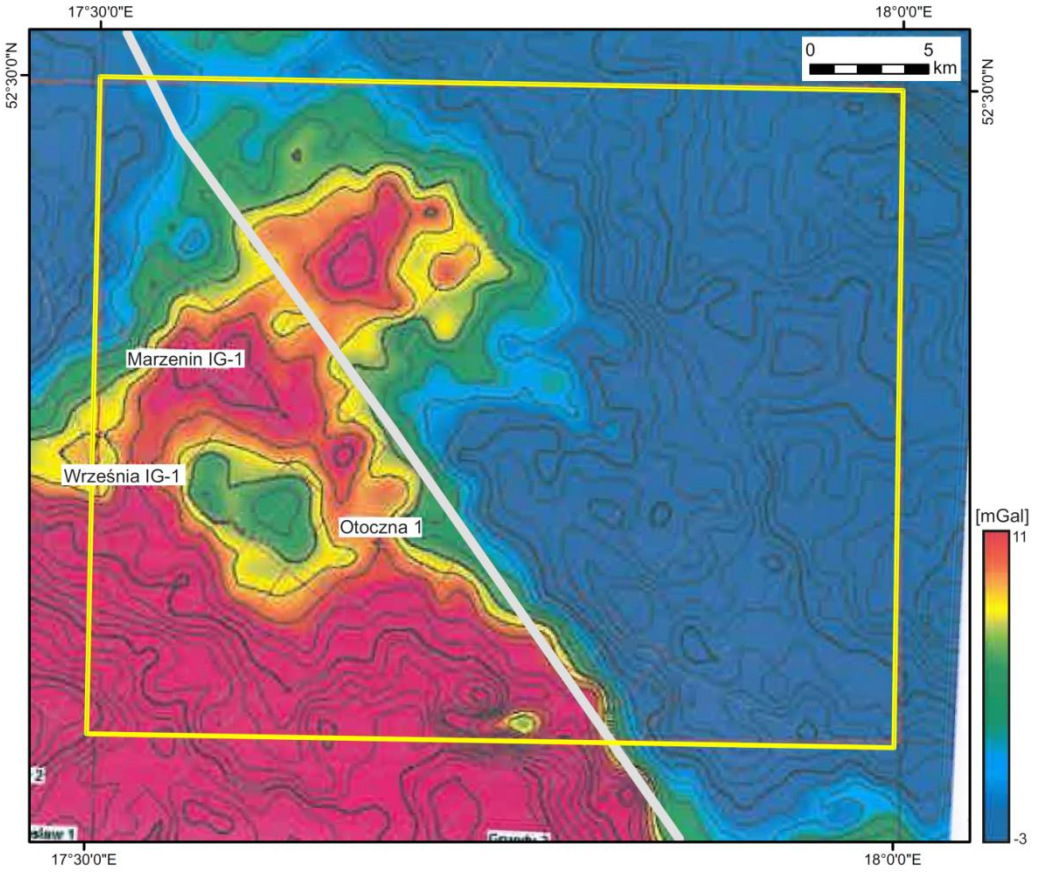

Fig. 7.3. Residual anomalies of Bouguer map for the depth range from 2 km to 50 km. Grey line – interpreted fault (after: Szpetnar-Skierniewska et al., 2015).

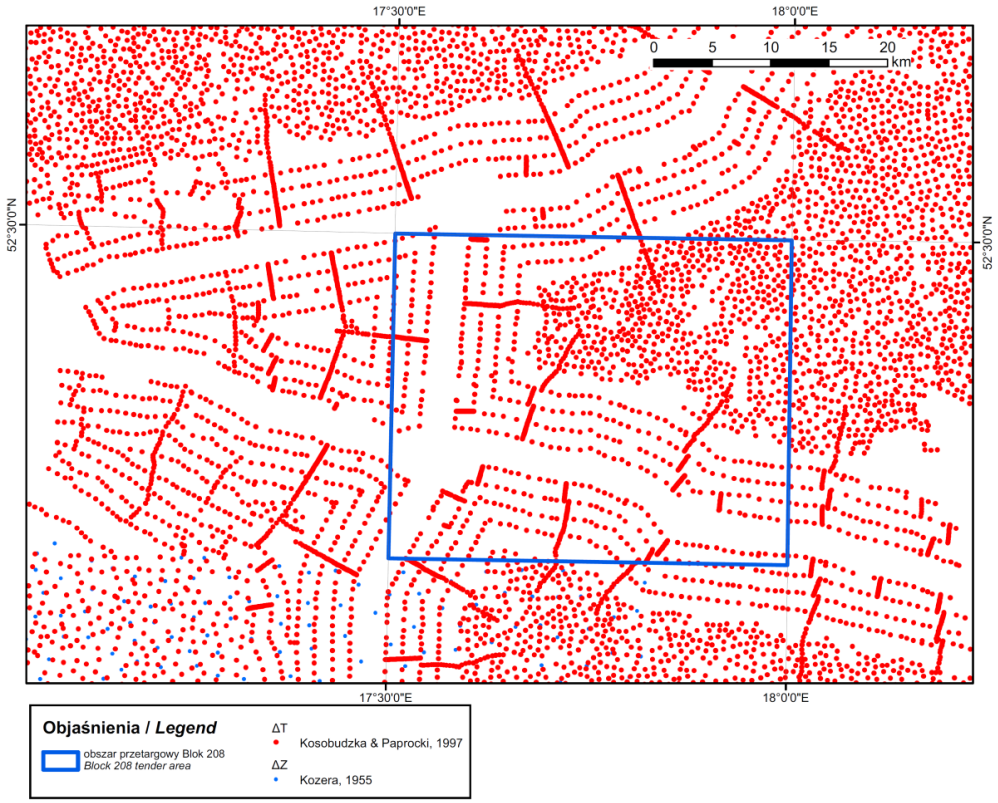

Fig. 7.4. Location of the Block 208 tender area in the magnetic anomaly map of Poland (Petecki and Rosowiecka, 2017).

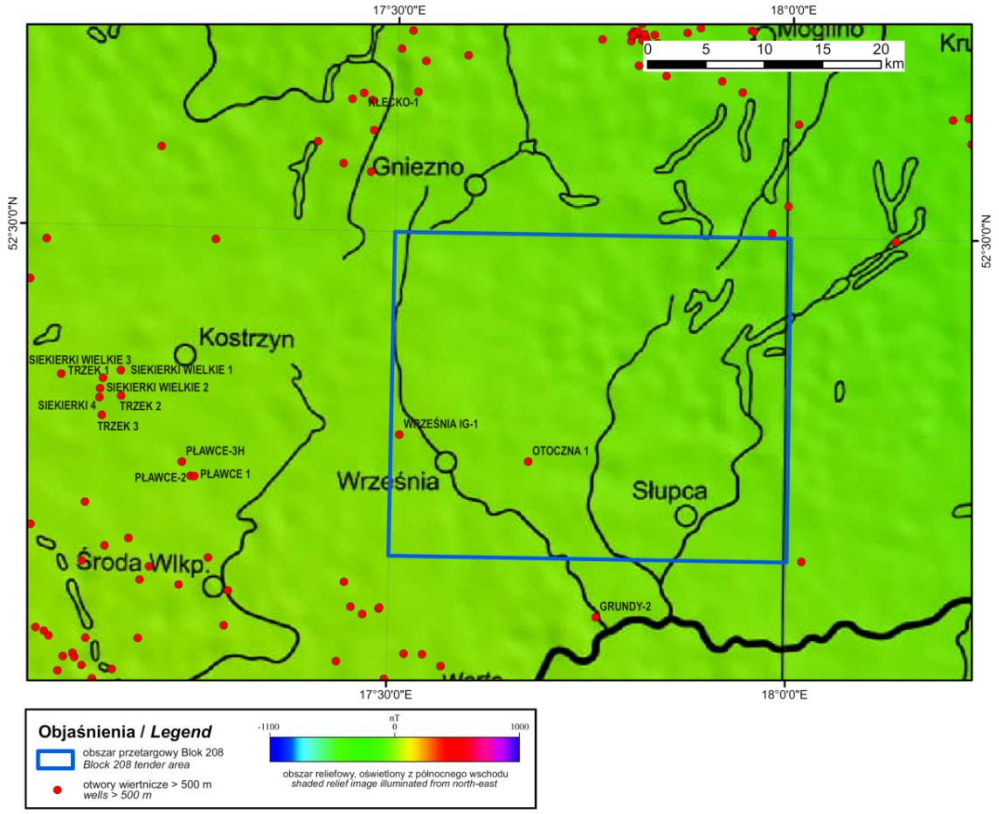

Fig. 7.5. Location of the Block 208 tender area in the magnetic anomaly map of Poland (Petecki and Rosowiecka, 2017).

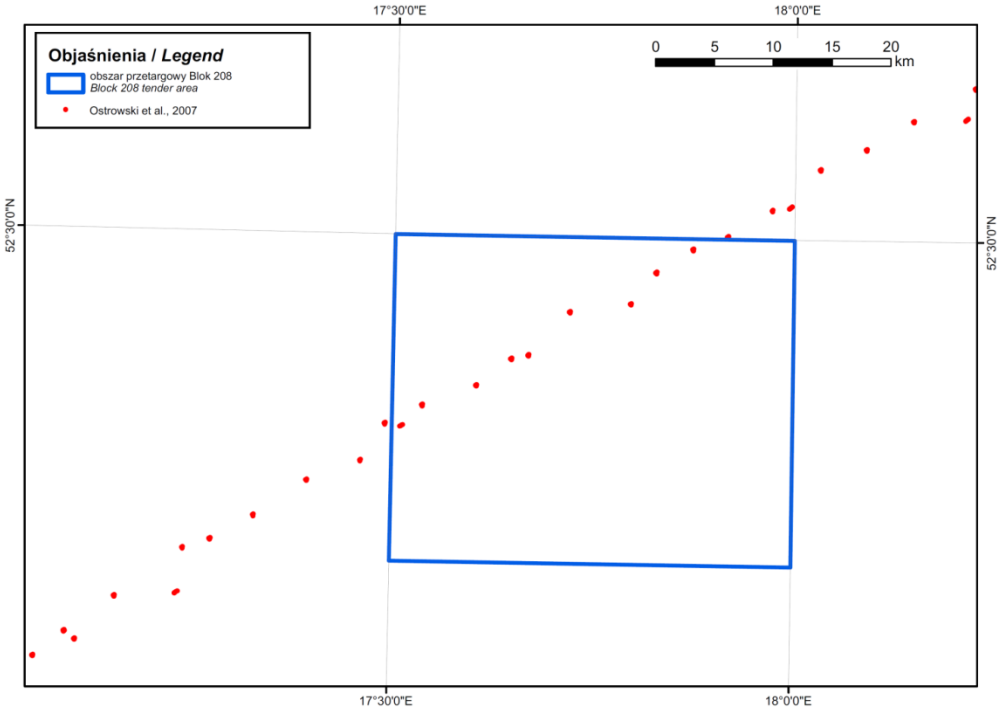

Fig. 7.6. Distribution of magnetotelluric survey in the Block 208 tender area (based on CGDB, 2023).

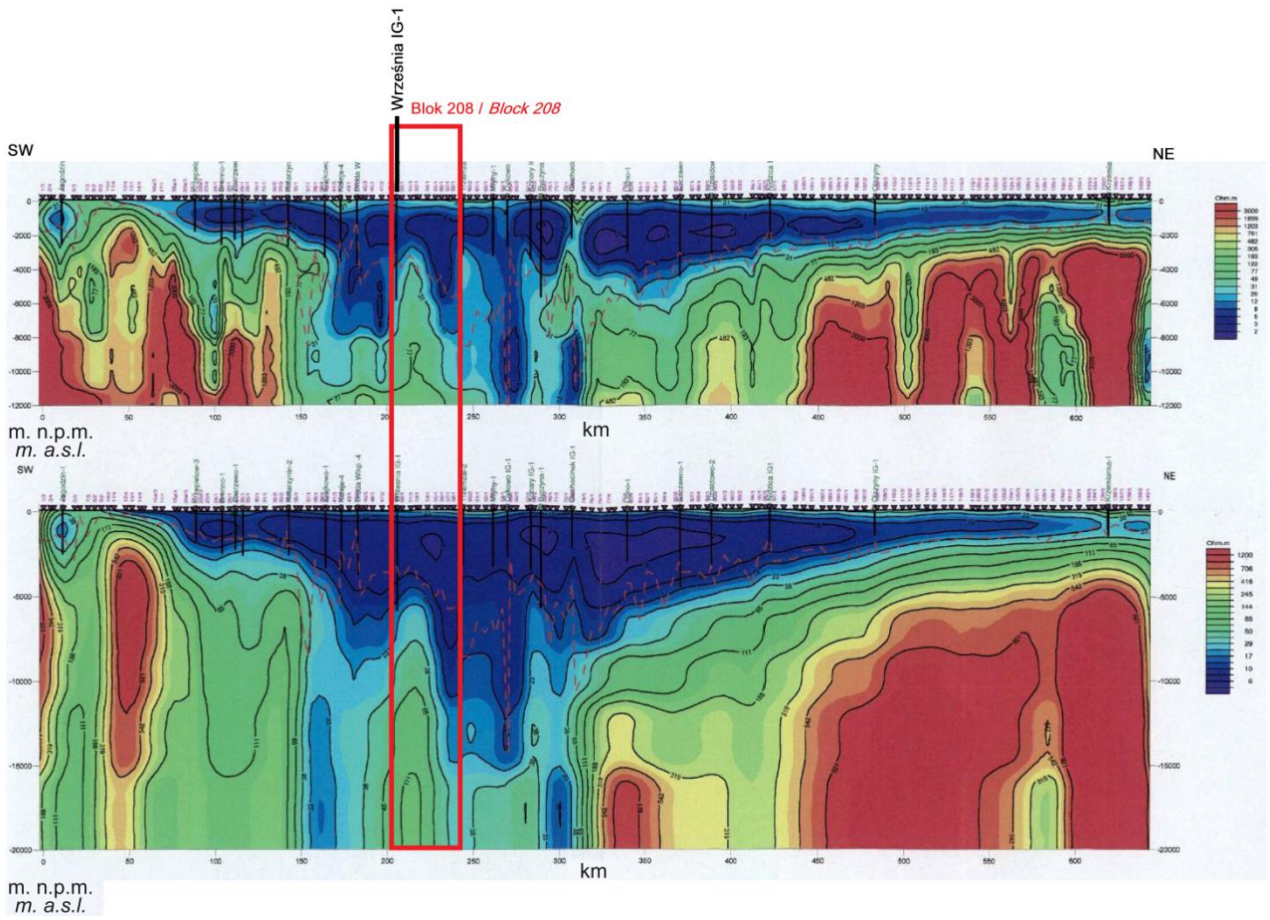

Fig. 7.7. Results of 2D inversion along Zgorzelec-Wiżajny profile (Ostrowski et al., 2007). The segment adjacent to the Block 208 tender area from north-west is marked with purple polygon.

8. SUMMARY CHART

General information:	**Tender area:**	**BLOCK 208**
	Location:	Onshore Hydrocarbon concession blocks: 208 Administrative location: Wielkopolskie Voivodeship, Gniezno county, communes: Witkowo (16.92%), Gniezno (0.33%), Gniezno (m.) (0.62%), Niechanowo (10.67%), Czerniejewo (6.44%), Łubowo (0.10%); Słupca country, communes: Strzałkowo (15.02%), Orchowo (1.28%), Powidz (7.65%), Ostrowite (4.16%), Słupca (10.91%), Słupca (m.) (1.09%); Września country, communes: Września (21.51%), Kołaczkowo (2.85%), Nekla (0.03%), Miłosław (0.42%)
	Concession type:	prospection and exploration of hydrocarbon deposits and production of hydrocarbons from a deposit
	Time:	concession for 30 years, including: prospection and exploration phase (5 years), production phase – after investment decision
Participation:		winner of the tender 100%
Acreage [km^2]:		946.1
Accumulation type:		I. unconventional tight gas accumulations in the Upper Rotliegend and Carboniferous sandstones II. conventional oil and gas accumulations in the Main Dolomite, possible accumulations of gas in the Zechstein Limestone
Structural stages:		Cenozoic Laramide Variscan
Petroleum plays:		I. unconventional (tight) petroleum system in the Upper Rotliegend and Carboniferous, , possible conventional accumulations of gas in the Zechstein Limestone II. conventional petroleum system in the Main Dolomite
Reservoir rocks:		I. Carboniferous and Upper Rotliegend sandstones, eventually carbonate rocks of the Zechstein Limestone II. carbonate rocks of the Main Dolomite
Source rocks:		I. Carboniferous fine-grained clastic rocks II. Main Dolomite mudstones, boundstones, packstones, and grainstones
Seal rocks:		I. Zechstein evaporates PZ1 II. Zechstein evaporates PZ12
Trap type:		I. structural-tectonic II. structural, lithological, mixed
Oil and gas fields in the neighborhood:		Miłosław, Miłosław E, Komorze
Seismic surveys (owner):		1974 Jarocin-Kalisz 2D, 1 line (State Treasury) 1974 Środa-Września 2D, 5 lines (State Treasury) 1975 Września-Słupca-Kłecko 2D, 20 lines (State Treasury) 1975 Września 2D, 6 lines (State Treasury) 1975 Profile Regionalne 2D, 1 line (State Treasury) 1976 Czarnków-Poznań-Strzelno 2D, 4 lines (State Treasury) 1981-1982 Poznań-Września 2D, 2 lines (State Treasury) 1990 Miłosław-Solec 2D, 1 line (ORLEN S.A.) 2005 Grundy 2D, 5 lines (State Treasury) 2006 Lubinia, 2 lines (State Treasury) 2011 Blok 208 2D, 11 lines (State Treasury) 2019 Września-Witkowo 2D, 19 lines (State Treasury) 2012 Miłosław 3D (State Treasury)
Wells (depth):		OTOCZNA 1 (3521.4 m) WRZEŚNIA IG-1 (5904.2 m)

Possible minimum work program for the prospection and exploration phase

- Archival data reinterpretation and analysis

- Conducting the 2D seismic survey (at least 50 km PW) or 3D seismic survey (at least 25 km^2)

- Drilling of one well to the maximal depth 5000 m TVD with obligatory coring of prospective intervals

9. REFERENCES

- **Aagaard P., Jahren J. S., Harstad A. O., Nilsen O., Ramm M. 2000.** Formation of grain-coating chlorite in sandstones. Laboratory synthesized vs. natural occurrences. *Clay Minerals*, **35**, 261–269.
- **Bochnia N., Duda W. 1968.** Dokumentacja półszczegółowych vadań grawimetrycznych. Temat: Synklinorium Szczecińsko-Mogileńskie. [Semidetailed gravimetric survey report: Szczecin-Mogilno Synclinorium, 1967]. Inv. 1435, CAG PIG, Warsaw. [in Polish]
- **Botor D., Papiernik B., Maćkowski T., Reicher B., Kosakowski P., Machowski G., Górecki W. 2013.** Gas generation in Carboniferous source rocks of the Variscan foreland basin: implications for a charge history of Rotliegend deposits with natural gases. *Annales Societatis Geologorum Poloniae*, **83**, 353–383.
- **Buniak A., Kuberska M., Kiersnowski H. 2009.** Petrograficzno-petrofizyczna charakterystyka piaskowców eolicznych strefy Siekierki-Winna Góra (koło Poznania) w aspekcie poszukiwań złóż gaz zamkniętego w osadach czerwonego spągowca. [Petrographical-petrophysical characteristics of the Rotliegend eolian sandstones of the Siekierki–Winna Góra Zone (the Poznań region) in the aspect of search for gas trapped in deposits]. *Przegląd Geologiczny*, **57**, 328–334. [in Polish with English summary]
- **Burzewski W., Górecki W., Maćkowski T., Papiernik B., Reicher B. 2009.** Zasoby prognostyczne - nieodkryty potencjał gazu ziemnego w polskim basenie czerwonego spągowca. [Prognostic gas reserves – undiscovered potential of gas in the Polish Rotliegend basin]. *Kwartalnik AGH Geologia*, **35**, 123–128. [in Polish with English summary]
- **CGDB, 2023.** Central Geological DataBase http://geoportal.pgi.gov.pl
- **Chruścińska J. 2014.** Dokumentacja geologiczna złoża gazu ziemnego Komorze w kat. C. [Komorze geological gas field documentation in cat. C]. Inv. 1570/2014, CAG PIG, Warsaw. [in Polish]
- **Chruścińska J. 2016.** Dokumentacja geologiczno-inwestycyjna złoża gazu ziemnego Miłosław E. [Miłosław E gas field geological-investment documentation]. Inv. 4013/2017, CAG PIG, Warsaw. [in Polish]
- **Chruścińska J., Czajka D. 2018.** Dokumentacja geologiczno-inwestycyjna złoża gazu ziemnego Miłosław. [Miłosław gas field geological-investment documentation]. Inv. 178/2019, CAG PIG, Warsaw. [in Polish]
- **Chruścińska J., Wiśniewska S., 2018.** Dokumentacja geologiczna likwidowanego otworu Grundy-2. [Grundy-2 report of well liquidation]. Inv. 5567/2019, CAG PIG, Warsaw. [in Polish]
- **Dadlez R., Franczyk M. 1976.** Znaczenie paleogeograficzne i paleotektoniczne garbu wielkopolskiego w czasie jury dolnej. [Palaeogeographic and palaeotectonic importance of the Wielkopolska Swell during the Early Jurassic]. *Biuletyn Instytutu Geologicznego*, **295**, 27–49. [in Polish]
- **Dadlez R., Narkiewicz M., Stephenson R.A., Visser M.T.M., Van Wees J-D., 1995.** Tectonic Evolution of the Mid-Polish Trough: Modelling Implications and Significance for Central European Geology. *Tectonophysics*, **252**, 179–195.
- **Dadlez R., Marek S., Pokorski J. 2000.** Geological map of Poland without Cenozoic deposits, 1 : 1 000 000. Polish Geological Institute, Warsaw.
- **Darłak B., Kowalska-Włodarczyk M., Leśniak G., Such P. 1998.** Przegląd wyników badań właściwości zbiornikowych i filtracyjnych wybranych skał zbiornikowych basenów młodopaleozoicznych Niżu Polskiego. [An overwier of the reservoir and filtration properties of selected reservoir horizons of the younger Paleozoic basins of the Polish Lowland]. (In): Analiza basenów sedymentacyjnych Niżu Polskiego [Sedimentary basin analysis of the Polish Lowland]; (Ed.): Narkiewicz M. *Prace Państwowego Instytutu Geologicznego*, **165**, 147–152. [in Polish with English summary]
- **Dayczak-Calikowska K., Moryc W. 1988.** Rozwój basenu sedymentacyjnego i paleotektonika jury środkowej na obszarze Polski. [Evolution of sedimentary basin and palaeotectonics of the Middle Jurassic in Po-

land]. *Geological Quarterly*, **32**, 117–136. [in Polish with English summary]

- **Dembowska J. 1979.** Systematyzowanie litostratygrafii jury górnej w Polsce północnej i środkowej. [Systematization of lithostratigraphy of the Upper Jurassic in northern and central Poland]. *Geological Quarterly*, **23**, 617–630. [in Polish with English summary]
- **Duda W. 1958.** Sprawozdanie. Półszczegółowe badania grawimetryczne w obszarze Mogilno-Gopło, 1957. [Semidetailed gravimetric survey report: Mogilno-Gopło, 1957]. Inv. 40920, CAG PIG, Warsaw. [in Polish]
- **Duda W., Kruk B. 1973.** Dokumentacja półszczegółowych badań grawimetrycznych. Temat: Gorzów-Jarocin, 1971-1972. [Semidetailed gravimetric survey report: Gorzów-Jarocin, 1971-1972]. Inw. 1754, CAG PIG, Warsaw. [in Polish]
- **Górecka-Nowak A., 2008.** New interpretations of the Carboniferous stratigraphy of SW Poland based on miospore data. *Bulletin of Geosciences*, **83**, 101–116.
- **Górecki W., Papiernik B., Maćkowski Reicher B., Botor D., Burzewski W., Machowski G. 2011.** Hydrocarbon potential of the Carboniferous – Lower Permian Total Petroleum System in the Polish part of the SPB. Extended abstracts, 73rd EAGE Conference & Exhibition incorporating SPE EUROPEC, 23–26 May, Vienna, P298. EarthDoc, EAGE Publications B.V.
- **Gościk D., Grelowski C., Mikołajewski Z., Zawierucha T. 2010.** Odwiert Grundy 2 – założenia projektowe a wynik wiercenia w aspekcie poszukiwania węglowodorów w poziomie dolomitu głównego (Ca2). [Grundy-2 well – project objectives vs. drilling results in the aspect of hydrocarbon exploration in the Main Dolomite (Ca2) level]. Międzynarodowa konferencja naukowo-techniczna Geopetrol 2010: nowe metody i technologie zagospodarowania złóż i wydobycia węglowodorów w warunkach lądowych i morskich. [Geopetrol 2010 International Conference: new methods and technology in development and production of Oil and Gas – Onshore and Offshore]. Zakopane, 20-23.09.2010 r. *Prace Naukowe Instytutu Nafty i Gazu*, **170**, 491–501. [in Polish with English summary]
- **Grzywacz J. 1958.** Sprawozdanie z półszczegółowych badań grawimetrycznych Oborniki-Czarnków. [Semidetailed gravimetric survey report: Oborniki-Czarnków]. Inv. 9963/3265, CAG PIG, Warsaw. [in Polish]
- **Hancock N.J. 1978.** Possible causes of Rotliegend sandstone diagenesis in northern West Germany. *Geological Society of London*, **135**, 35–40.
- **Iciek A., Królikowski C., Linowski H., Midura A., Oleksiak J., Piwocki M., Soćko A. 1989.** Budowa geologiczna Polski i poszukiwanie złóż surowców mineralnych. Cel nr 28. Opracowanie kompleksu nowoczesnych metod geofizycznych do poszukiwania i rozpoznawania złóż węgli brunatnych. [Geology of Poland and mineral resources. Target 28. Development of new geophysical methods for prospecting and exploration of brown coals]. Kat. 3921/287, Arch. CAG PIG, Warsaw. [in Polish]
- **Jaskowiak-Schoeneichowa M. 1977.** Kreda górna. Budowa geologiczna wschodniej części niecki mogileńsko-łódzkiej (strefa Gopło-Ponętów-Pabianice). [Upper Cretaceous. Geology of the eastern part of the Mogilno-Łódź Synclinorium (Gopło-Ponętów-Pabianice area)]. *Prace Instytutu Geologicznego*, **80**. [in Polish with English summary]
- **Karnkowski P. 1993.** Złoża gazu ziemnego i ropy naftowej w Polsce. Tom 1 – Niż Polski. [Oil and gas fields in Poland. Polish Lowland]. Tow. Geosynopt. GEOS AGH, Kraków, 214 pp. [in Polish]
- **Kiersnowski H., Buniak A., Kuberska M., Srokowska-Okońska A. 2010.** Występowanie gazu ziemnego zamkniętego w piaskowcach czerwonego spągowca Polski. [Tight gas accumulations in Rotliegend sandstones of Poland]. *Przegląd Geologiczny*, **58**, 335–346. [in Polish with English summary]
- **Kiersnowski H., Buniak A., Waśkiewicz K. 2020.** Mapa litofacji stropu osadów czerwonego spągowca górnego. [Lithofacies map of the top of the Upper Rotliegend]. Polish Geological Institute – National Research Institute, Warsaw. [in Polish with English abbreviations]

- **Kondracki J. 2013.** Geografia regionalna Polski. [Regional geography of Poland]. PWN, Warsaw. [in Polish]
- **Kosakowski P., Wróbel M. 2010.** Source-rock Evaluation and Basin Modelling in the Western Part of the Fore-sudetic Monocline -SW Poland (P343). Conference: 72nd EAGE Conference & Exhibition incorporating SPE EUROPEC 2010, at Barcelona, Spain. DOI: 10.3997/2214-4609.201401214.
- **Kosobudzka I., Paprocki A. 1997.** Wykonanie półszczegółowych badań magnetycznych „T" w Polsce zachodniej, centralnej i południowo-wschodniej w latach 1995-1997. [Semidetailed magnetic T research in Western, Central, and South-Western Poland, 1995-1997). Inw. 812/98, Arch. CAG PIG, Warsaw. [in Polish]
- **Kotarba M., Wagner R. 2007.** Generation potential of the Zechstein Main Dolomite (Ca2) carbonates in the Gorzów Wielkopolski-Międzychód-Lubiatów area: geological and geochemical approach to microbial-algal source rock. *Przegląd Geologiczny*, **55**, 1025–1036.
- **Kotarba M.J., Więcław D., Kowalski A. 2000.** Skład, geneza i środowisko generowania ropy naftowej w utworach dolomitu głównego zachodniej części obszaru przedsudeckiego. [Composition, origin and habitat of oils in the Zechstein Main Dolomite strata of the western part of the Fore-Sudetic area (SW Poland)]. *Przegląd Geologiczny*, **48**, 436–442. [in Polish with English summary]
- **Kotarba M., Bilinkiewicz E., Kosakowski P. 2020.** Origin of hydrocarbon and non-hydrocarbon (H_2S, CO_2 and N_2) components of natural gas accumulated in the Zechstein Main Dolomite carbonate reservoir of the western part of the Polish sector of the Southern Permian Basin. *Chemical Geology*, **554**, 1–21.
- **Kozłowska A., Kuberska M. 2015.** Piaskowce dolnego karbonu strefy wielkopolsko-śląskiej jako utwory perspektywiczne pod względem poszukiwań złóż gazu zamkniętego (badania wstępne). [The Lower Carboniferous sandstones in the Wielkopolska-Silesia zone prospective for tight gas exploration (preliminary studies)]. *Biuletyn Państwowego Instytutu Geologicznego*, **464**, 49–60. [in Polish with English summary]
- **Królikowski C., Petecki Z. 1995.** Atlas grawimetryczny Polski. [Gravimetric Atlas of Poland]. Polish Geological Institute, Warsaw. [in Polish]
- **Krzemiński L. 2005.** Proweniencja materiału okruchowego piaskowców karbońskich z waryscyjskich basenów przedpola w południowo-zachodniej Polsce i na Morawach. [Provenance of Carboniferous sandstones from the Variscan foreland basins in south-western Poland and Moravia]. *Biuletyn Państwowego Instytutu Geologicznego*, **417**, 27–108. [in Polish with English summary]
- **Kuberska M. 1999.** Etapy cementacji piaskowców czerwonego spągowca w kujawsko-pomorskim segmencie strefy T-T. [Cementation stages of the Rotliegend sandstones in the Kuyavian-Pomerania segment of the T-T Zone]. *Przegląd Geologiczny*, **47**, 477–478. [in Polish]
- **Kuberska M. 2001.** Spoiwa ilaste piaskowców czerwonego spągowca w kujawsko-pomorskim segmencie bruzdy środkowopolskiej. [Clayey cements of the Rotliegend sandstones in the Kuyavian-Pomerania segment of the Mid Polish Trough]. *Przegląd Geologiczny*, **49**, 345. [in Polish]
- **Kuberska M. 2004.** Diageneza osadów czerwonego spągowca w strefie Szczecinek-Bydgoszcz (Pomorze Zachodnie). [Diagenesis of the Rotliegend rocks in the Szczecinek-Bydgoszcz area (Western Pomerania)]. *Biuletyn Państwowego Instytutu Geologicznego*, 411, **87**–168. [in Polish with English summary]
- **Kudrewicz R. 2007.** Mapy strukturalne powierzchni podcechsztyńskiej i podpermskiej, 1 : 500 000. [Structural maps of the Permian and Zechstein basement surfaces]. (In): Zasoby prognostyczne, nieodkryty potencjał gazu ziemnego w utworach czerwonego spągowca i wapienia cechsztyńskiego w Polsce – badania geologiczne. [Prognostic resources, undiscovered gas potential in the Rotliegend and Zechstein Limestone in Poland – geological research]. (Eds): Wagner R. et al., 2008. Inw. 2293/2009, Arch. CAG PIG, Warsaw. [in Polish]
- **Łaszczyńska B., Okulus H., Wojas A. 1982.** Dokumentacja badań geofizycznych;

temat: Poszukiwania złóż węgla brunatnego w obrębie anomalii grawimetrycznych (obszary: Oborniki, Kłecko, Pogorzela, Świebodzin-Boryszyn, Studzieniec, Bobrowice), 1981. [Geophysical documentation; topic: Searching of brown coal fields gravimetric annomalies (Oborniki, Kłecko, Pogorzela, Świebodzin-Boryszyn, Studzieniec, Bobrowice regions), 1981]. Inw. 2189, Arch. CAG PIG, Warsaw. [In Polish]

- **Maćkowski T., Reicher B. 2008.** Przestrzenne modelowania procesu generowania, ekspulsji i symulacji migracji węglowodorów. [3D modeling of hydrocarbon generation, expulsion and migration processess]. (In): Zasoby prognostyczne, nieodkryty potencjał gazu ziemnego w utworach czerwonego spągowca i wapienia cechsztyńskiego w Polsce. [Prognostic resources and undiscovered potential for gas occurrence in the Rotliegend and Zechstein Limestone]; (Ed): Górecki W. Inv. 2293/2009, CAG PIG, Warsaw. [In Polish]
- **Maćkowski T., Reicher B., Burzewski W., Botor D., Papiernik B., Górecki W., 2008.** Rekonstrukcja czasowo-przestrzennych parametrów, model ekspulsji i migracji węglowodorów oraz ocena potencjału generacyjnego. [Reconstruction of hydrocarbon parameters in space and time, expulsion and migration models, and evaluation of generation potential]. (In): Zasoby prognostyczne, nieodkryty potencjał gazu ziemnego w utworach czerwonego spągowca i wapienia cechsztyńskiego w Polsce. [Prognostic resources and undiscovered potential for gas occurrence in the Rotliegend and Zechstein Limestone]; (Ed): Górecki W. Inv. 2293/2009, CAG PIG, Warsaw. [In Polish]
- **Maliszewska A. 1997.** Charakterystyka petrograficzna – skały osadowe czerwonego spągowca w Polsce na obszarach platformowych. [Petrographic characteristics – Rotliegend sedimentary rocks on the platform areas of Poland]. (In): Epikontynentalny perm i mezozoik w Polsce. [The epicontinental Permian and Mesozoic in Poland]. (Eds): Marek., Pajchlowa M. *Prace Państwowego Instytutu Geologicznego*, **153**, 38–42. [in Polish with English summary]
- **Maliszewska A., Kuberska M. 2008.** Spoiwa skał górnego czerwonego spągowca w zachodniej części Niżu Polskiego w ujęciu kartograficznym. [Mapping of cement types in the Upper Rotliegend rocks from the western Polish Lowlands]. *Biuletyn Państwowego Instytutu Geologicznego*, **429**, 79–90. [in Polish with English summary]
- **Maliszewska A., Kuberska M. 2009.** O badaniach izotopowych diagenetycznego illitu z piaskowców czerwonego spągowca Wielkopolski i Pomorza Zachodniego. [Isotopic investigations of diagenetic illite of Rotliegend sandstones from the Wielkopolska and Western Pomerania regions]. *Przegląd Geologiczny*, **57**, 322–327. [in Polish with English summary]
- **Maliszewska A., Pokorski J. 1978.** Piroklastyczne skały ogniwa obrzyckiego autunu w zachodniej części Niżu Polskiego. [Pyroclastic rocks of the Obrzycko Member (Autunian) in western part of the Polish Lowlands]. *Geological Quarterly*, **22**, 511–532. [in Polish with English summary]
- **Maliszewska A., Kuberska M., Such P., Leśniak G. 1998.** Ewolucja przestrzeni porowej utworów czerwonego spągowca. [Evolution of the pore space of the Rotliegend sandstones]. (In): Analiza basenów sedymentacyjnych Niżu Polskiego [Sedimentary basin analysis of the Polish Lowland]; (Ed.): Narkiewicz M. *Prace Państwowego Instytutu Geologicznego*, **165**, 177–194. [in Polish with English summary]
- **Maliszewska A., Kiersnowski H., Jackowicz E. 2003.** Wulkanoklastyczne osady czerwonego spągowca dolnego na obszarze Wielkopolski. [Lower Rotliegend volcaniclastic rocks at wielkopolska (Western Poland)]. *Prace Państwowego Instytutu Geologicznego*, **179**, 1–59. [in Polish with English summary]
- **Maliszewska A., Jackowicz E., Kuberska M., Kiersnowski H. 2016.** Skały permu dolnego (czerwonego spągowca) zachodniej Polski – monografia petrograficzna. [Lower Permian (Rotliegend) rocks of western Poland : a petrographic monograph]. *Prace Państwowego Instytutu Geologicznego*, **204**, 5–115. [in Polish with English summary]
- **Marek S. 1977.** Kreda dolna. [Upper Cretaceous]. (In): Budowa geologiczna wschodniej części niecki mogileńsko-łódzkiej (strefa Gopło-Ponętów-Pabianice). [Geology of

the eastern part of the Mogilno-Łódź Trough (Gopło-Ponętów-Pabianice area)]. (Ed.): Marek S. *Prace Instytutu Geologicznego*, **80**, 83–99. [in Polish with English summary]

- **MIDAS, 2022.** System of management and protection of mineral resources in Poland. http://geoportal.pgi.gov.pl/portal/page/portal/midas
- **Nawrocki J., Becker A. 2017.** Geological Atlas of Poland. Polish Geological Institute – National Research Institute, Warsaw.
- **Ostrowska K., Pisuła M. 1991.** Dokumentacja szczegółowych badań grawimetrycznych dla tematu: Poszukiwanie złóż węgla brunatnego w obrębie anomalii grawimetrycznych, II faza 1990 rok. [Detailed gravimetric survey report for recognition of brown coal deposits on gravimetric anomalies, stage II, 1990]. Inv. 1281/91, CAG PIG, Warsaw. [In Polish]
- **Ostrowski C., Stefaniuk M., Wojdyła M., Kosobudzka I. 2007.** Dokumentacja badań geofizycznych. Temat: Pomiary polowe magnetotelluryczne, magnetyczne i grawimetryczne wzdłuż profilu Zgorzelec–Wiżajny wraz z ich przetworzeniem i in-terpretacją, 2005-2007. [Geophysical sur-vey report. Field magnetotelluric, magnetic and gravimetric measurements along Zgorzelec–Wiżajny line with its processing and interpretation]. Inw. 3093/2014, Arch. CAG PIG, Warsaw. [in Polish]
- **Parka Z., Ślusarczyk S., 1988.** Stratygrafia osadów karbońskich podłoża monokliny przedsudeckiej. [Stratigraphy of the Carboniferous deposits of the Fore-Sudetic Monocline basement]. *Prace Naukowe Instytutu Górnictwa Politechniki Wrocławskiej*, **43**, 1–47. [in Polish]
- **Peryt T.M. 1981.** Dolomityzacja osadów wapienia cechsztyńskiego w rejonie Wrześni. [Dolomitization of the Zechstein Limestone deposits of the Września Region (Fore-Sudetic area, western Poland)]. *Geological Quarterly*, **22**, 477–493. [in Polish with English summary]
- **Peryt T.M, Ważny H. 1978.** Skondensowane profile wapienia cechsztyńskiego w północnej części monokliny przedsudeckiej. [Condensed profiles of the Zechstein Limestone in the northern part of the Fore-Sudetic Monocline]. *Geological Quarterly*, **25**, 549–568. [in Polish with English summary]
- **Petecki Z. 2008.** Magnetic basement in the Pomeranian segment of the Trans-European Suture Zone (NW Poland) (in Polish with English summary). *Prace Państwowego Instytutu Geologicznego*, **191**, 5–72.
- **Petecki Z., Rosowiecka O. 2017.** A new magnetic anomaly map of Poland and its contribution to the recognition of crystalline basement rocks. *Geological Quarterly*, **61**, 934–945.
- **Petijohn F. J., Potter P. E., Siever R. 1972.** Sand and sandstone. Springer Verlag. Berlin.
- **Pieńkowski G. 2004.** The epicontinental Lower Jurassic of Poland. *Polish Geological Institute Special Papers*, **12**, 1–154
- **Pletsch T., Appel J., Botor D., Clayton C.J., Duin E.J.T., Faber E., Górecki W., Kombrink H., Kosakowski P., Kuper G., Kus J., Lutz R., Mathiesen A., Ostertag C., Papiernik B., Van Bergen F. 2010.** Petroleum generation and migration. [W:] Doornenbal i Stevenson, 2010 [red.], Petroleum Geological Atlas of the Southern Permian, Basin Area. 225–253. EAGE Publications b.v., Houten.
- **Podhalańska T., Adamczak-Biały T., Becker A., Dyrka I., Feldman-Olszewska A., Głuszyński A., Grotek I., Janas M., Jarmołowicz-Szulc K., Jachowicz M., Karcz P., Klimuszko E., Kozłowska A., Krzyżak E., Kuberska M., Nowak G., Pachytel R., Pacześna J., Roman M., Sikorska-Jaworowska M., Skowroński L., Sobień K., Trela W., Trzepierczyńska A., Waksmundzka M. I., Wołkowicz K., Wójcicki A. 2016.** Rozpoznanie stref perspektywicznych dla występowania niekonwencjonalnych złóż węglowodorów w Polsce, stałe zadanie psg, etap I, Opracowanie końcowe z realizacji projektu. [Investigations of prospective zones for the unconventional hydrocarbon accumulation occurrences in Poland, Stage I, final report]. Inv. 4878/2016, CAG PIG, Warsaw. [in Polish]
- **Podhalańska T., Adamczak-Biały T., Becker A., Dyrka I., Feldman-Olszewska A., Głuszyński A., Grotek I., Janas M., Jarmołowicz-Szulc K., Jachowicz M., Karcz P., Klimuszko E., Kozłowska A.,**

Krzyżak E., Kuberska M., Nowak G., Pachytel R., Pacześna J., Roman M., Sikorska-Jaworowska M., Skowroński L., Sobień K., Trela W., Trzepierczyńska A., Waksmundzka M. I., Wołkowicz K., Wójcicki A. 2018. Rozpoznanie stref perspektywicznych dla występowania niekonwencjonalnych złóż węglowodorów w Polsce, stałe zadanie psg, etap II, Opracowanie końcowe z realizacji projektu. [Investigations of prospective zones for the unconventional hydrocarbon accumulation occurrences in Poland, Stage II, final report]. Inv. 9051/2019, CAG PIG, Warsaw. [in Polish]

- **Pokorski J. 1981**. Propozycja formalnego podziału litostratygraficznego czerwonego spągowca na Niżu Polskim. [Formal lithostratigraphic subdivision proposed for the Rotliegendes of the Polish Lowlands]. *Geological Quarterly*, **25**, 41–58. [in Polish with English summary]
- **Pokorski J. 1988.** Rotliegendes lithostratigraphy in north-western Poland. *Bulletin of the Polish Academy of Sciences, Earth Sciences*, **36**, 99–108.
- **Pokorski J. 1997.** Perm dolny (czerwony spągowiec). Litostratygrafia i litofacje. Formalne i nieformalne jednostki litostratygraficzne. [Lower Permian (Rotliegend). Lithostratigraphy and lithofacies. Formal and informal lithostratigraphic units]. (In): The epicontinental Permian and Mesozoic in Poland; (Eds): Marek S., Pajchlowa M. *Prace Państwowego Instytutu Geologicznego*, **153**, 35–38. [in Polish with English summary]
- **Poprawa P., Grotek I., Żywiecki M.M. 2005.** Impact of the Permian magmatic activity on the thermal maturation of the Carboniferous sediments in the outer Variscan orogen (SW Poland). *Mineralogical Society of Poland, Special Papers*, **26**, 253–259.
- **Reczek J. 1958.** Półszczegółowe badania grawimetryczne w rejonie Kłecka, 1958. [Semidetailed gravimetric survey in the Kłecko region, 1958]. Inv. 12315, CAG PIG, Warsaw. [in Polish]
- **Reczek J. 1963.** Opracowanie profilowych badań grawimetrycznych, temat: Kłecko, 1962. [Gravimetric survey summary report, Kłecko, 1962]. Inv. 2093, CAG PIG, Warsaw. [in Polish]
- **Reczek J. 1967.** Dokumentacja półszczegółowych badań grawimetrycznych, temat: Mogilno-Konin-Uniejów, 1965/66. [Semidetailed gravimetric survey report, Mogilno-Konin-Uniejów, 1965/66]. Kat. G-215 PBG, CAG PIG, Warsaw. [in Polish]
- **Richter-Bernburg, G. 1955.** Stratigraphische Gliederung des deutschen Zechsteins. *Zeitschrift der Deutschen Geologischen Gesellschaft*, **105**, 843–854.
- **Rochewicz A. 1980.** Wpływ procesów illityzacji i chlorytyzacji na własności kolektorskie piaskowców czerwonego spągowca SW Polski. [Impact of the illitization and chloritization processess on the Rotliegend sandstones reservoir properties in the SW Poland]. *Archiwum Mineralogiczne*, **36**, 55–61. [in Polish]
- **Sikorska-Jaworowska M., Kuberska M., Kozłowska A. 2016.** Petrografia i mineralogia łupków niższego paleozoiku kratonu wschodnioeuropejskiego oraz piaskowców karbonu podłoża monokliny przedsudeckiej. [Petrography and mineralogy of the lower Palaeozoic shales from the East European Craton and Carboniferous sandstones from the basement of the Fore-Sudetic Homocline]. *Przegląd Geologiczny*, **64**, 963–967. [in Polish with English summary]
- **Słowakiewicz M., Gąsiewicz A. 2013**. Palaeoclimatic imprint, distribution, and genesis of Zechstein Main Dolomite (Upper Permian) petroleum source rocks in Poland: Sedimentological and geochemical rationales. *Geological Society, London, Special Publications*, **376**, 523–538.
- **Słowakiewicz M., Perri E., Tucker M.E. 2016.** Micro- and Nanopores in Tight Zechstein 2 Carbonate Facies from the Southern Permian Basin, NW Europe. *Journal of Petroleum Geology*, **39**, 149–168.
- **Soćko A. 1982.** Dokumentacja badań grawimetrycznych na złożu solnym Mogilno, 1980 r. [Gravimetric survey report around the Mogilno rock-salt deposit, 1980]. Kat. G-446 PBG, CAG PIG, Warsaw. [in Polish]
- **Sokołowski J., Bojarski L., Dutkiewicz N., Cywiński T., Deczkowski Z., Dembowska J., Fuglewicz R., Gajewska I., Gapowski G., Giżejewski J., Karnkowski P., Kuhn D., Jaskowiak-Schoeinechowa N., Jakubowska L., Jasińska H., Kopik J., Lato-**

szyńska T., Maliszewska A., Majewski Z., Nieznalski M., Osiecka H., Peryt T., Raczyńska A., Roniewicz P., Szczebło J., Sztukowski M., Żelichowski A., Zielińska H. 1977. Dokumentacja wynikowa głębokiego wiercenia Września IG-1. [Września IG-1 final well report]. Inv. 123272, CAG PIG, Warsaw. [in Polish]

- **Solon J., Borzyszkowski J., Bidłasik M., Richling A., Badora K., Balon J., Brzezińska-Wójcik T., Chabudziński Ł., Dobrowolski R., Grzegorczyk I., Jodłowski M., Kistowski M., Kot R., Krąż P., Lechnio J., Macias A., Majchrowska A., Malinowska E., Migoń P., Myga-Piątek U., Nita J., Papińska E., Rodzik J., Strzyż M., Terpiłowski S., Ziaja W. 2018.** Physico-geographic mesoregions of Poland – verification and adjustment of boundaries on the basis of contemporary spatial data. *Geographia Polonica*, **91**.
- **Szpetnar-Skierniewska A., Łojek M., Kiersnowski H., Dusak K. 2015.** Dokumentacja geologiczna z wykonania prac geologicznych na koncesji nr 5/03/p na obszarze bloku koncesyjnego nr 208 niekończących się udokumentowaniem zasobów złóż kopalin (ropy naftowej i gazu ziemnego). [Concession No. 5/03/p final geological report, block 208]. Inv. 2644/2015, CAG PIG, Warsaw. [in Polish]
- **Wagner R. 1994.** Stratygrafia osadów i rozwój basenu cechsztyńskiego na Niżu Polskim. [Stratigraphy and evolution of the Zechstein Basin in the Polish Lowland]. *Prace Państwowego Instytutu Geologicznego*, **194**, 1–74.
- **Wagner R. 1998.** Mapy paleogeograficzne cechsztynu. [Zechstein Palaeogeographic maps]. (In): Atlas paleogeograficzny epikontynentalnego permu i mezozoiku w Polsce, 1 : 2 500 000. [Palaeogeographic atlas of the epicontinental Permian and Mesozoic in Poland, 1 : 2 500 000]. (Eds): Dadlez R., Marek Sy., Pokorski A. Inv. 3417/98, 4610/2015, CAG PIG, Warsaw. [in Polish]
- **Wagner, R. 2012.** Mapa paleogeograficzna dolomitu głównego (Ca2) w Polsce. [Palaeogeographic map of the Main Dolomite (Ca2) in Poland]. Polish Geological Institute – National Research Institute, Warsaw. [in Polish]
- **Wagner R., Peryt T.M. 1997.** Possibility of sequence stratigraphic subdivision of the Zechstein in the Polish Basin. *Geological Quarterly*, **41**, 457–474.
- **Wagner R., Buniak A., Dadlez R., Grotek I., Kiersnowski H., Kuberska M., Kudrewicz R., Lis P., Maliszewska A., Mikołajewski Z., Papiernik B., Pokorski J., Poprawa P., Skowroński L., Słowakiewicz M., Szewczyk J., Wolnowski T. 2008.** Zasoby prognostyczne, nieodkryty potencjał gazu ziemnego w utworach czerwonego spągowca i wapienia cechsztyńskiego w Polsce – badania geologiczne. [Prognostic resources, undiscovered potential of natural gas in the Rotliegend and Zechstein Limestone in Poland – geological investigations]. Inv. 2293/2009, CAG PIG, Warsaw. [in Polish]
- **Wasiak J. 1990.** Dokumentacja szczegółowych badań grawimetrycznych, temat: Poszukiwanie złóż węgla brunatnego w obrębie anomalii grawimetrycznych, II faza – 1989 r. [Detailed gravimetric survey report. Topic: Searching for brown coal deposits on gravimetric anomalies, stage II, 1989]. Kat. G-570, Arch. PBG, Warsaw. [in Polish]
- **Wójcicki A., Kiersnowski H., Dyrka I., Adamczak-Biały T., Becker A., Głuszyński A., Janas M., Kozłowska A., Krzemiński L., Kuberska M., Pacześna J., Podhalańska T., Roman M., Skowroński L., Waksmundzka M.I. 2014.** Prognostyczne zasoby gazu ziemnego w wybranych zwięzłych skałach zbiornikowych Polski. Szacowanie zasobów złóż węglowodorów – zadanie ciągłe PSG (etap I, 2014-2017 r.). [Prognostic resources of tight gas in Poland]. Polish Geological Institute – National Research Institute, Warsaw, 1–65. [in Polish]
- **Wróbel J., Szewc A. 1977.** Dokumentacja wynikowa otworu badawczego Otoczna-1. [Otoczna-1 final well report]. Inv. 122593, CAG PIG, Warsaw. [in Polish]

Żelaźniewicz A., Aleksandrowski P., Buła Z., Karnkowski P.H., Konon A., Ślączka A., Żaba J., Żytko K. 2011. Regionalizacja tektoniczna Polski. [Tectonic subdivision of Poland]. Komitet Nauk Geologicznych PAN, Wrocław. [in Polish]